# Supporting Information

# New 3-Acyl Tetramic acid Derivatives from the Deep-Sea-Derived Fungus *Lecanicillium fusisporum*

**Xinya Xu [1,†], Yanhui Tan [2,†], Chenghai Gao [1], Kai Liu[1], Zhenzhou Tang [1], Chunju Lu [1], Haiyan Li [1], Xiaoyong Zhang [3,*] and Yonghong Liu [1,*]**

[1] Institute of Marine Drugs, Guangxi University of Chinese Medicine, Nanning 530200, P. R. China; xyxu@gxtcmu.edu.cn (X. X.); gaoch@gxtcmu.edu.cn (C. G); liuk@gxtcmu.edu.cn (K. L.); tangzz@gxtcmu.edu.cn (Z. T.); luchunjv@stu.gxtcmu.edu.cn (C. L.); lihaiyan12368@163.com (H. L.); yonghongliu@scsio.ac.cn (Y. L.)

[2] School of Chemistry and Pharmaceutical Science, State Key Laboratory for the Chemistry and Molecular Engineering of Medicinal Resources, Guangxi Normal University, Guilin 541004, P. R. China; tyh533@smu.edu.cn

[3] College of Marine Sciences, South China Agricultural University, Guangzhou 510642, P. R. China; zhangxiaoyong@scau.edu.cn

* Correspondence: zhangxiaoyong@scau.edu.cn; yonghongliu@scsio.ac.cn

† These authors contributed equally to this paper.

# Table of Contents

Figure S1. The colonies and the ITS rRNA sequences data of deep-sea-derived fungus *Lecanicillium fusisporum* GXIMD00542 ....4
Figure S2. $^{1}$H NMR spectrum of 1 ....4
Figure S3. $^{13}$C NMR spectrum of 1 ....5
Figure S4. HSQC spectrum of 1 ....5
Figure S5. $^{1}$H-$^{1}$H COSY spectrum of 1 ....6
Figure S6. HMBC spectrum of 1 ....6
Figure S7. NOESY spectrum of 1 ....7
Figure S8. HR-ESI-MS spectrum of 1 ....7
Table S1. Crystal data and structure refinement for compound 1 ....8
Figure S9. $^{1}$H NMR spectrum of 2 ....9
Figure S10. $^{13}$C NMR spectrum of 2 ....9
Figure S11. HSQC spectrum of 2 ....10
Figure S12. $^{1}$H-$^{1}$H COSY spectrum of 2 ....10
Figure S13. HMBC spectrum of 2 ....11
Figure S14. NOESY spectrum of 2 ....11
Figure S15. HR-ESI-MS spectrum of 2 ....12
Figure S16. $^{1}$H NMR spectrum of 3 ....12
Figure S17. $^{13}$C NMR spectrum of 3 ....13
Figure S18. HSQC spectrum of 3 ....13
Figure S19. $^{1}$H-$^{1}$H COSY spectrum of 3 ....14
Figure S20. HMBC spectrum of 3 ....14
Figure S21. NOESY spectrum of 3 ....15
Figure S22. HR-ESI-MS spectrum of 3 ....15
Figure S23. $^{1}$H NMR spectrum of 4 ....16
Figure S24. $^{13}$C NMR spectrum of 4 ....16
Figure S25. HSQC spectrum of 4 ....17
Figure S26. $^{1}$H-$^{1}$H COSY spectrum of 4 ....17
Figure S27. HMBC spectrum of 4 ....18
Figure S28. NOESY spectrum of 4 ....18
Figure S29. HR-ESI-MS spectrum of 4 ....19
Figure S30. $^{1}$H NMR spectrum of 5 ....19
Figure S31. $^{13}$C NMR spectrum of 5 ....20
Figure S32. HSQC spectrum of 5 ....20
Figure S33. $^{1}$H-$^{1}$H COSY spectrum of 5 ....21
Figure S34. HMBC spectrum of 5 ....21
Figure S35. NOESY spectrum of 5 ....22
Figure S36. 1D selective NOESY spectrum of 5 ....22
Figure S37. 1D selective NOESY spectrum of 5 ....23
Figure S38. HR-ESI-MS spectrum of 5 ....23
Figure S39. $^{1}$H NMR spectrum of 6 ....24
Figure S40. $^{13}$C NMR spectrum of 6 ....24

Figure S41. HSQC spectrum of 6 ..... 25
Figure S42. $^{1}$H-$^{1}$H COSY spectrum of 6 ..... 25
Figure S43. HMBC spectrum of 6 ..... 26
Figure S44. NOESY spectrum of 6 ..... 26
Figure S45. HR-ESI-MS spectrum of 6 ..... 27
Figure S46. $^{1}$H NMR spectrum of 7 ..... 27
Figure S47. $^{13}$C NMR spectrum of 7 ..... 28
Figure S48. HSQC spectrum of 7 ..... 28
Figure S49. $^{1}$H-1H COSY spectrum of 7 ..... 29
Figure S50. HMBC spectrum of 7 ..... 29
Figure S51. NOESY spectrum of 7 ..... 30
Figure S52. HR-ESI-MS spectrum of 7 ..... 30
Figure S53. $^{1}$H NMR spectrum of (*R*)-MTPA ester of 7 ..... 31
Figure S54. $^{1}$H NMR spectrum of (*S*)-MTPA ester of 7 ..... 31
Table S2. Relative free energies[a] and equilibrium populations[b] of conformers for (3*S*, 6*S*, 10*R*)-2a [c] ..... 31
Figure S55. The optimized structures (left) and the calculated CD spectra of conformers (3*S*, 6*S*, 10*R*)-2a in MeOH at M06-2X/def2TZVP level (right). σ=0.30 eV. ..... 34
Table S3. Relative free energies[a] and equilibrium populations[b] of conformers for (3*S*, 6*R*, 10*S*)-2b[c] ..... 34
Figure S56. The optimized structures (left) and the calculated CD spectra of conformers (3*S*, 6*R*, 10*S*)-2b in MeOH at M06-2X/def2TZVP level (right). σ=0.30 eV. ..... 35
Table S4. Relative free energies[a] and equilibrium populations[b] of conformers for (3*S*, 6*S*, 9*R*)-3a[c] ..... 35
Figure S57. The optimized structure of conformers for (3*S*, 6*S*, 9*R*)-3a in MeOH at B3LYP/6-31G (d) level ..... 36
Table S5. Relative free energies[a] and equilibrium populations[b] of conformers for (3*S*, 6*R*, 9*S*)-3b[c] ..... 36
Figure S58. The optimized structure of conformers for (3*S*, 6*R*, 9*S*)-3b in MeOH at B3LYP/6-31G (d) level ..... 37
Figure S59. Correlation plots of experimental $^{13}$C NMR chemical shifts versus the corresponding calculated data for (3*S*, 6*S*, 9*R*)-3a and (3*S*, 6*R*, 9*S*)-3b ..... 38
Figure S60. DP4+ probabilities (%) for conformers (3*S*, 6*S*, 9*R*)-3a (isomer 1) and (3*S*, 6*R*, 9*S*)-3b (isomoer 2) ..... 38
Table S6. Relative free energies[a] and equilibrium populations[b] of conformers for (3*S*,6*S*,9*S*)-4a[c] .38
Figure S61. The optimized structures (left) and the calculated CD spectra for conformers (3*S*,6*S*,9*S*)-4a in MeOH at M06-2X/def2TZVP level (right). σ=0.30 eV. ..... 40
Table S7. Relative free energies[a] and equilibrium populations[b] of conformers for (3*S*,6*R*,9*R*)-4b[c] 40
Figure S62. The optimized structures (left) and the calculated CD spectra for conformers (3*S*,6*R*,9*R*)-4b in MeOH at M06-2X/def2TZVP level (right). σ=0.30 eV. ..... 41
Table S8. Relative free energies[a] and equilibrium populations[b] of conformers for (3*R*,6*R*,9*R*)-4c[c] 41
Figure S63. The optimized structures (left) and the calculated CD spectra for conformers (3*R*,6*R*,9*R*)-4c in MeOH at M06-2X/def2TZVP level (right). σ=0.30 eV. ..... 43
Table S9. Relative free energies[a] and equilibrium populations[b] of conformers for (3*R*,6*S*,9*S*)-4d[c].43

Figure S64. The optimized structures (left) and the calculated CD spectra for conformers (3*R*,6*S*,9*S*)-4d in MeOH at M06-2X/def2TZVP level (right). σ=0.30 eV. .....44
Figure S65. Correlation plots of experimental $^{13}$C NMR chemical shifts versus the corresponding calculated data for (3*S*, 6*S*, 9*S*)-4a and (3*S*, 6*R*, 9*R*)-4b .....45
Figure S66. DP4+ probabilities (%) for conformers of (3*S*, 6*S*, 9*S*)-4a (isomer 1) and (3*S*, 6*R*, 9*R*)-4b (isomoer 2). .....46
Table S10. Relative free energies[a] and equilibrium populations[b] of conformers for (3*S*, 6*R*, 8S, 9*S*)-5a[c] .....46
Figure S67. The optimized structure of conformers for (3*S*,6*R*,8*S*,9*S*)-5a in MeOH at B3LYP/6-31G (d) level.....47
Table S11. Relative free energies[a] and equilibrium populations[b] of conformers for (3*S*,6*S*,8*R*,9*R*)-5b [c] .....47
Figure S68. The optimized structure of conformers for (3*S*,6*S*,8*R*,9*R*)-5b in MeOH at B3LYP/6-31G (d) level.....48
Figure S69. Correlation plots of experimental $^{13}$C NMR chemical shifts versus the corresponding calculated data for (3*S*,6*R*,8*S*,9*S*)-5a and (3*S*,6*S*,8*R*,9*R*)-5b. .....48
Figure S70. DP4+ probabilities (%) for conformers of (3*S*,6*R*,8*S*,9*S*)-5a (isomer 1) and (3*S*,6*S*,8*R*,9*R*)-5b (isomoer 2). .....49
Table S12. Relative free energies[a] and equilibrium populations[b] of conformers for (3*S*,6*S*,8*R*,9*S*)-6a [c].....49
Figure S71. The optimized structure of conformers for (3*S*,6*S*,8*R*,9*S*)-6a in MeOH at B3LYP/6-31G (d) level.....50
Table S13. Relative free energies[a] and equilibrium populations[b] of conformers for (3*S*,6*R*,8*S*,9*R*)-6b [c] .....50
Figure S72. The optimized structure of conformers for (3*S*,6*R*,8*S*,9*R*)-6b in MeOH at B3LYP/6-31G (d) level.....51
Figure S73. Correlation plots of experimental $^{13}$C NMR chemical shifts versus the corresponding calculated data for (3*S*,6*S*,8*R*,9*S*)-6a and (3*S*,6*R*,8*S*,9*R*)-6b .....51
Figure S74. DP4+ probabilities (%) for conformers of (3*S*,6*S*,8*R*,9*S*)-6a (isomer 1) and (3*S*,6*R*,8*S*,9*R*)-6b (isomoer 2). .....52
Figure S74. Proposed biosynthetic pathway of compounds 1–7. .....52

CAACCCTTATGTGACATACCAATCGTTGCTTCGGCGGACTCGCCCCGGTGTCCGGCAGGCCCTCGCGG
CCGGCCGCGACCCGGATCCAGGCGGACGCCGGAGACCATCCAAAAACTCTTTGTATTCTAGCAAGTCT
TCTGAATGAGCCGCAAGGCAACACAAATGAATCAAAACTTTCAACAACGGATCTCTTGGTTCTGGCATC
GATGACTAGCGCAGCGAAAGGAGATAACTAATGTGAATTGCACACATCCGCGAACTTGAACACACTGG
AGGCCCATAGCGGTCCCAACCAATCGCCCCGGTTGAGGAGGACGGGCAACGACTTGATTCGTGGCTA
CCATGCAGGCACCCTTTTCGGCCGTGAAGCTTCACCCACAACTTGCATTCAAAGACTCGATGGTTCCCG
GGATTCTGCAATTCGCTCATGATTGACATGACTTCAGCATTATTTTAGCTTTGTACTGTAATGAAAAAGG
AAAGGAACGTTTAATTTATTGGGCTTGAAAATCCGATCAATACTCCACTCTTTTATTTCCCAAAAAAGAG
AATACTACTTGTATATAGTTACA

**Figure S1.** The colonies and the ITS rRNA sequences data of deep-sea-derived fungus *Lecanicillium fusisporum* GXIMD00542

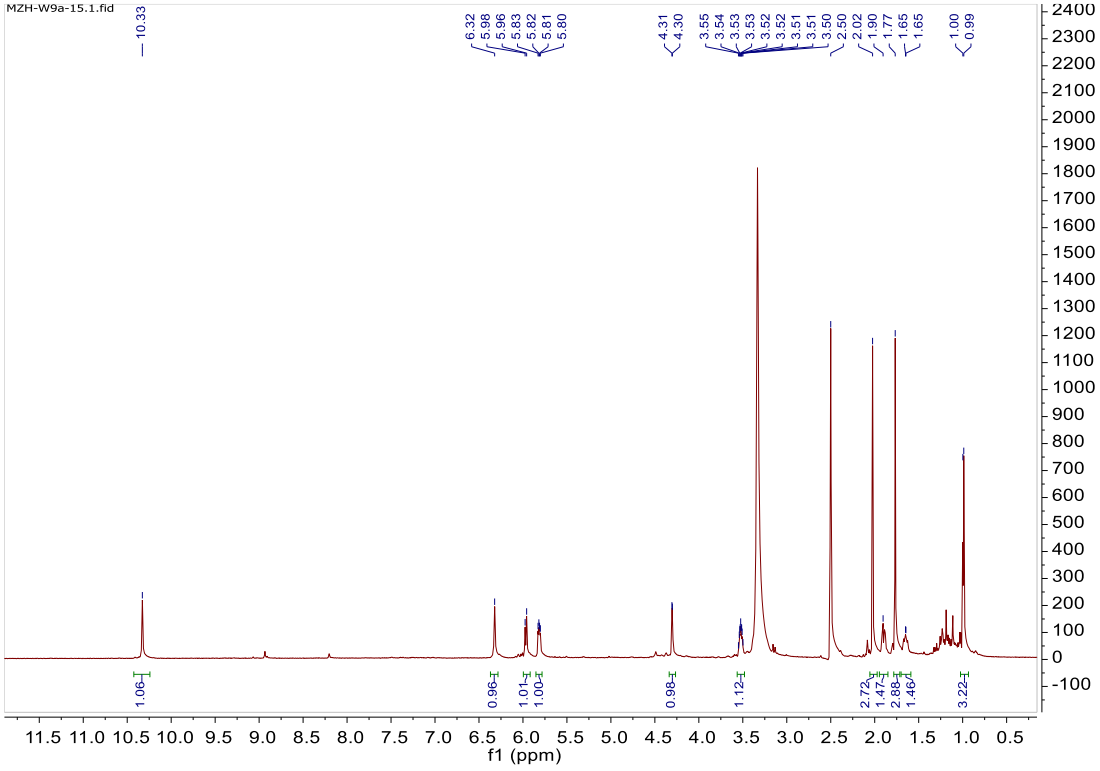


**Figure S2**. $^{1}$H NMR spectrum of **1**

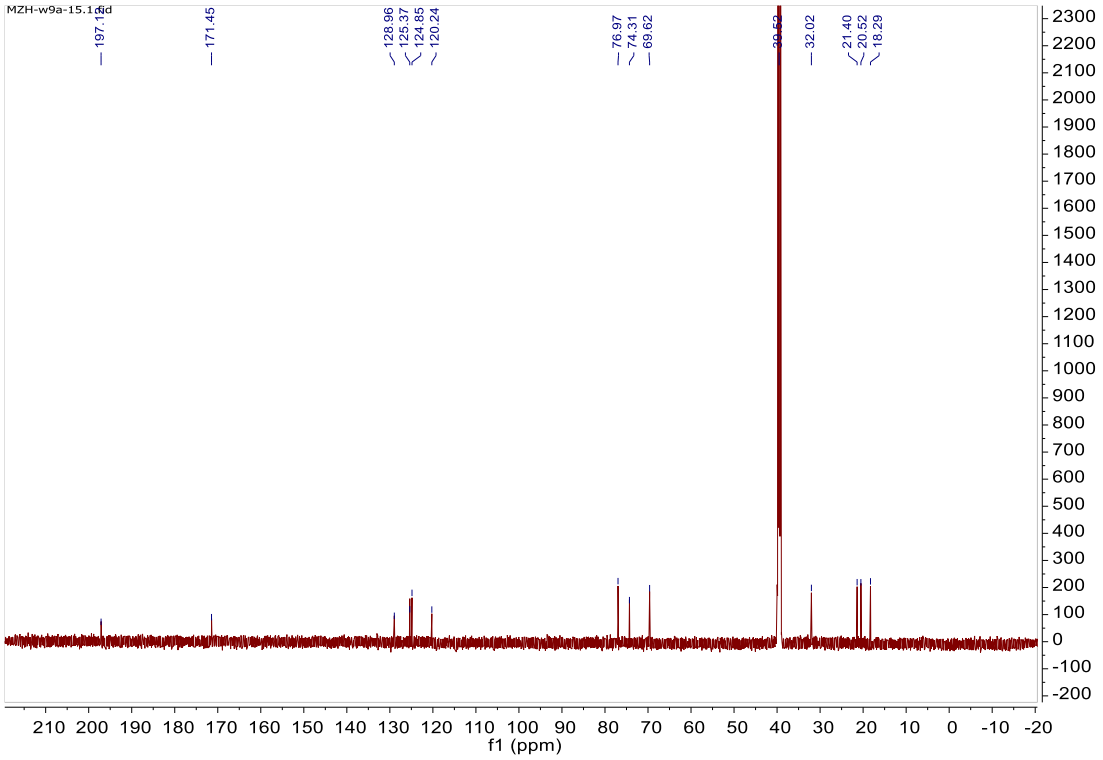


Figure S3. $^{13}C$ NMR spectrum of **1**

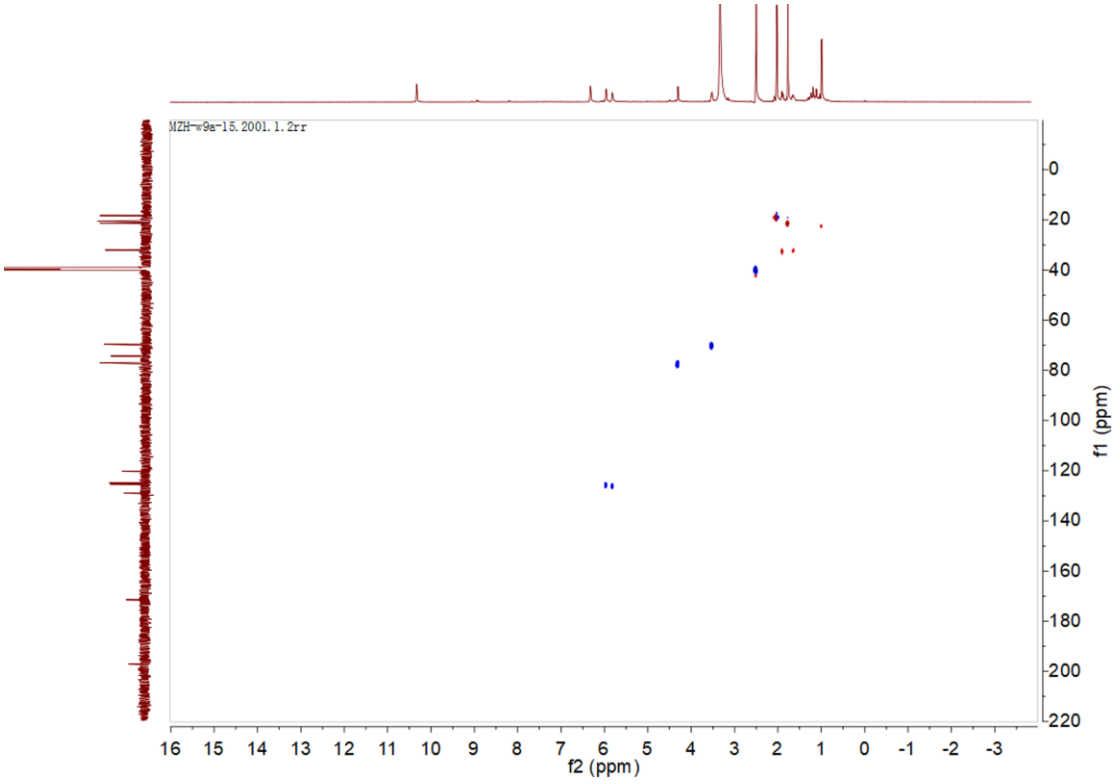


Figure S4. HSQC spectrum of **1**

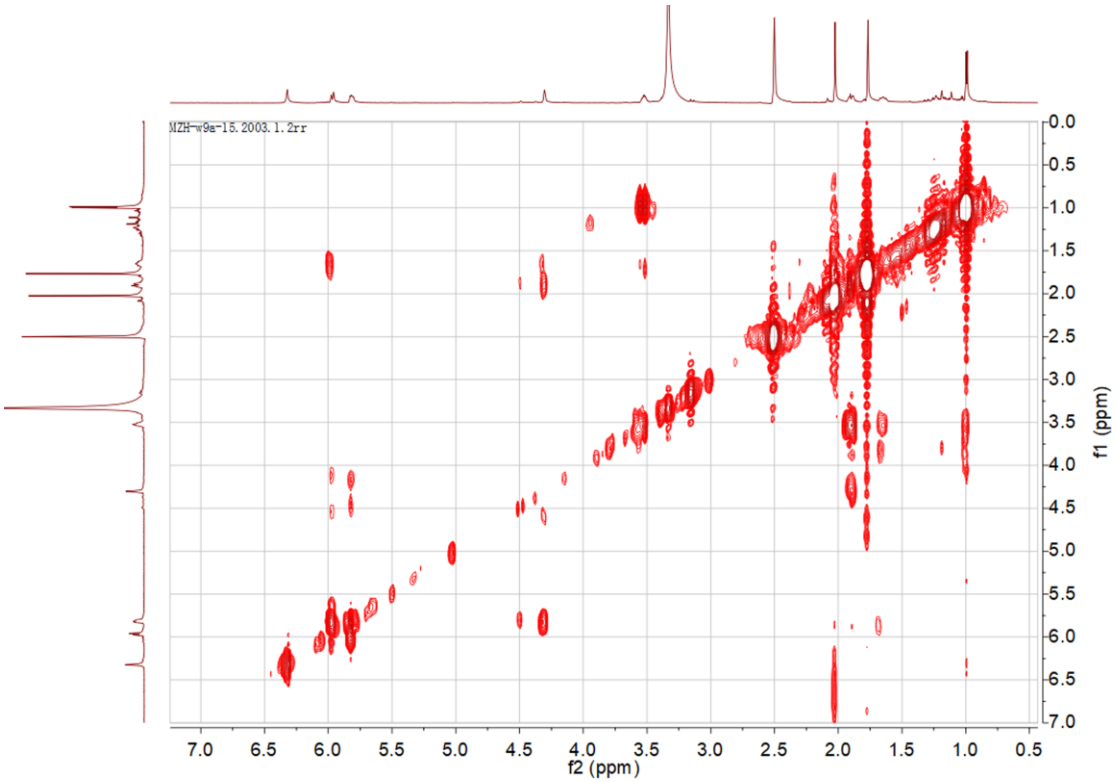


Figure S5. $^{1}H$-$^{1}H$ COSY spectrum of **1**

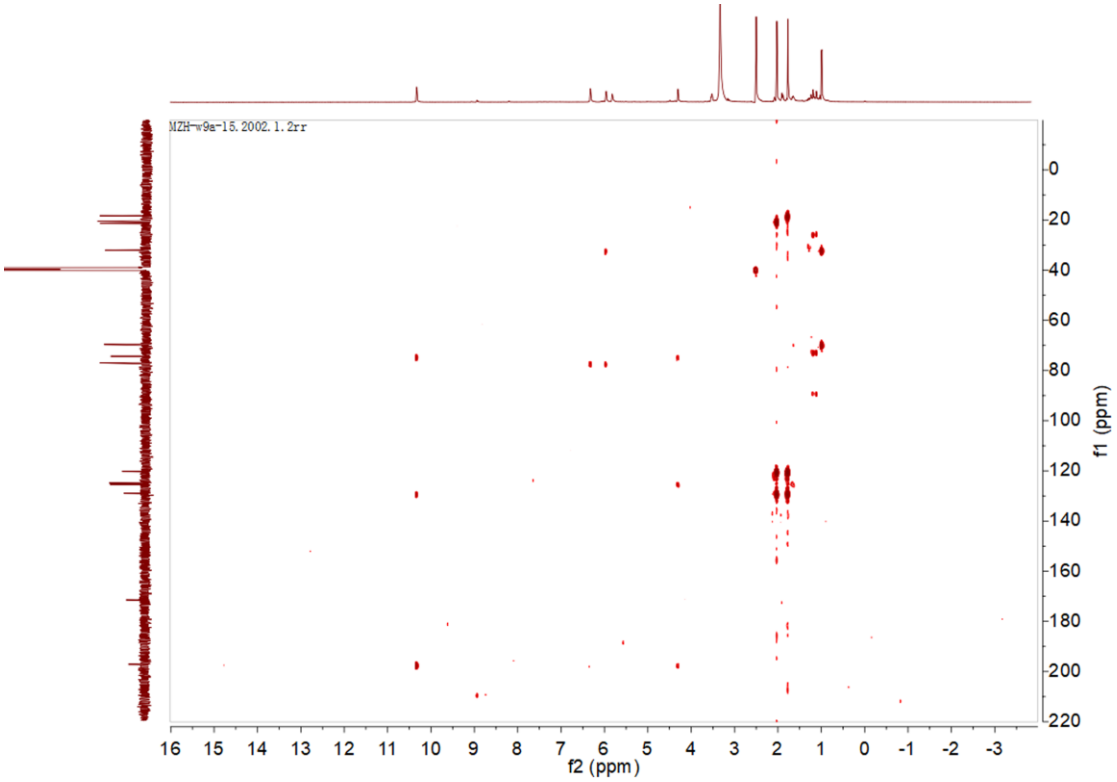


Figure S6. HMBC spectrum of **1**

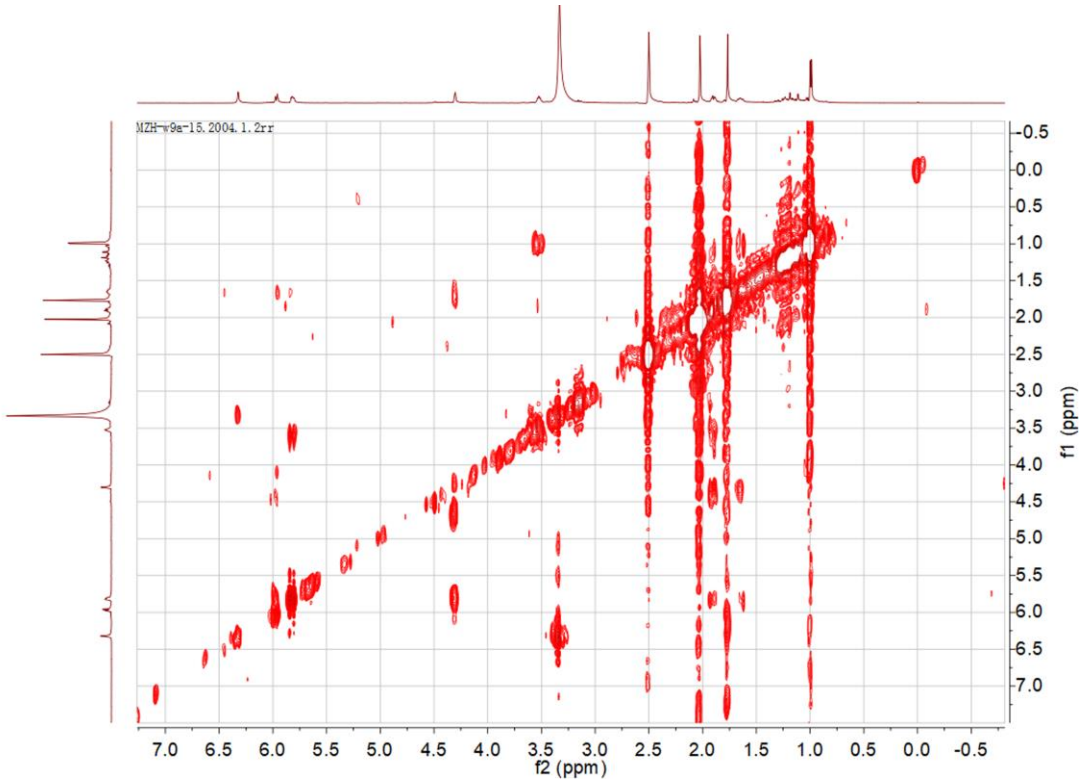


**Figure S7**. NOESY spectrum of **1**

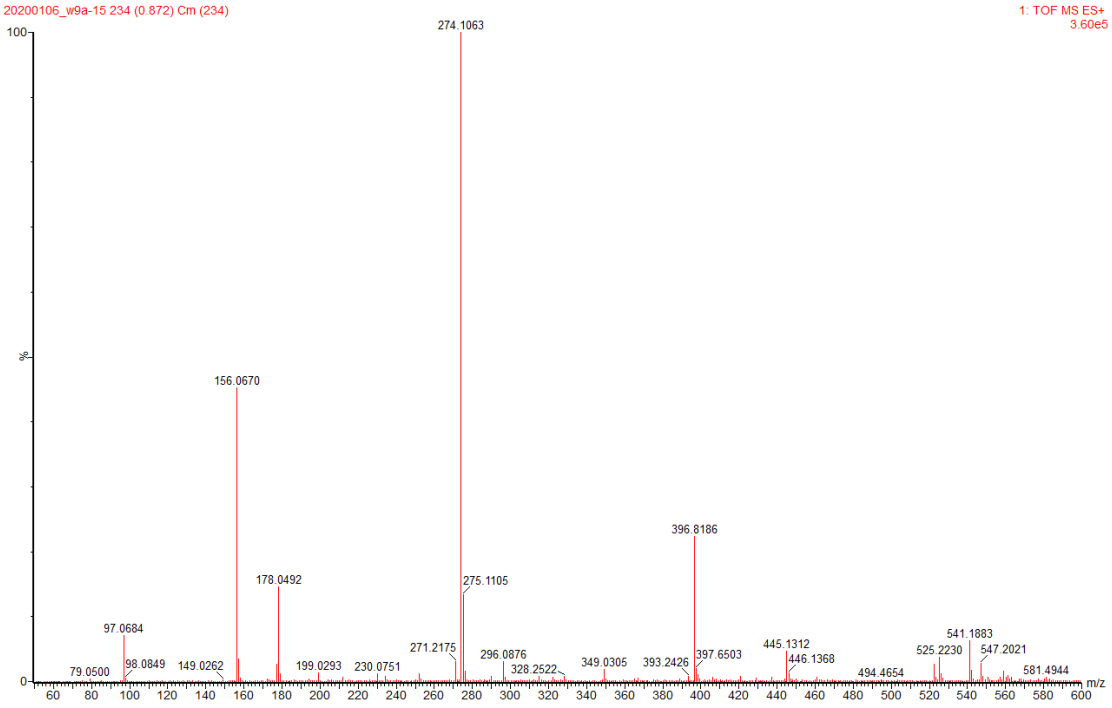


**Figure S8**. HR-ESI-MS spectrum of **1**

Table S1. Crystal data and structure refinement for compound 1

| | |
|---|---|
| Empirical formula | $C_{26}H_{36}N_2O_9$ |
| Formula weight | 520.57 |
| Temperature/K | 100.00(10) |
| Crystal system | orthorhombic |
| Space group | $P2_12_12_1$ |
| a/Å | 11.32560(10) |
| b/Å | 12.19970(10) |
| c/Å | 18.5233(2) |
| α/° | 90 |
| β/° | 90 |
| γ/° | 90 |
| Volume/Å$^3$ | 2559.34(4) |
| Z | 4 |
| $\rho_{calc}$g/cm$^3$ | 1.351 |
| μ/mm$^{-1}$ | 0.851 |
| F(000) | 1112.0 |
| Crystal size/mm$^3$ | 0.16 × 0.08 × 0.08 |
| Radiation | Cu Kα (λ = 1.54184) |
| 2Θ range for data collection/° | 8.678 to 148.214 |
| Index ranges | -13 ≤ h ≤ 12, -13 ≤ k ≤ 14, -22 ≤ l ≤ 22 |
| Reflections collected | 14388 |
| Independent reflections | 5046 [$R_{int}$ = 0.0182, $R_{sigma}$ = 0.0192] |
| Data/restraints/parameters | 5046/0/345 |
| Goodness-of-fit on $F^2$ | 1.045 |
| Final R indexes [I>=2σ (I)] | $R_1$ = 0.0266, w$R_2$ = 0.0702 |
| Final R indexes [all data] | $R_1$ = 0.0270, w$R_2$ = 0.0705 |
| Largest diff. peak/hole / e Å$^{-3}$ | 0.18/-0.27 |
| Flack parameter | 0.03(4) |

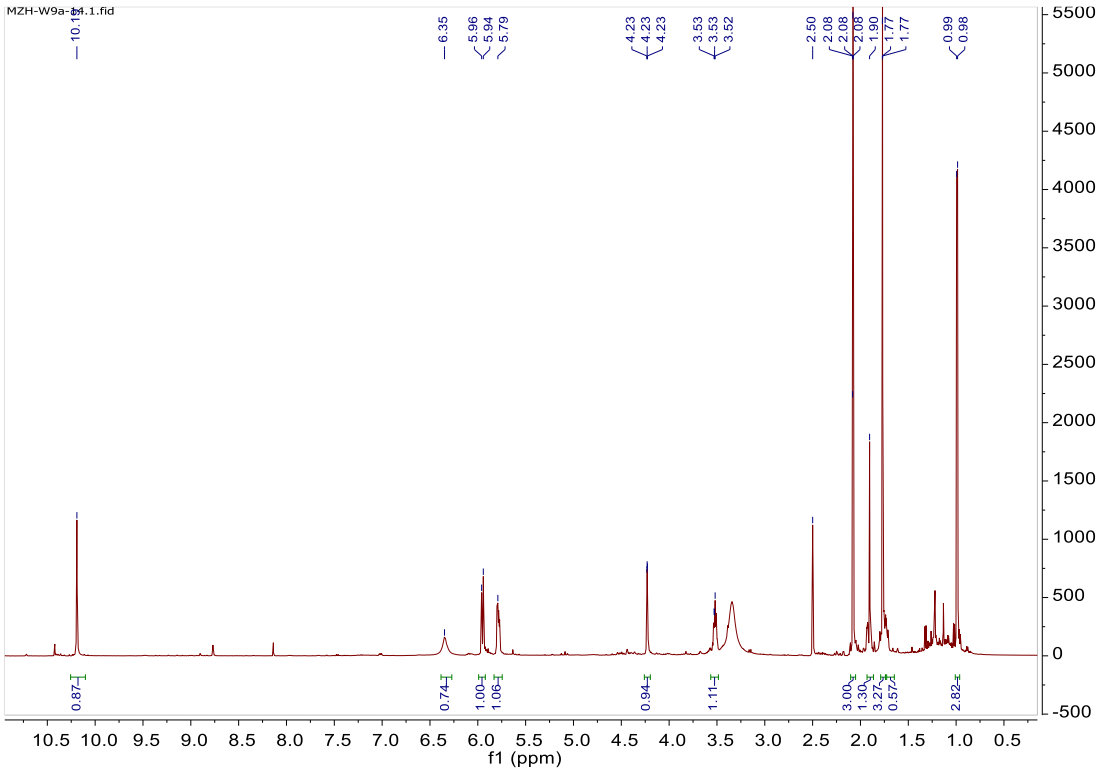


**Figure S9**. $^{1}$H NMR spectrum of **2**

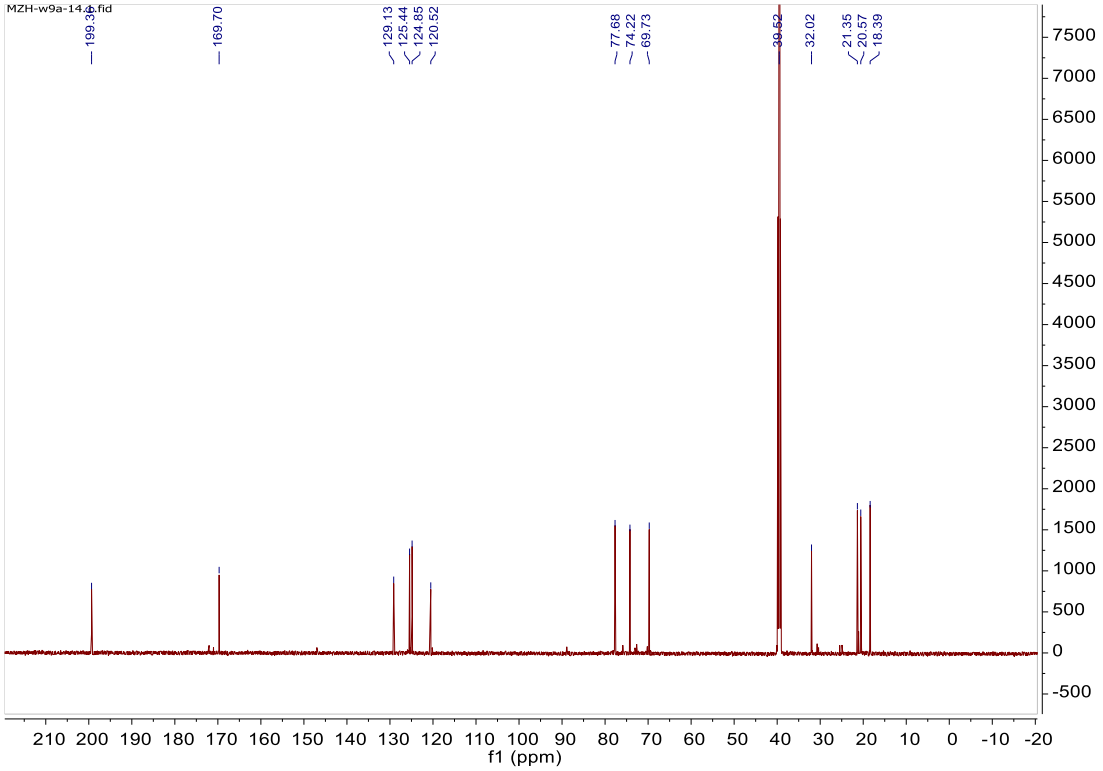


**Figure S10**. $^{13}$C NMR spectrum of **2**

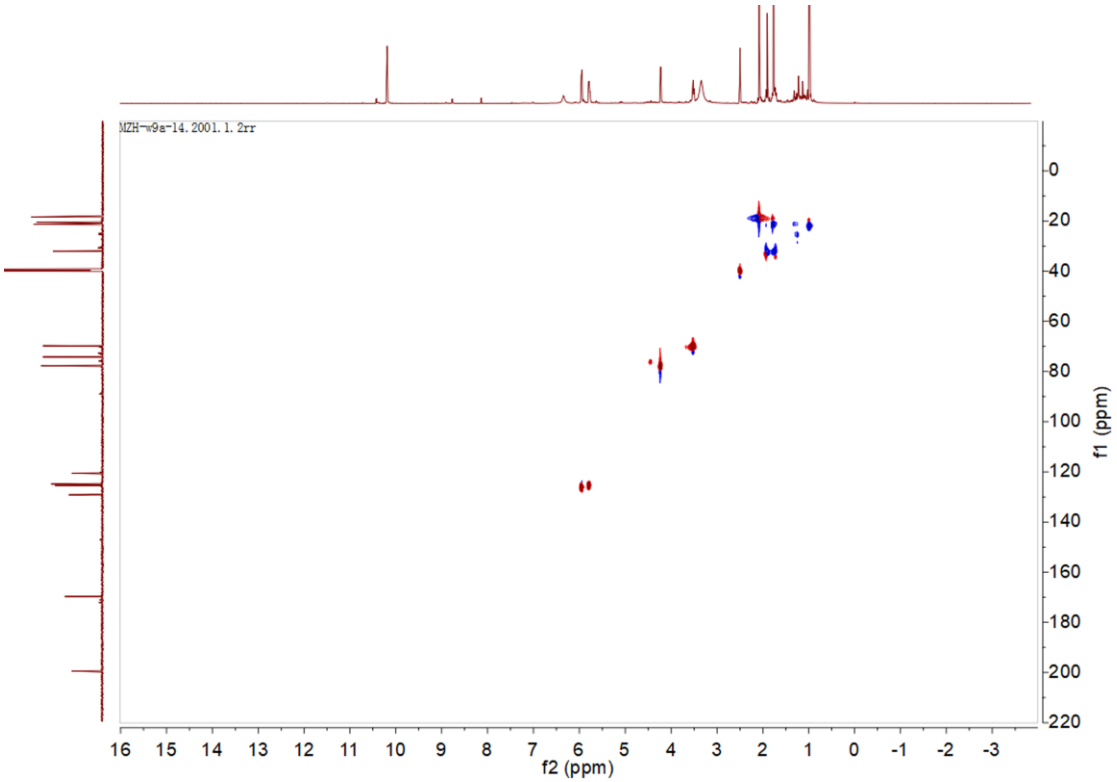


Figure S11. HSQC spectrum of 2

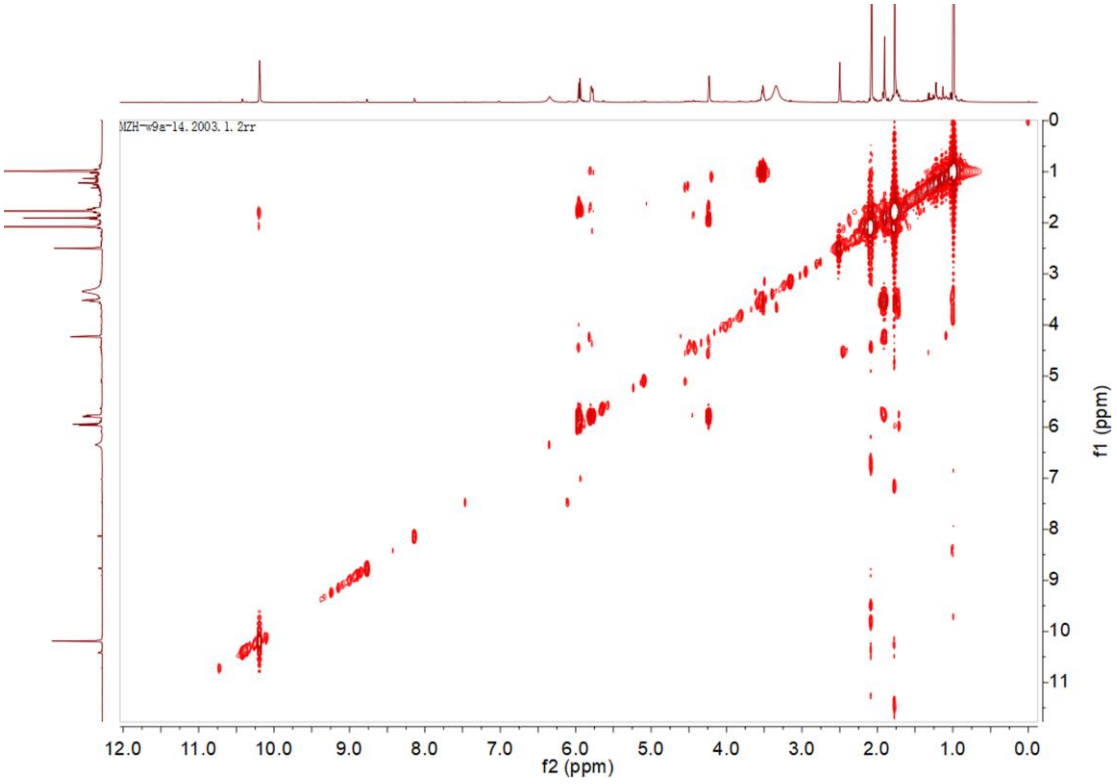


Figure S12. $^{1}$H-$^{1}$H COSY spectrum of 2

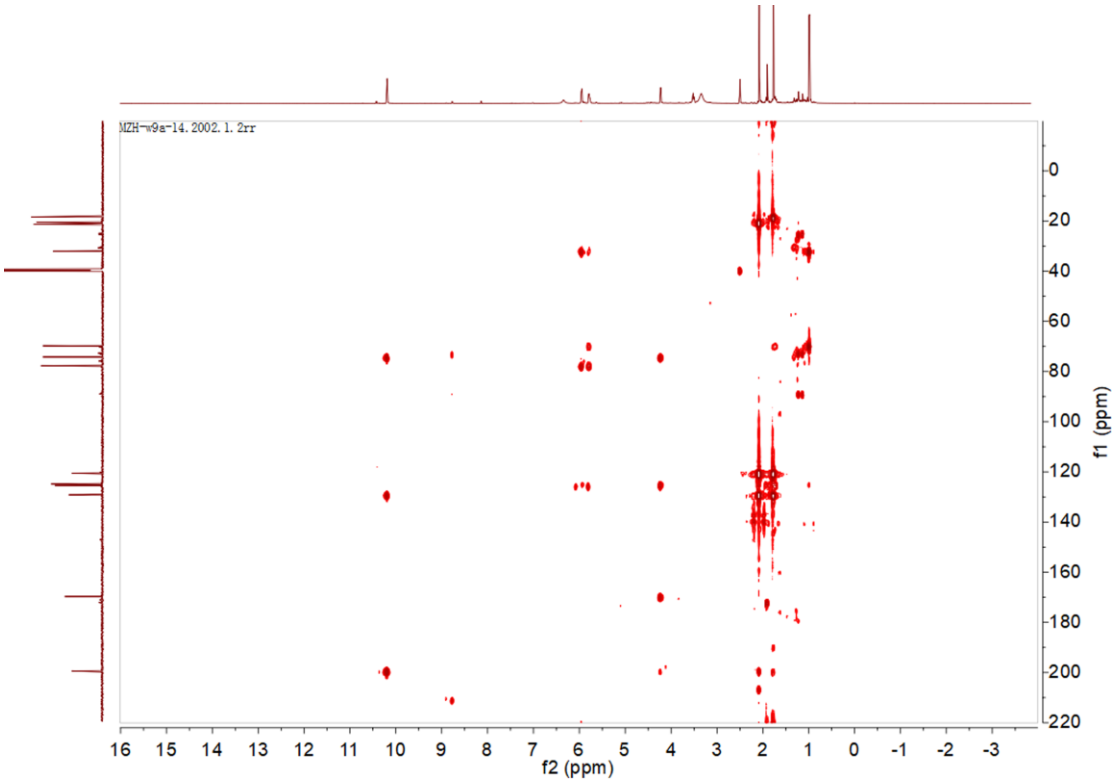


Figure S13. HMBC spectrum of 2

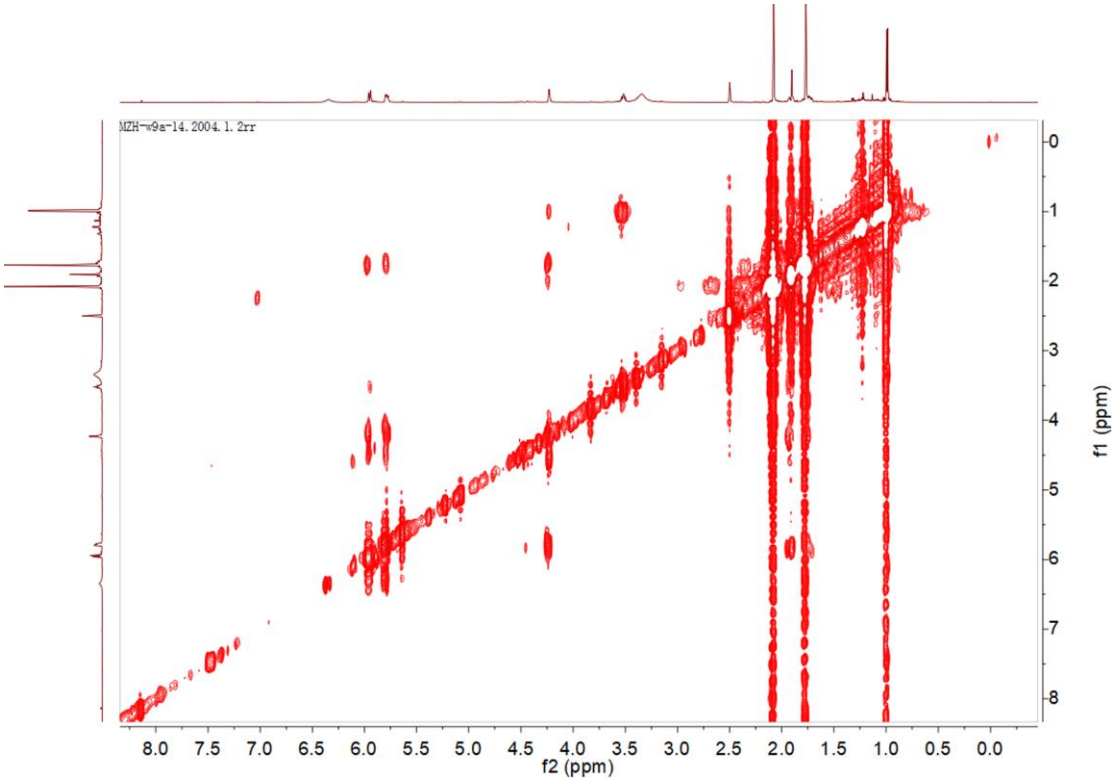


Figure S14. NOESY spectrum of 2

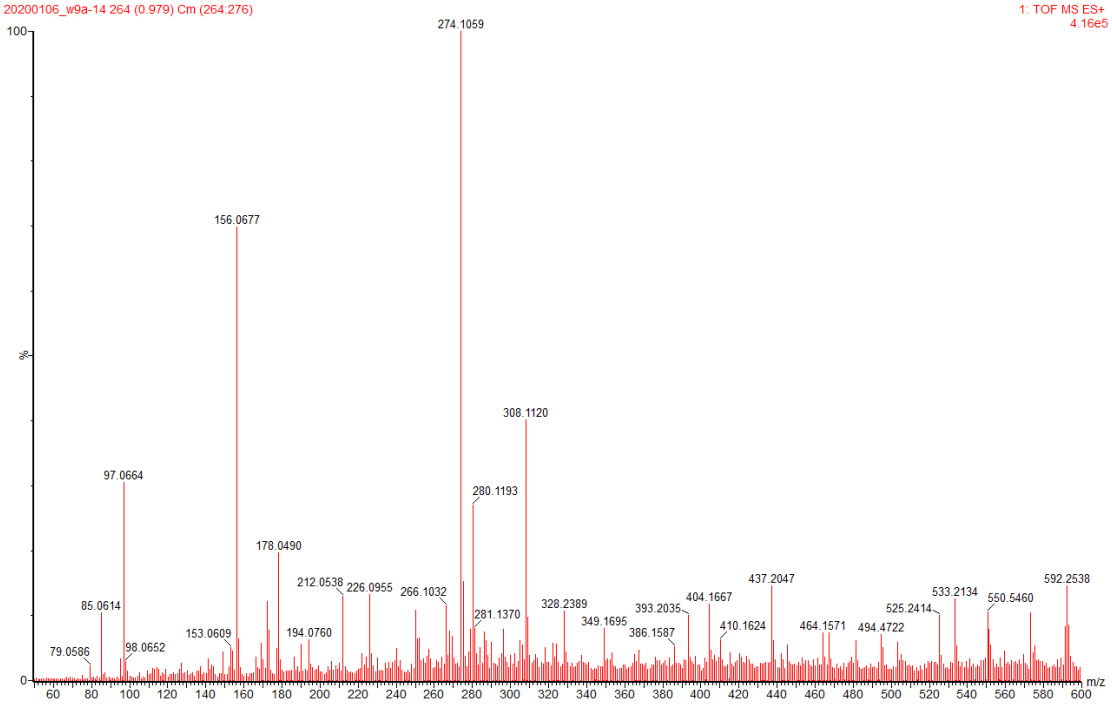


**Figure S15.** HR-ESI-MS spectrum of **2**

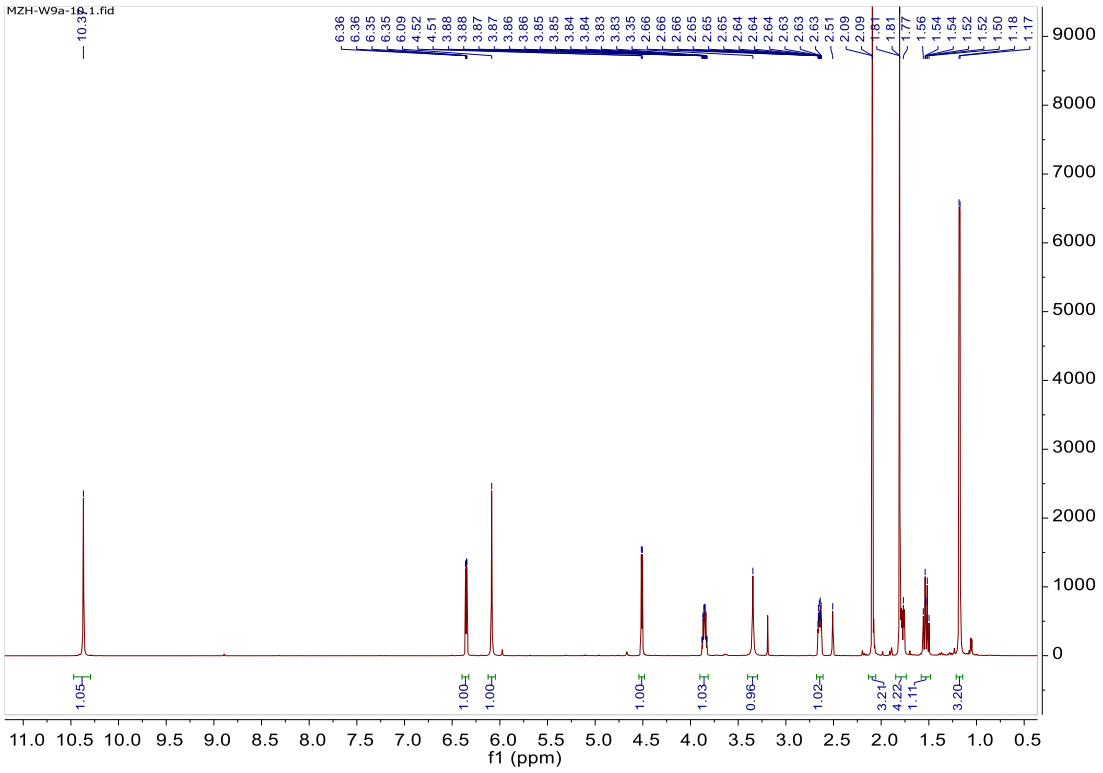


**Figure S16.** $^{1}$H NMR spectrum of **3**

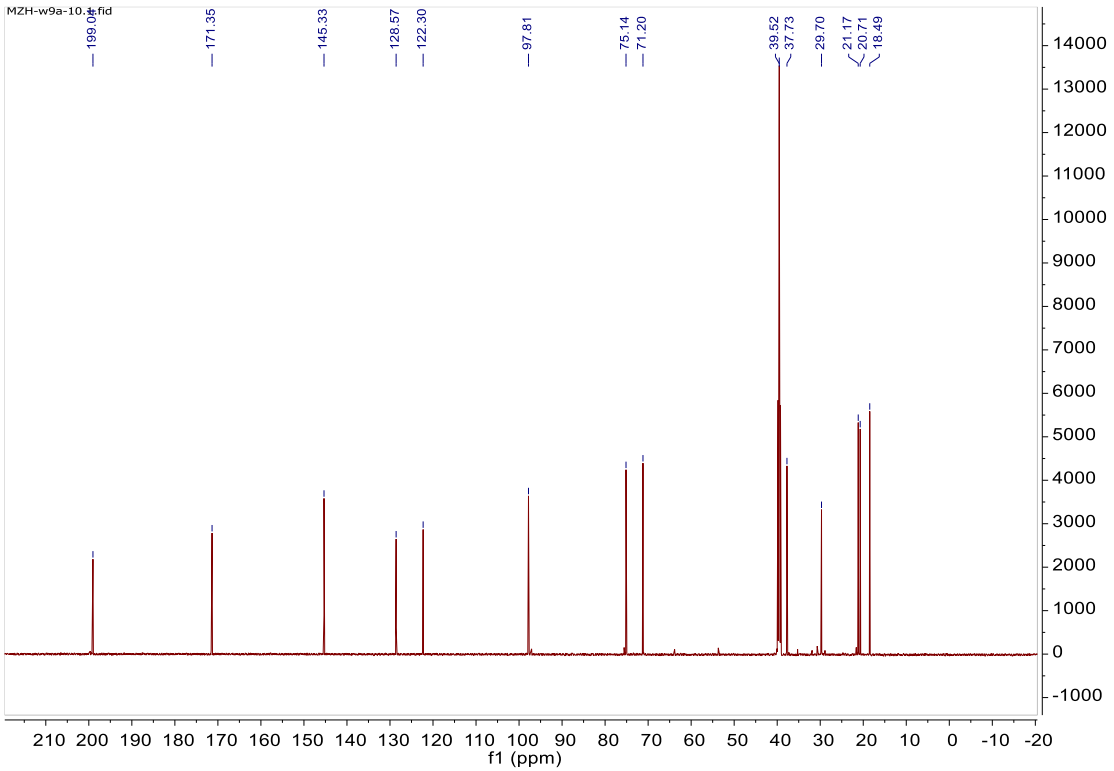


Figure S17. $^{13}C$ NMR spectrum of **3**

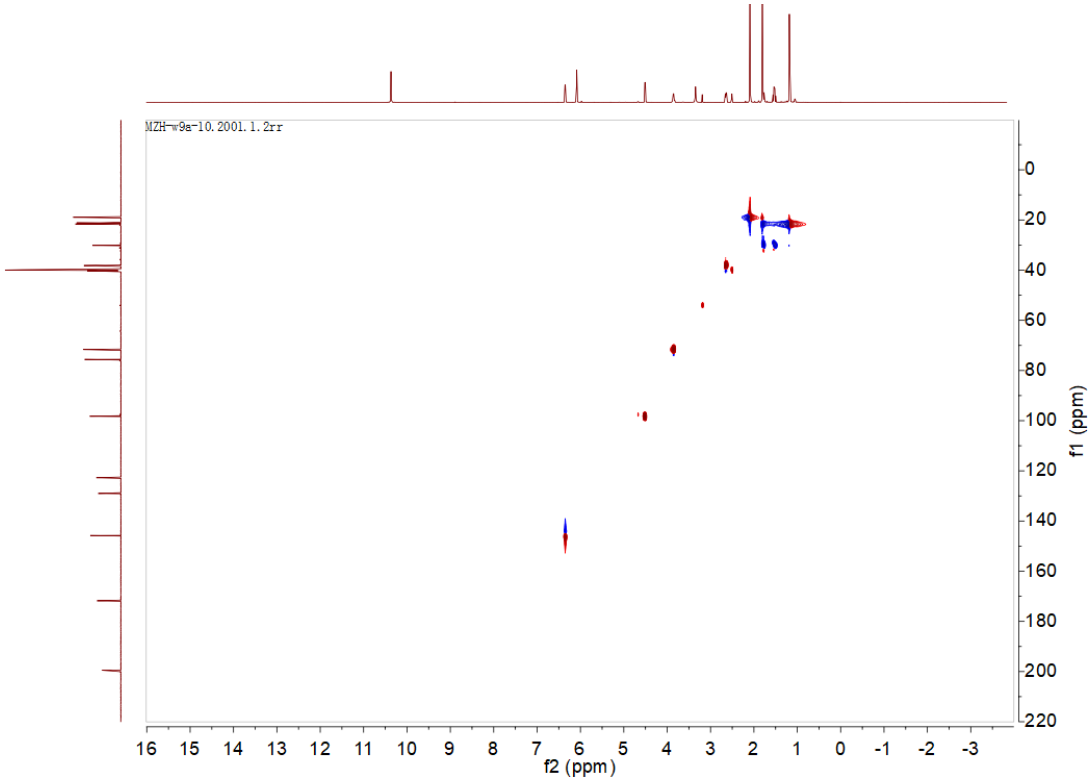


Figure S18. HSQC spectrum of **3**

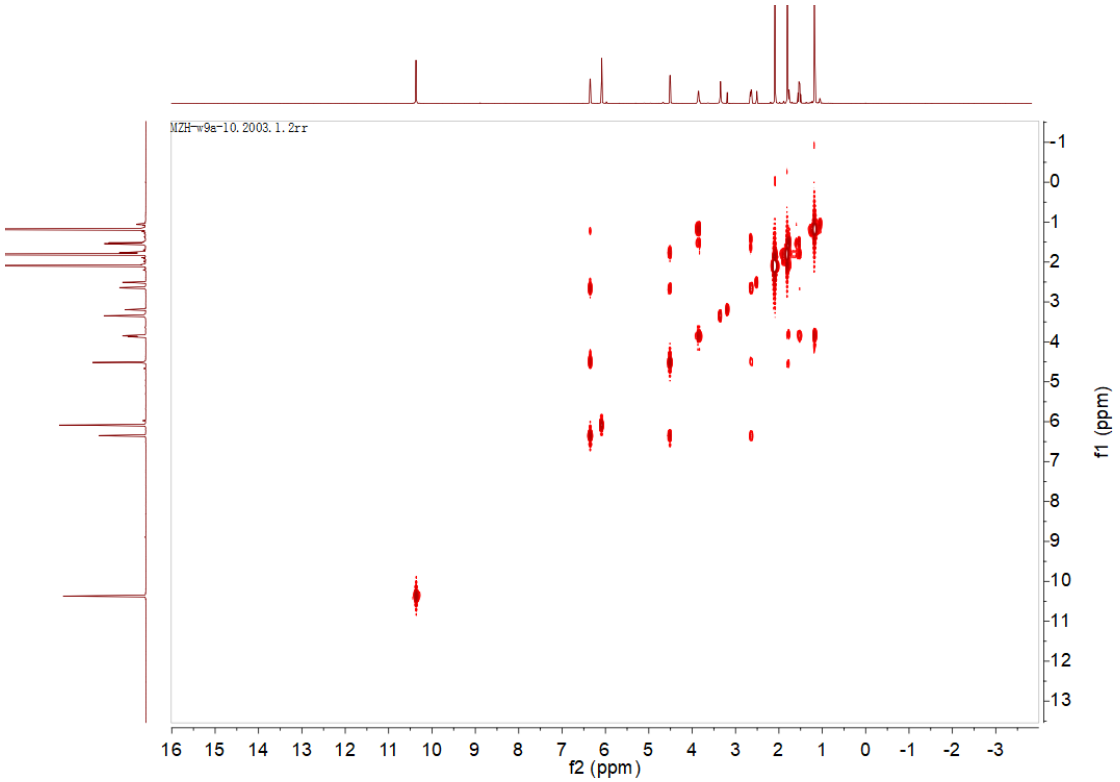


Figure S19. $^{1}$H-$^{1}$H COSY spectrum of 3

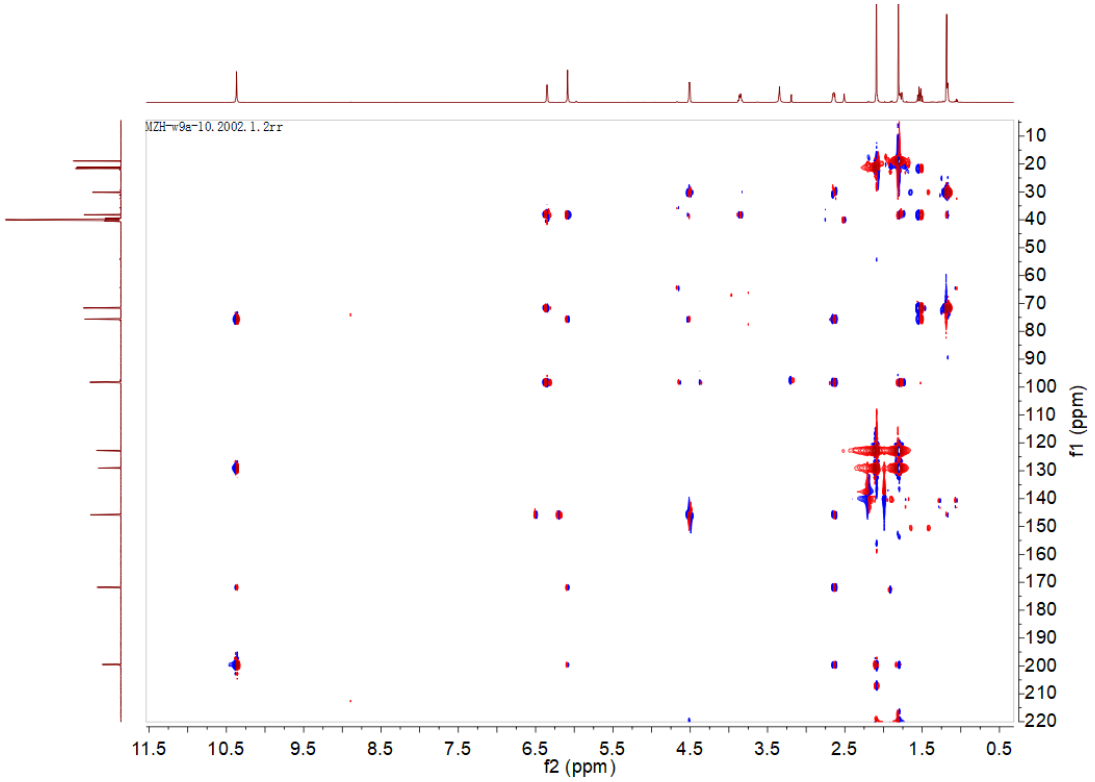


Figure S20. HMBC spectrum of 3

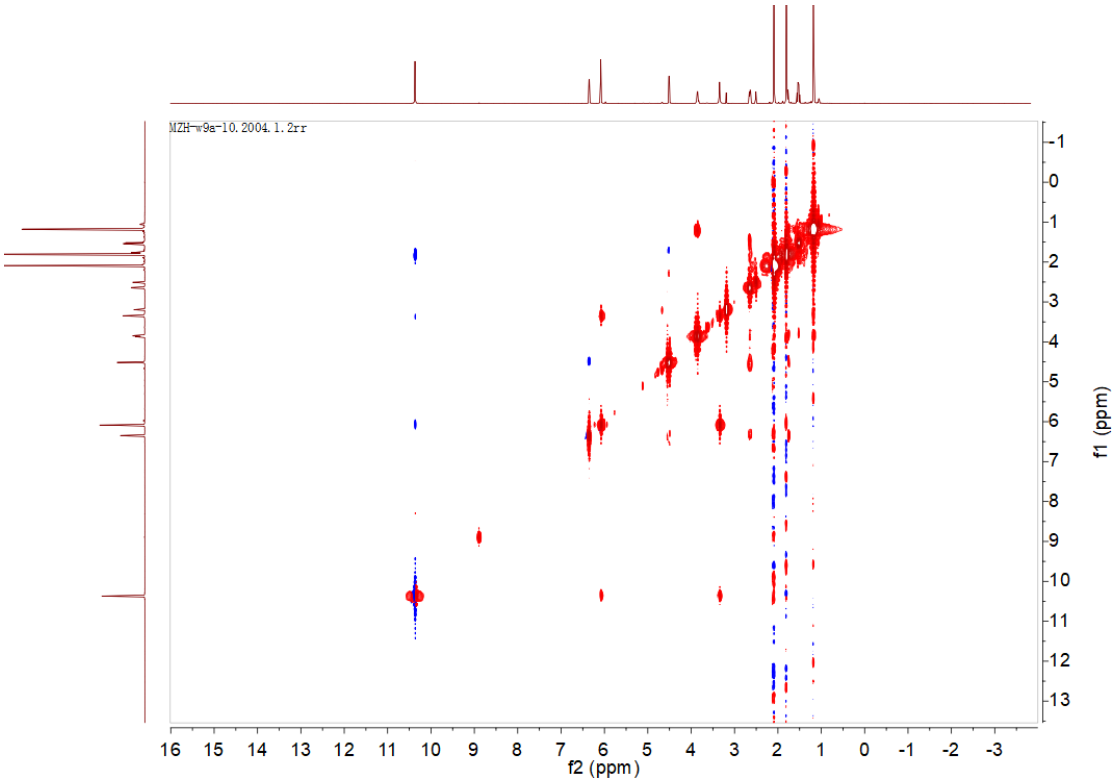


**Figure S21**. NOESY spectrum of **3**

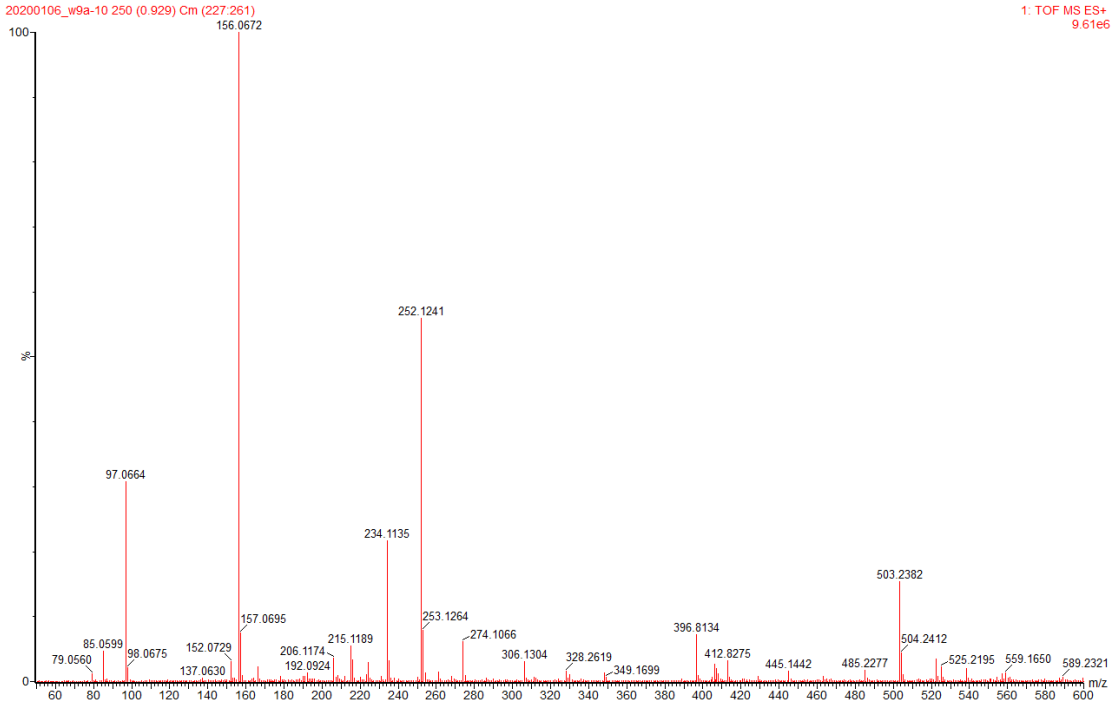


**Figure S22.** HR-ESI-MS spectrum of **3**

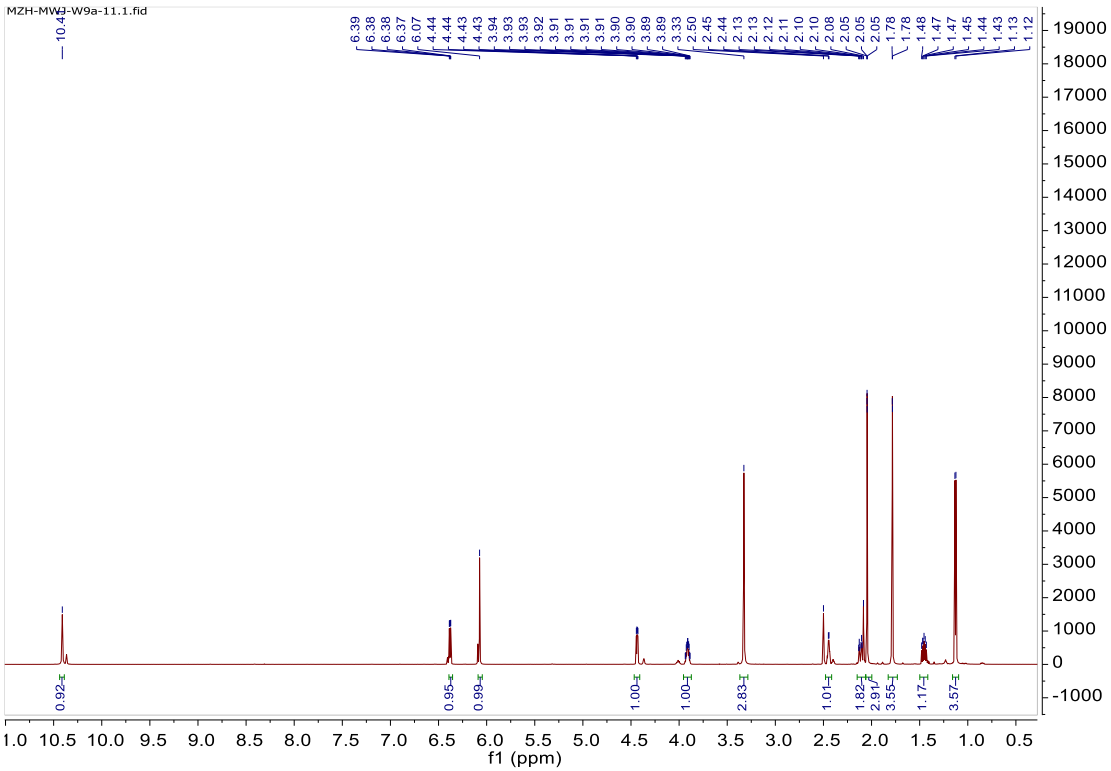


**Figure S23**. $^{1}$H NMR spectrum of **4**

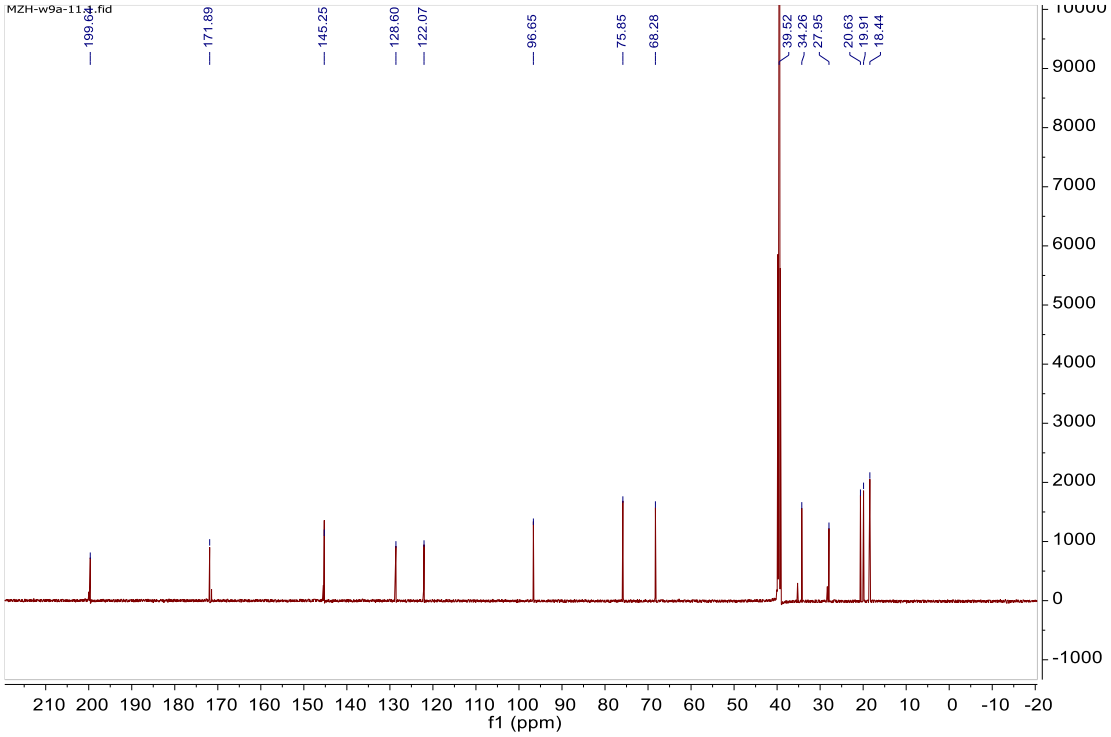


**Figure S24.** $^{13}$C NMR spectrum of **4**

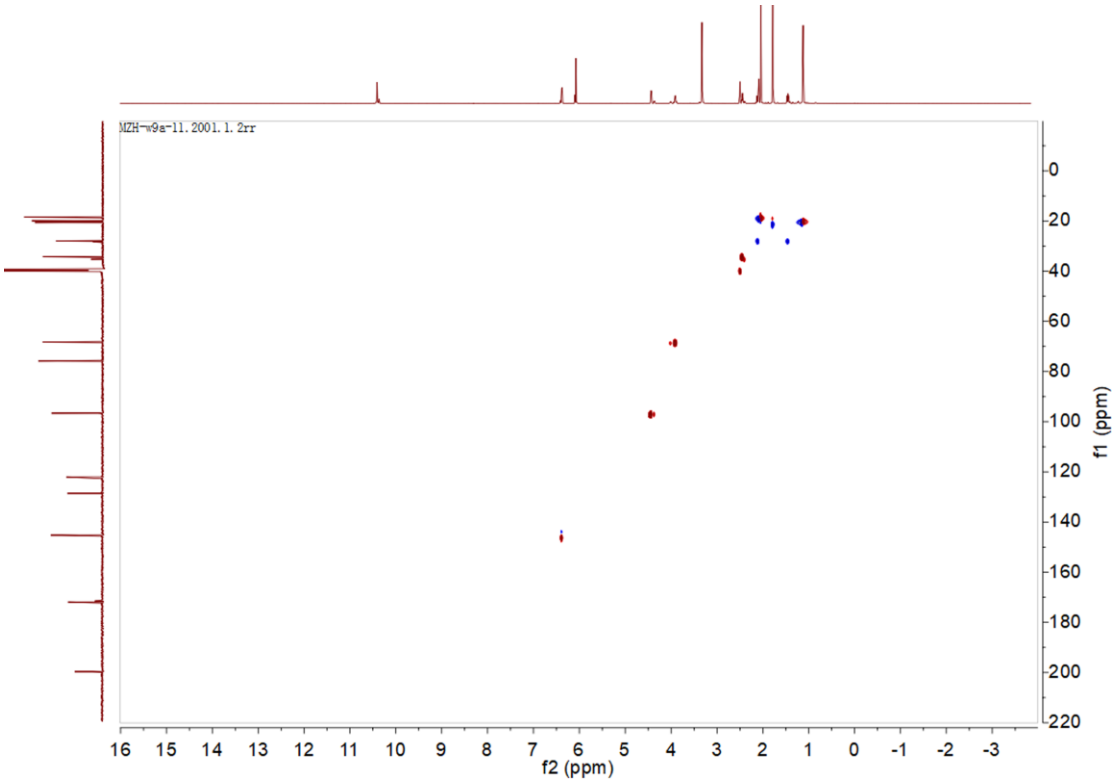


Figure S25. HSQC spectrum of **4**

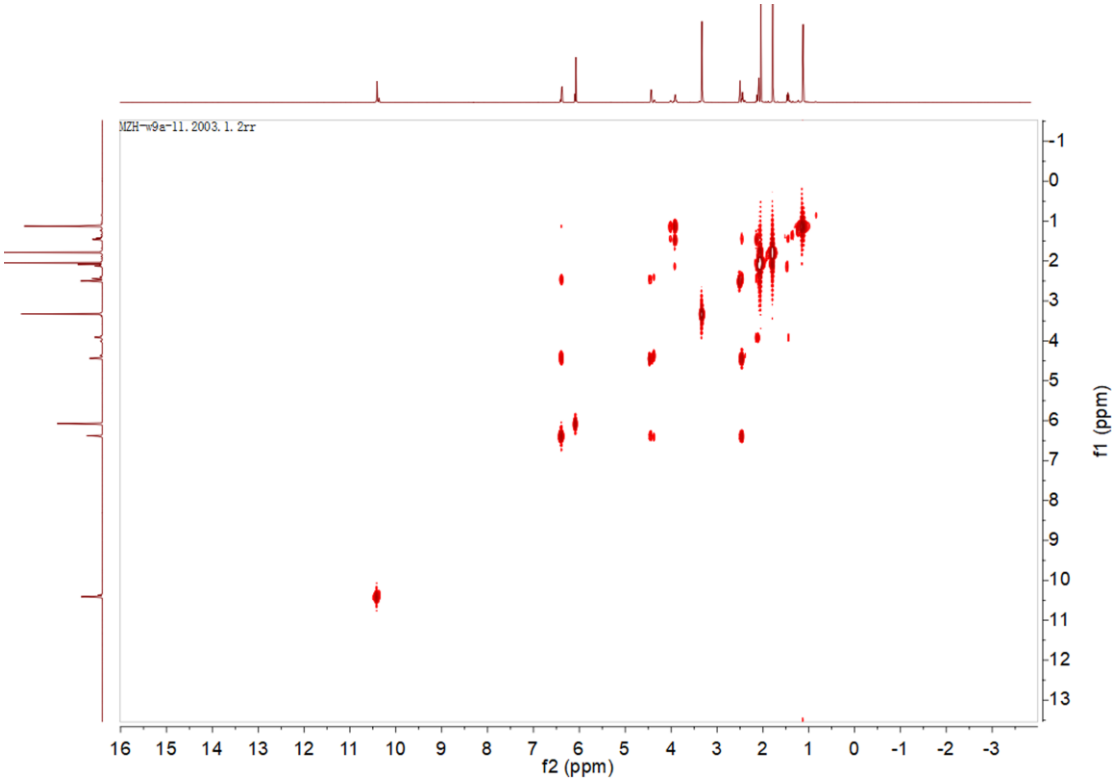


Figure S26. $^{1}$H-$^{1}$H COSY spectrum of **4**

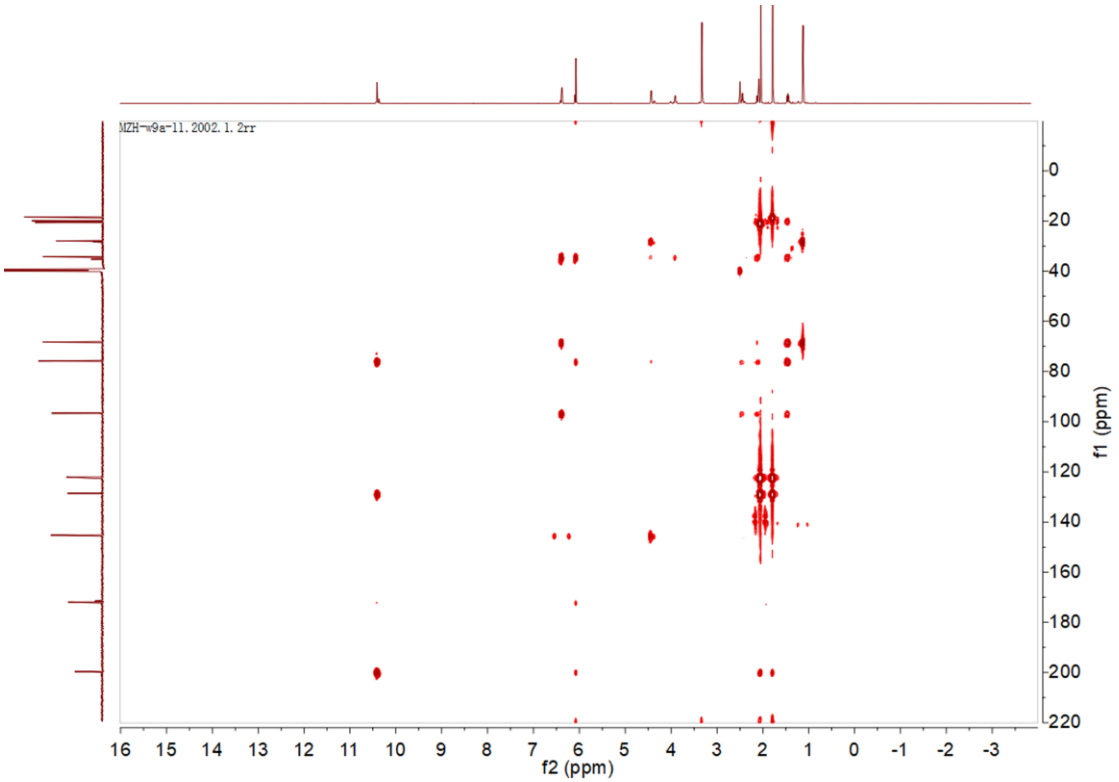


Figure S27. HMBC spectrum of **4**

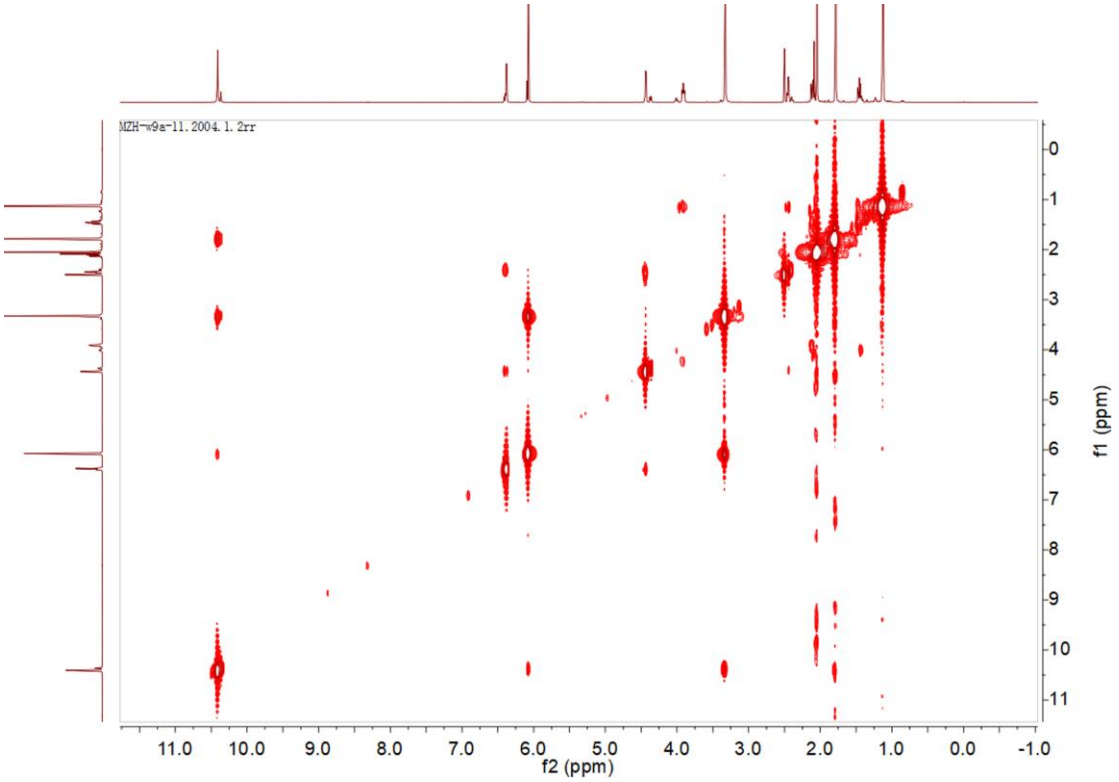


Figure S28. NOESY spectrum of **4**

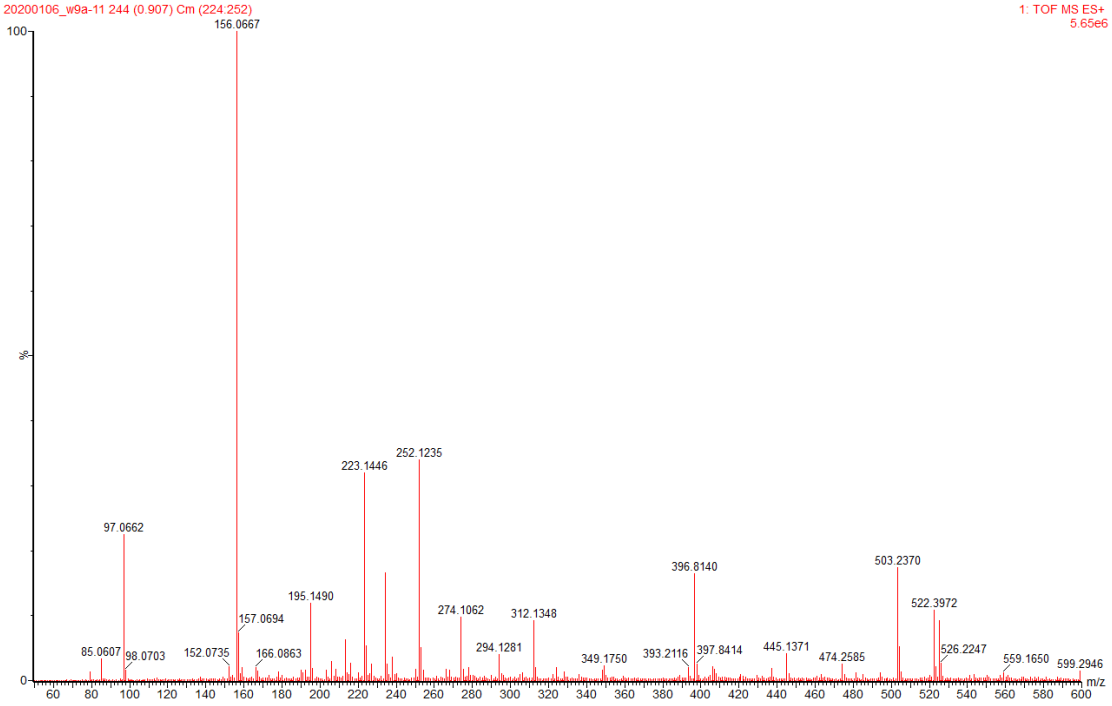


**Figure S29**. HR-ESI-MS spectrum of **4**

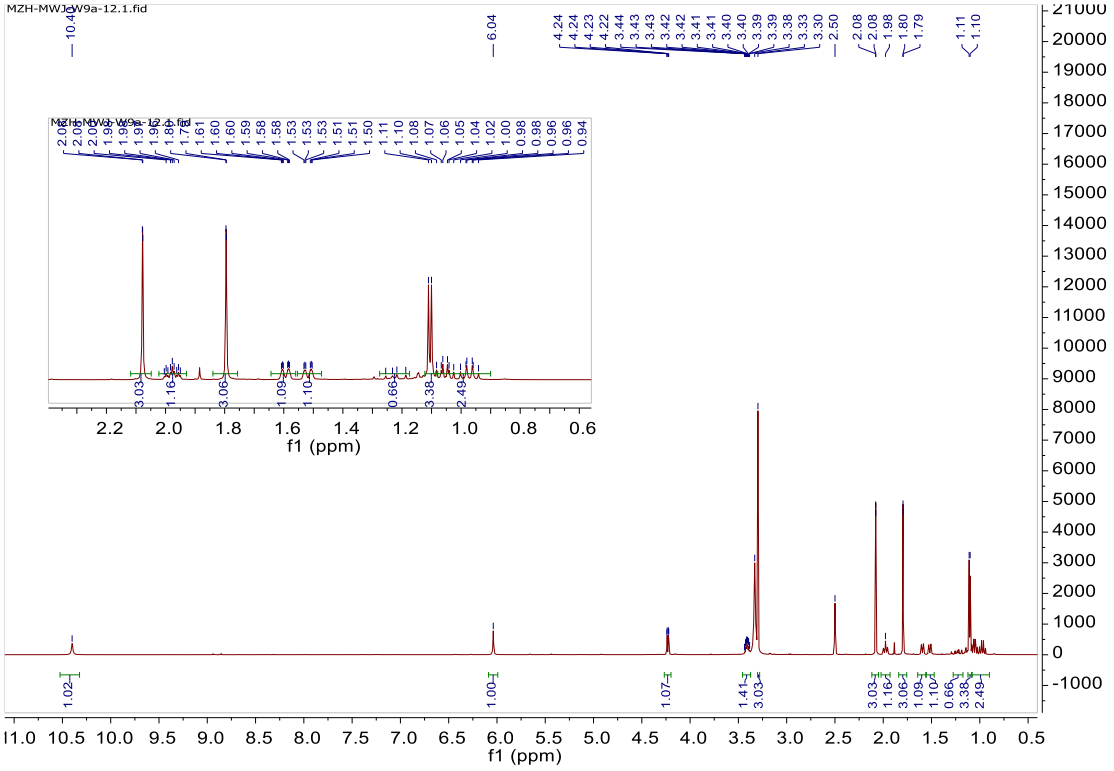


**Figure S30**. $^{1}$H NMR spectrum of **5**

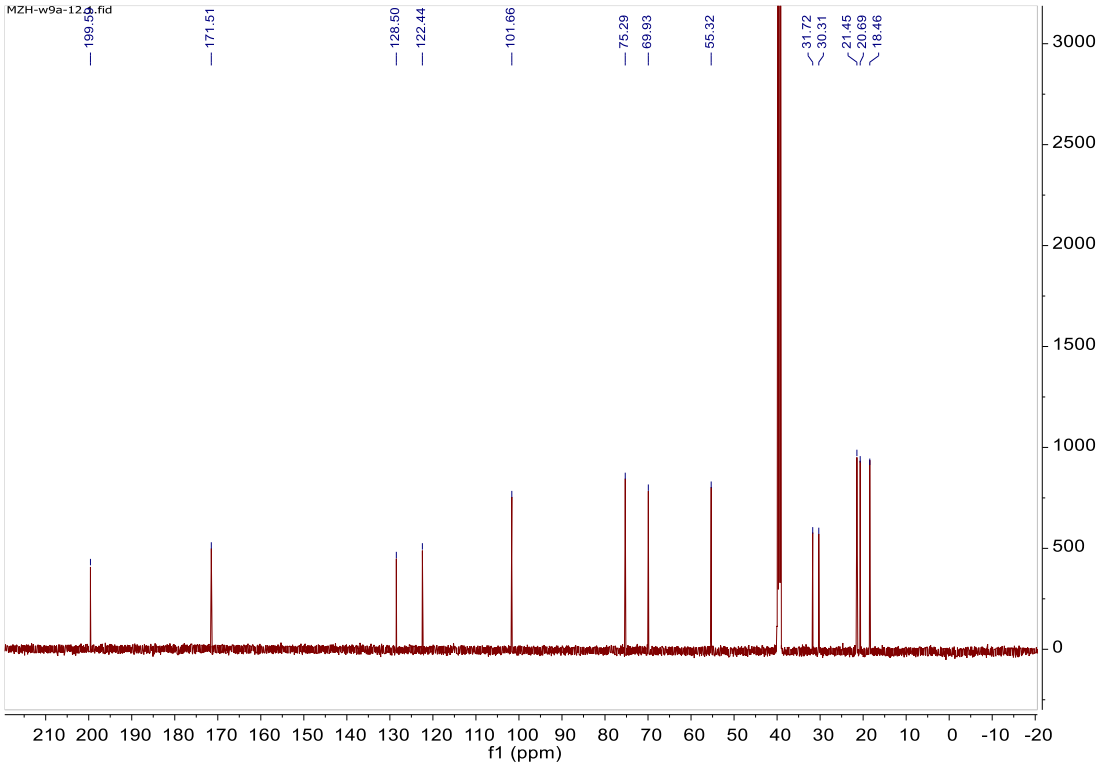


Figure S31. $^{13}$C NMR spectrum of **5**

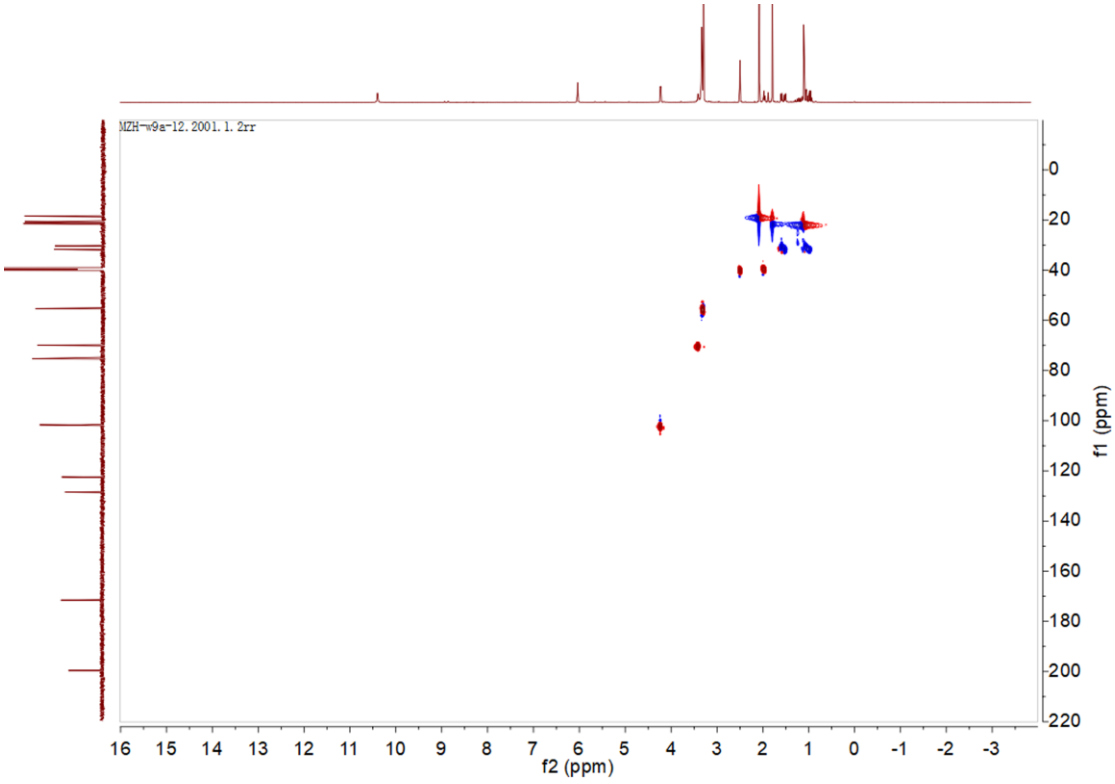


Figure S32. HSQC spectrum of **5**

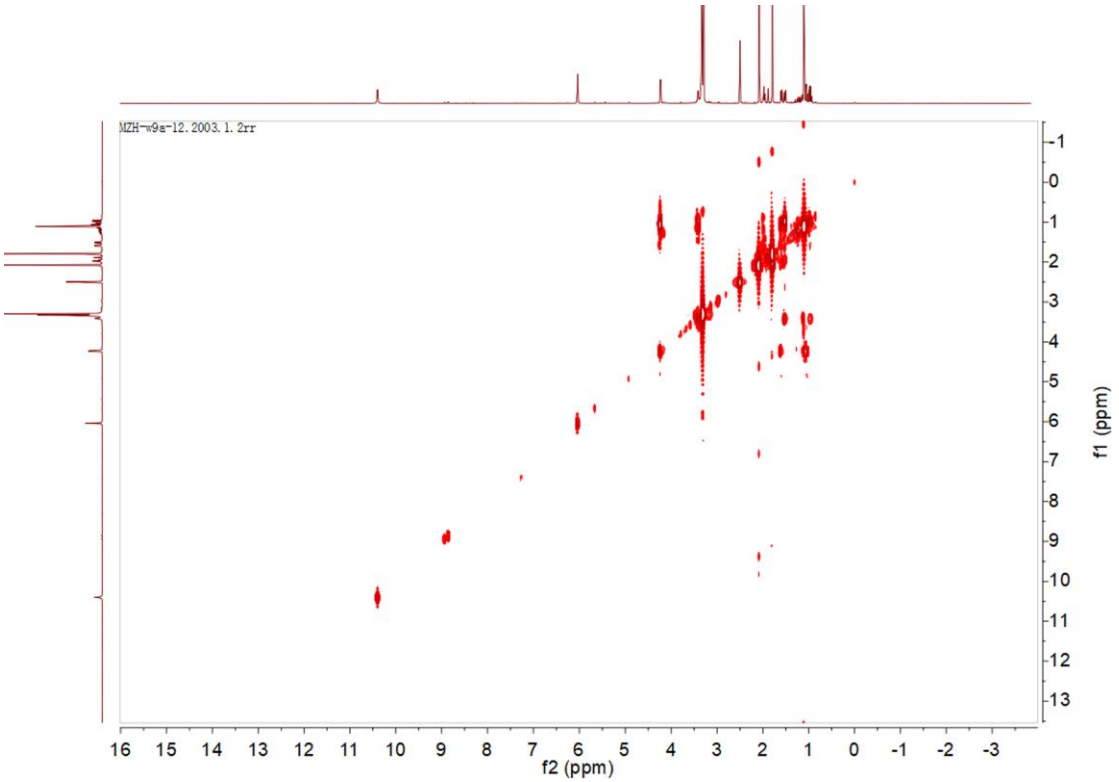


Figure S33. $^{1}H$-$^{1}H$ COSY spectrum of 5

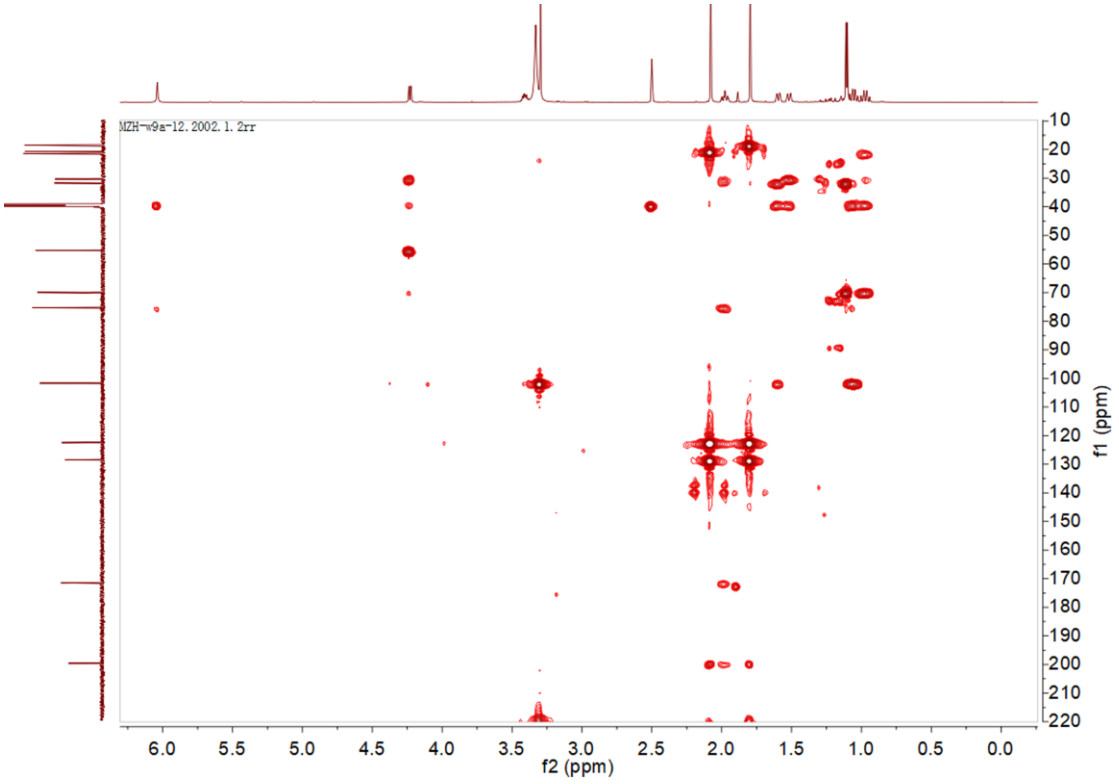


Figure S34. HMBC spectrum of 5

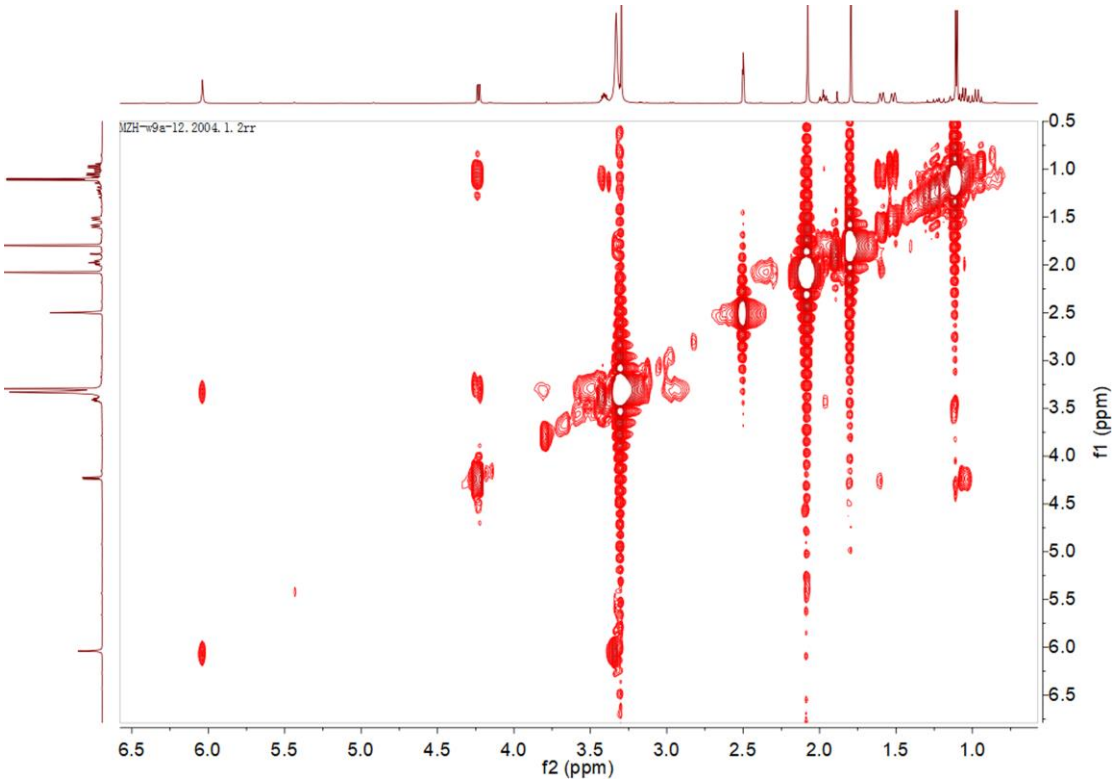


Figure S35. NOESY spectrum of 5

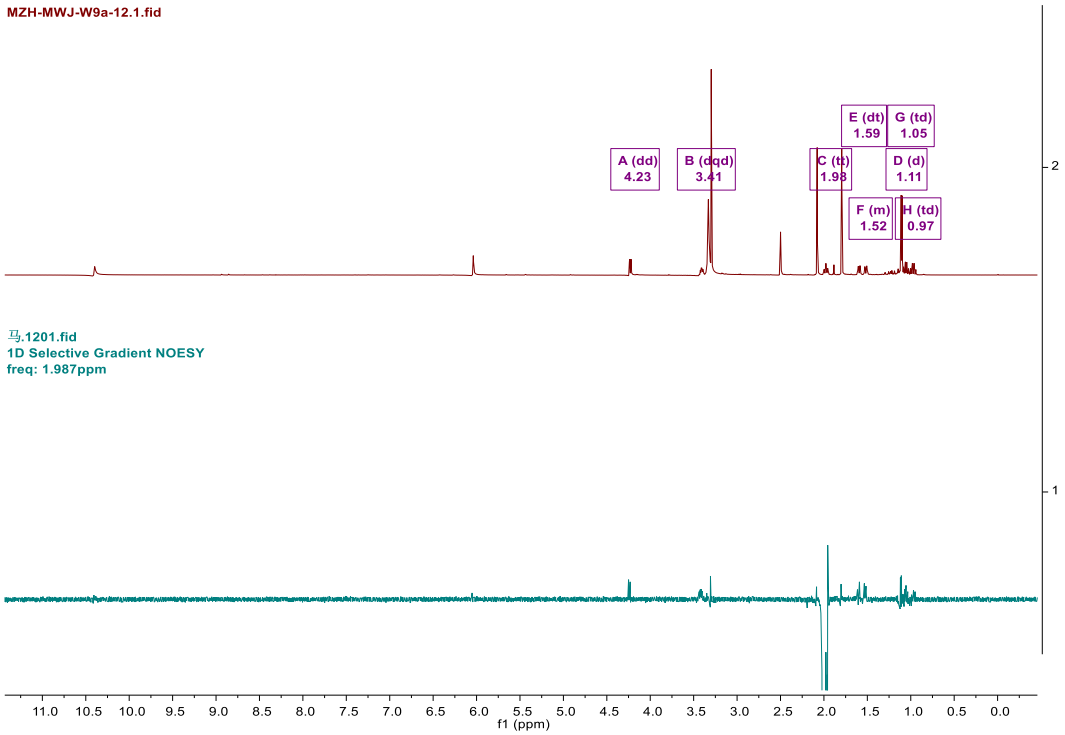


Figure S36. 1D selective NOESY spectrum of 5 (1.98ppm)

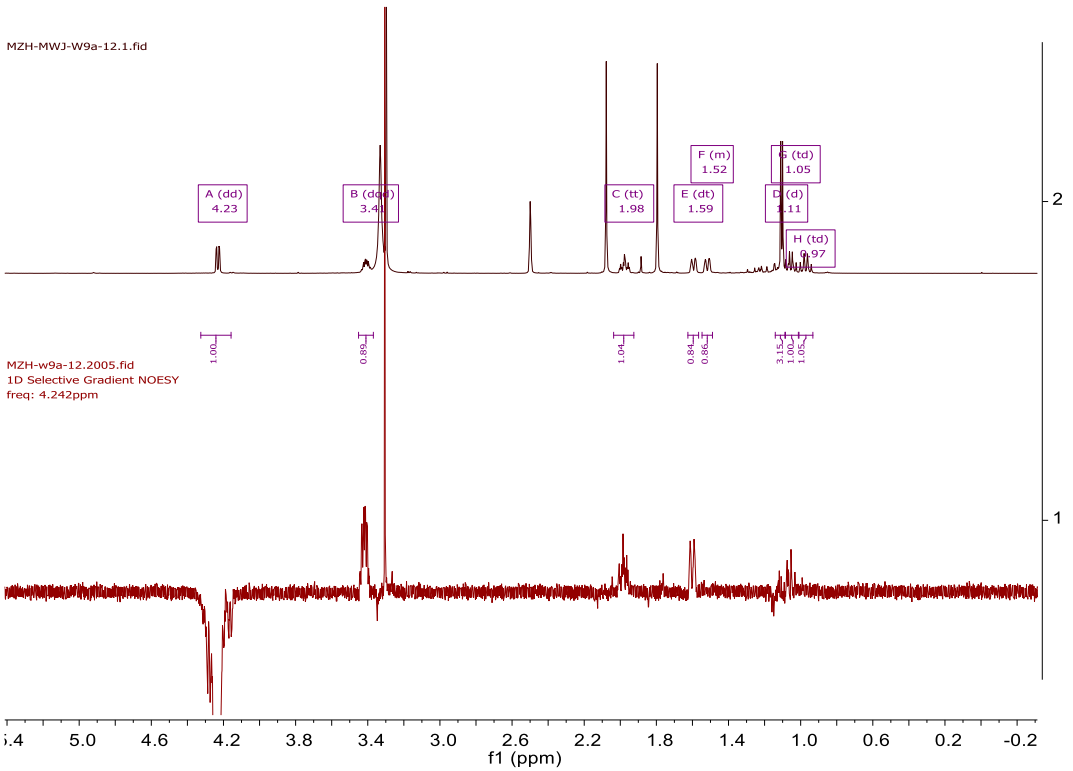


Figure S37. 1D selective NOESY spectrum of **5** (4.24ppm)

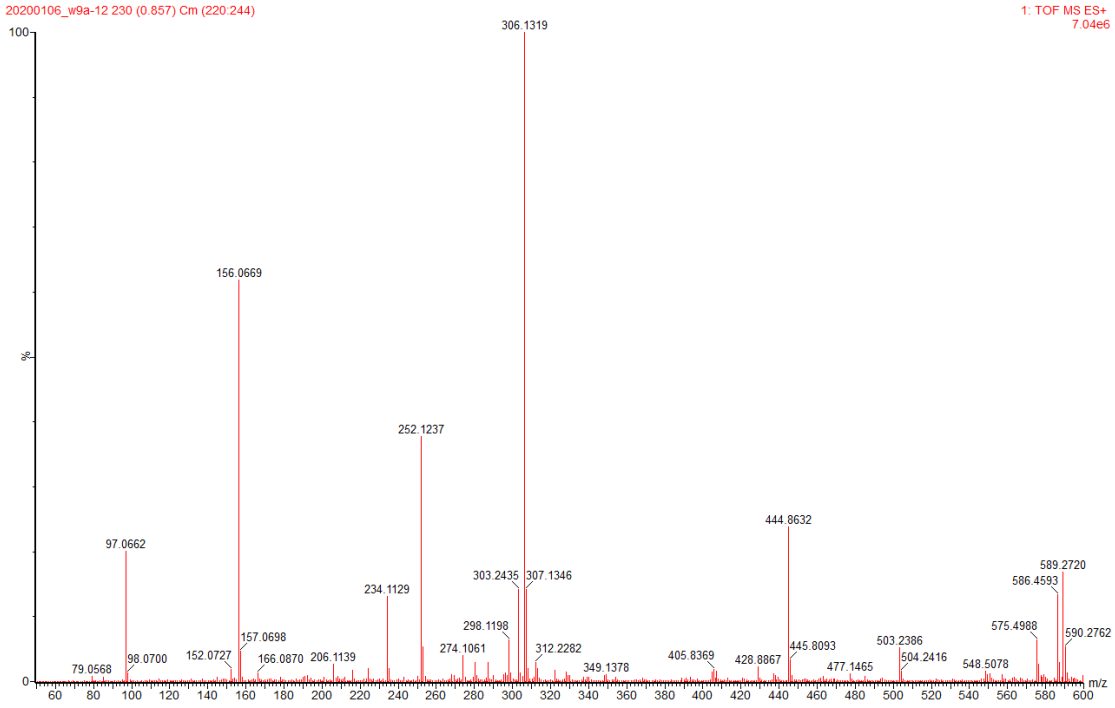


Figure S38. HR-ESI-MS spectrum of **5**

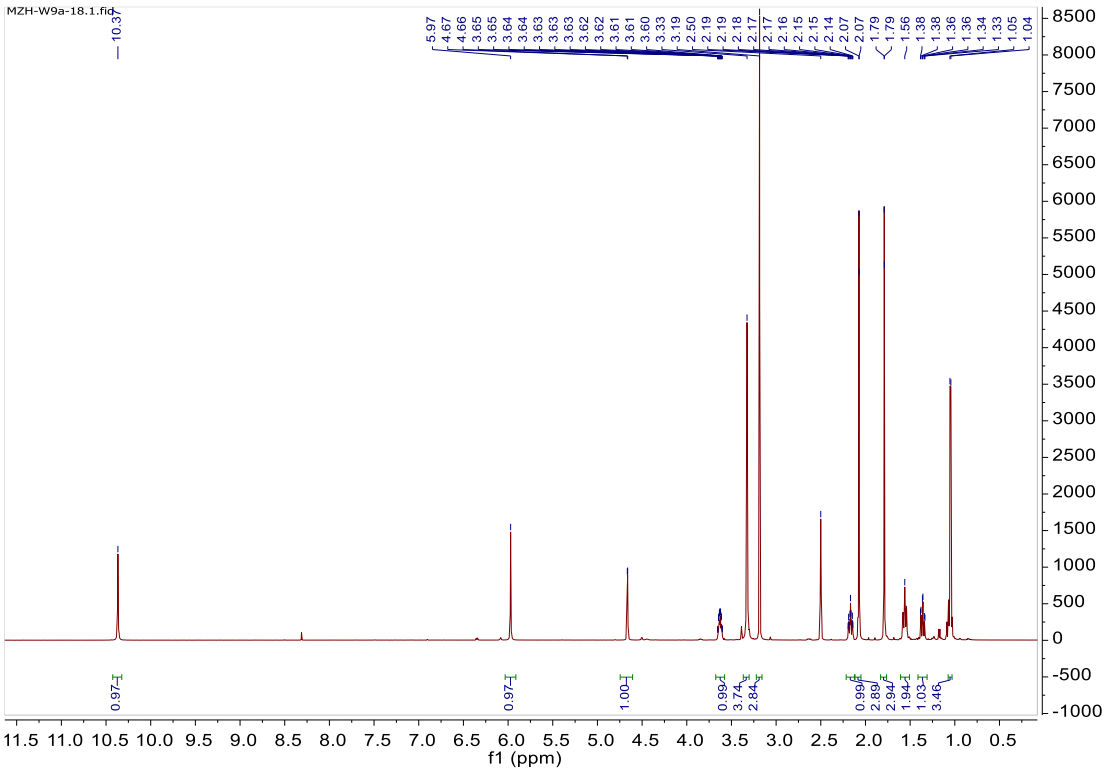


Figure S39. $^{1}$H NMR spectrum of **6**

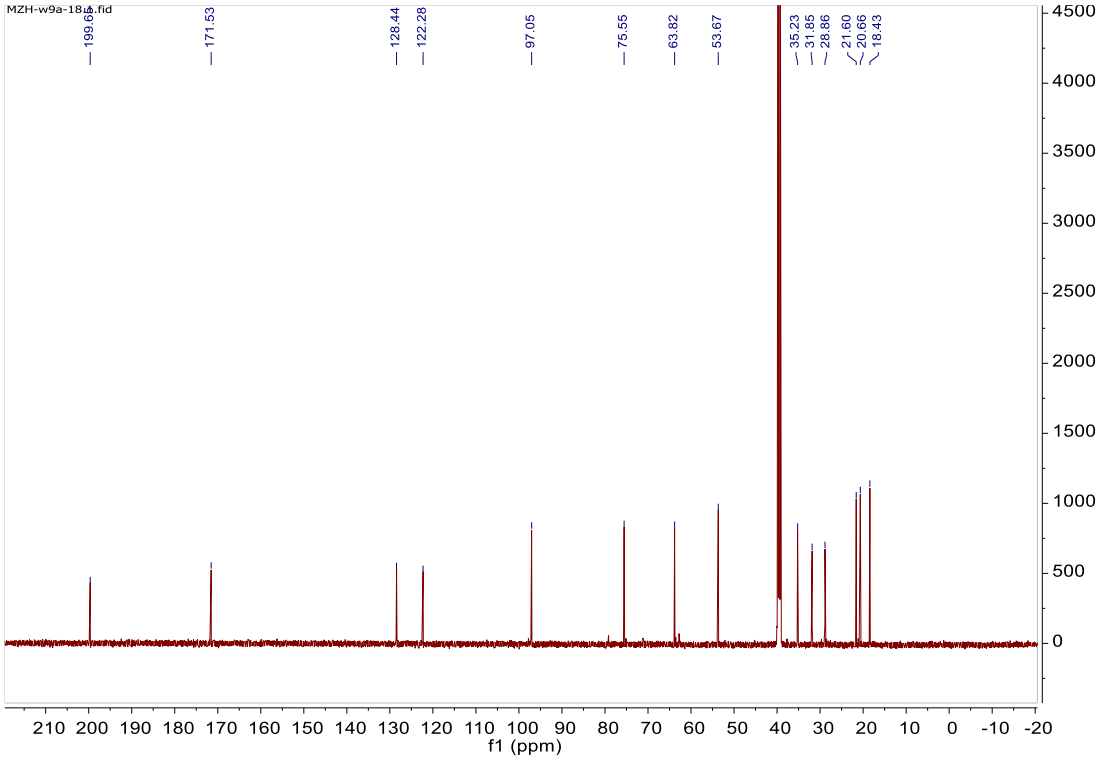


Figure S40. $^{13}$C NMR spectrum of **6**

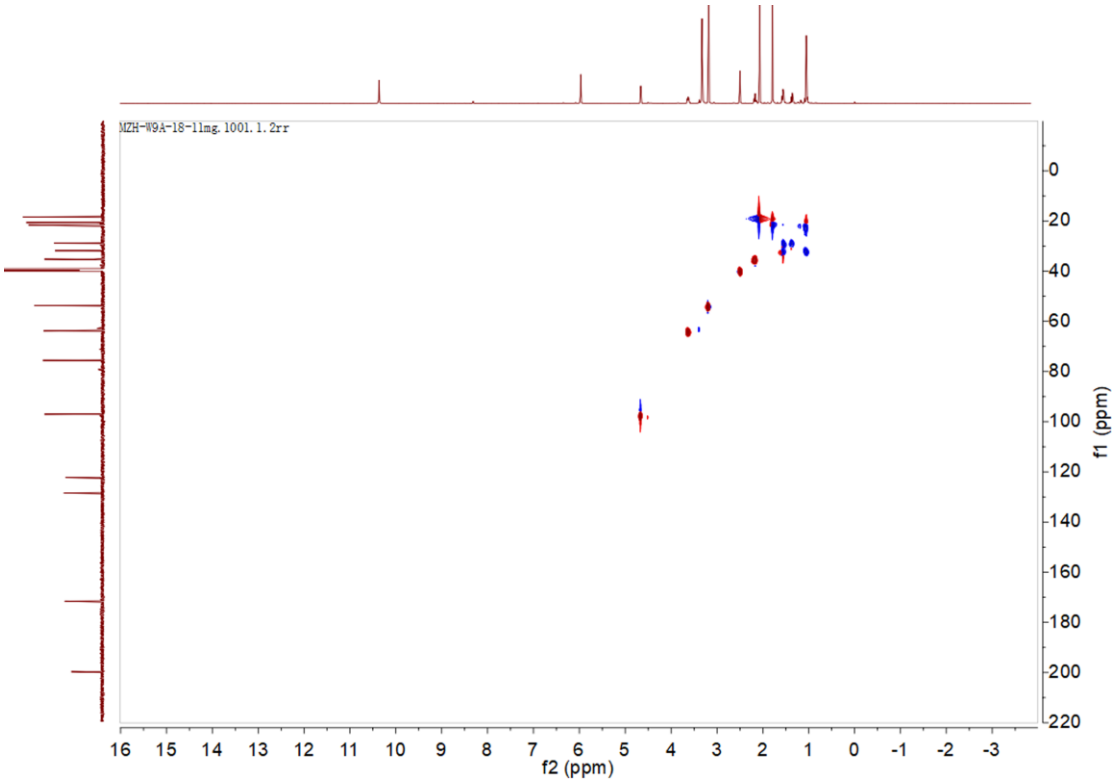


Figure S41. HSQC spectrum of 6

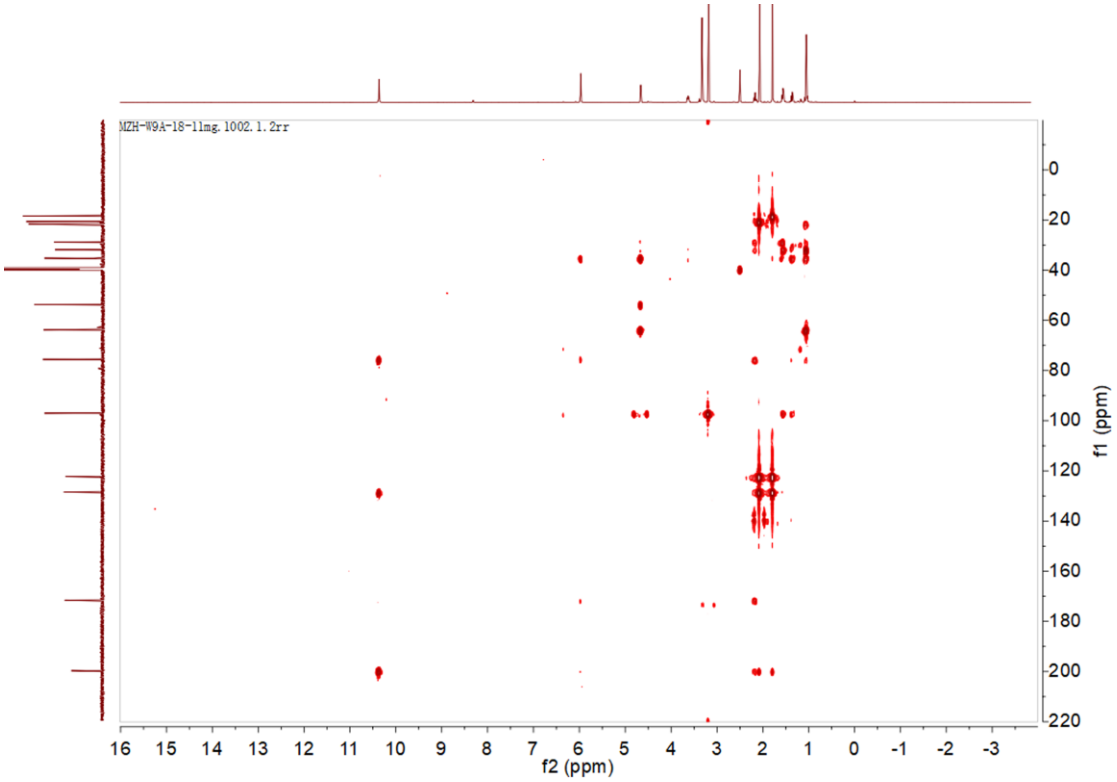


Figure S42. $^{1}$H-$^{1}$H COSY spectrum of 6

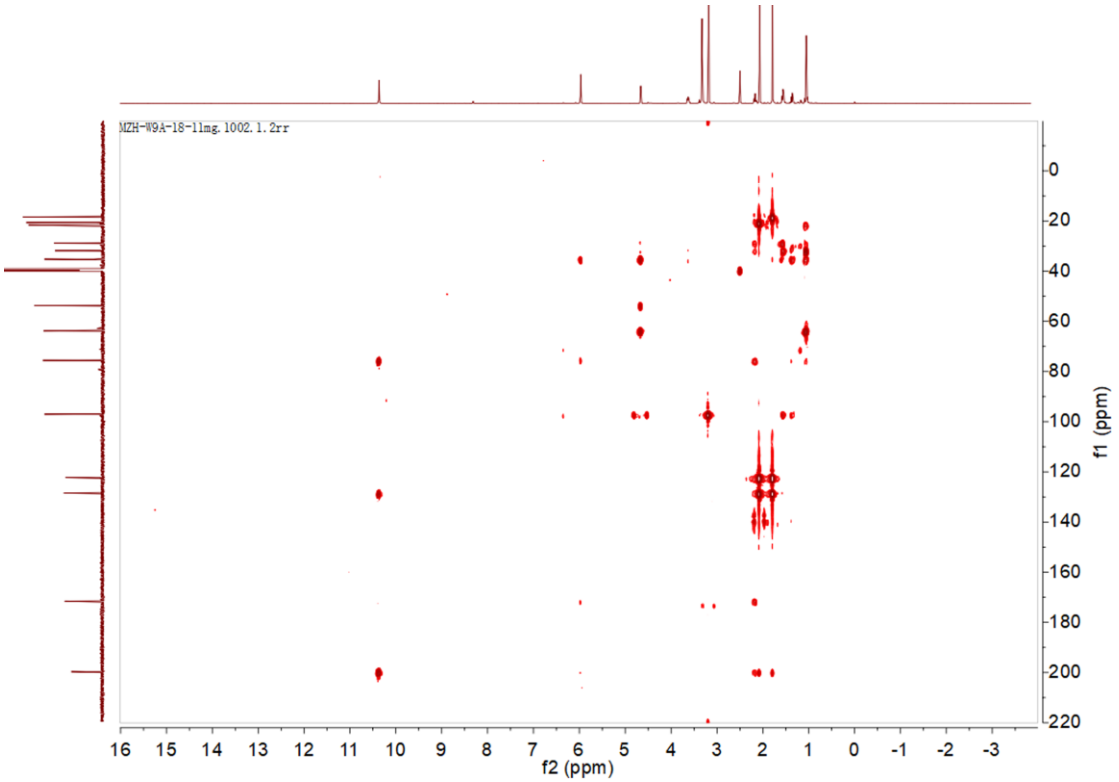


Figure S43. HMBC spectrum of 6

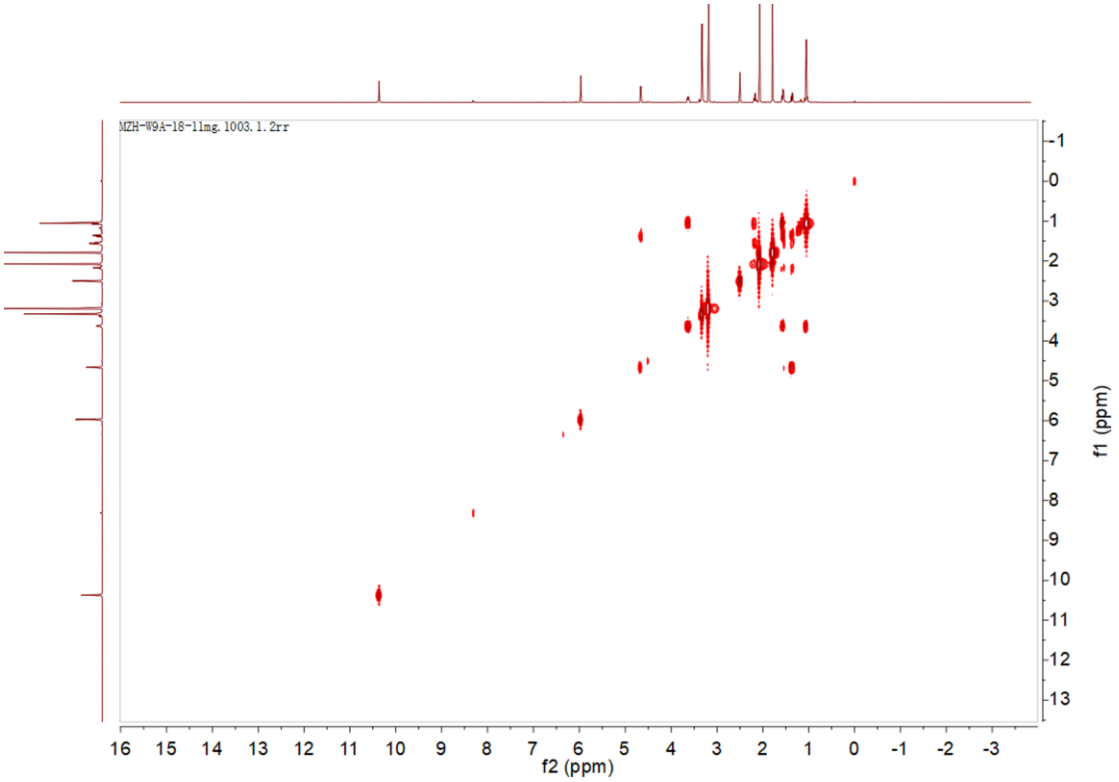


Figure S44. NOESY spectrum of 6

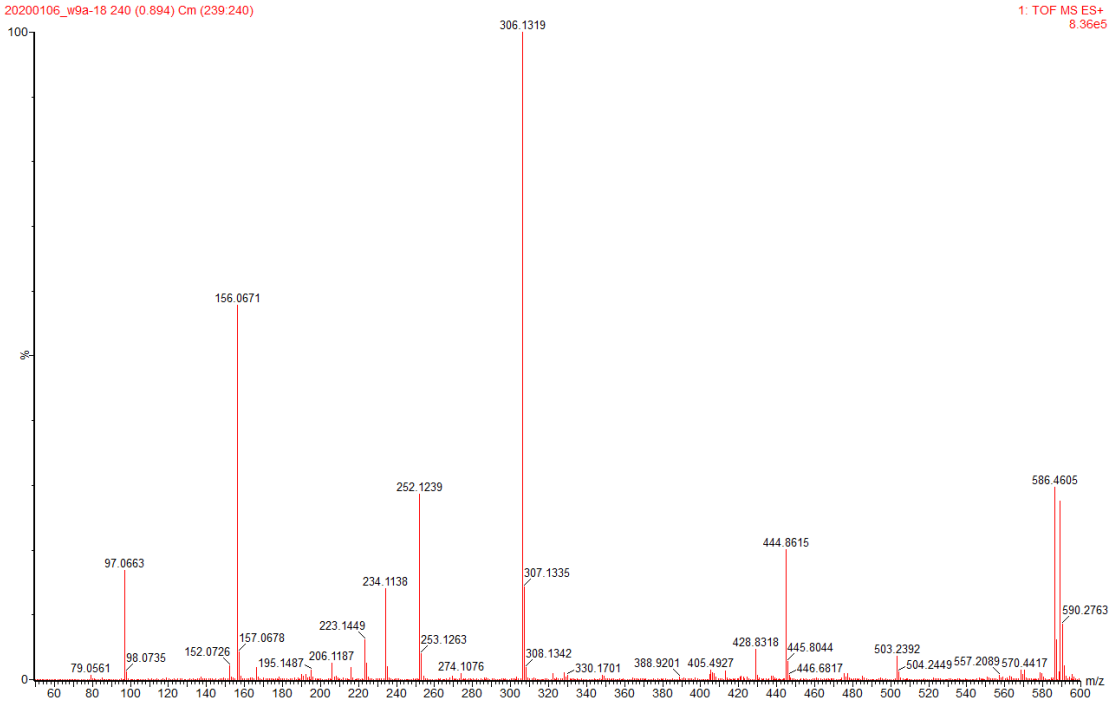


Figure S45. HR-ESI-MS spectrum of **6**

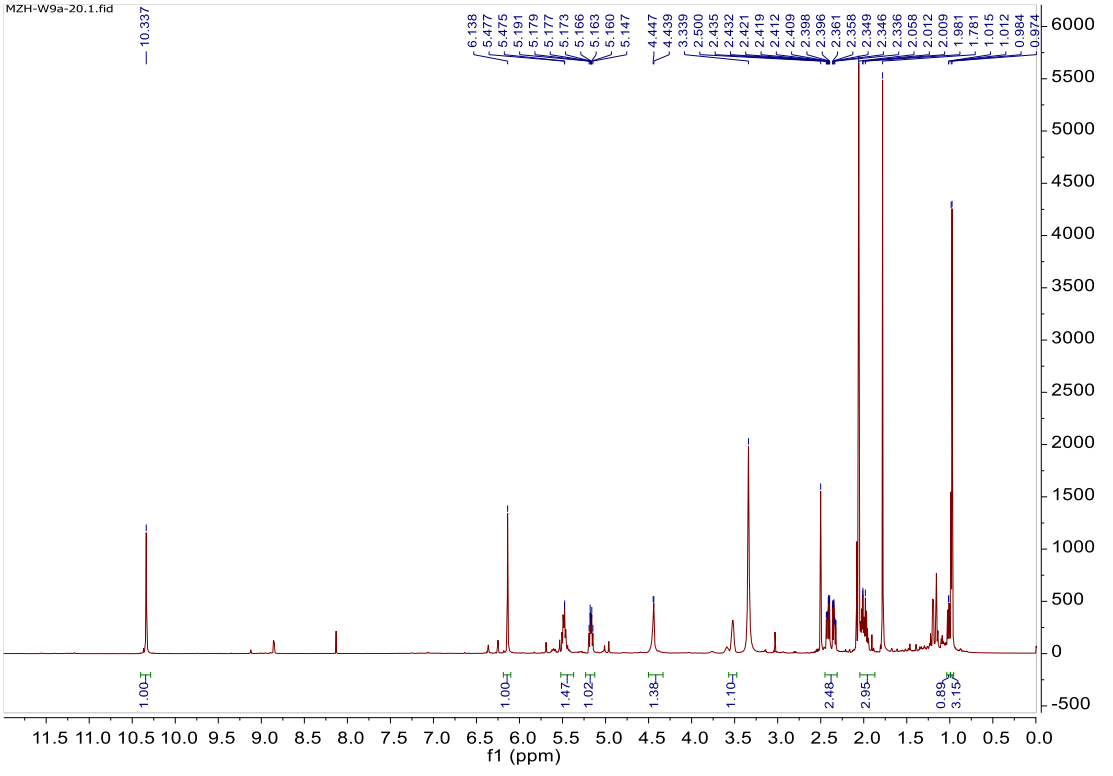


Figure S46. $^{1}$H NMR spectrum of **7**

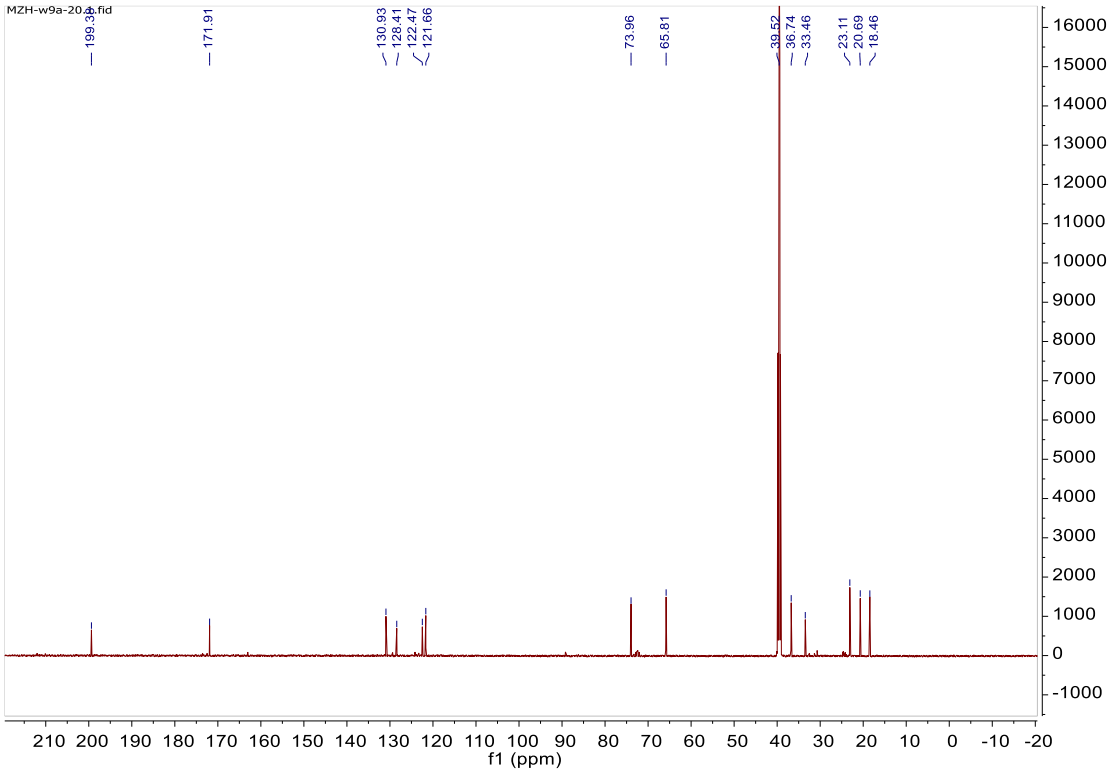


Figure S47. $^{13}C$ NMR spectrum of **7**

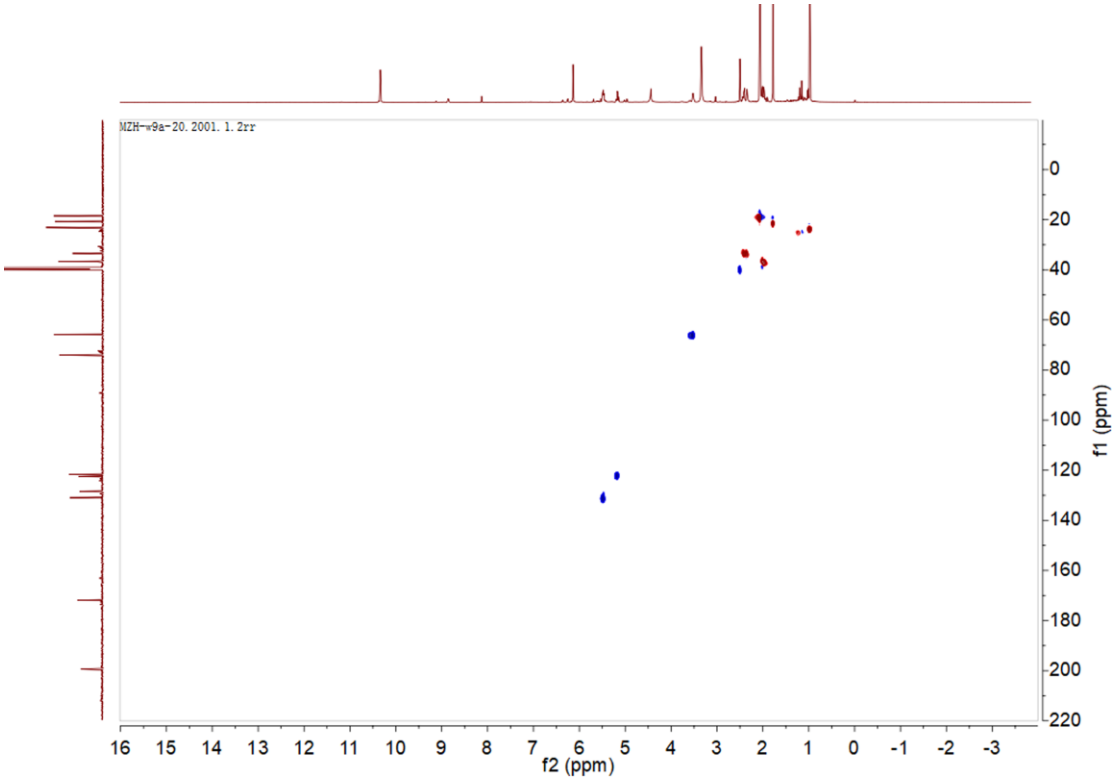


Figure S48. HSQC spectrum of **7**

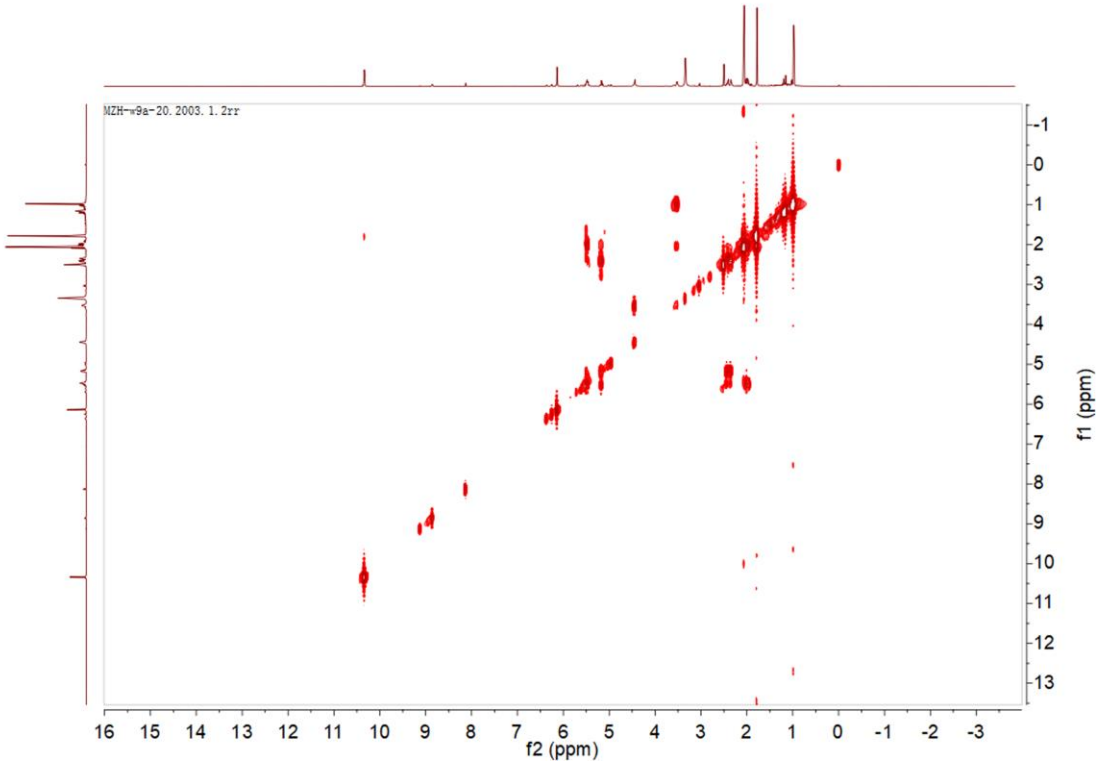


Figure S49. $^{1}$H-1H COSY spectrum of **7**

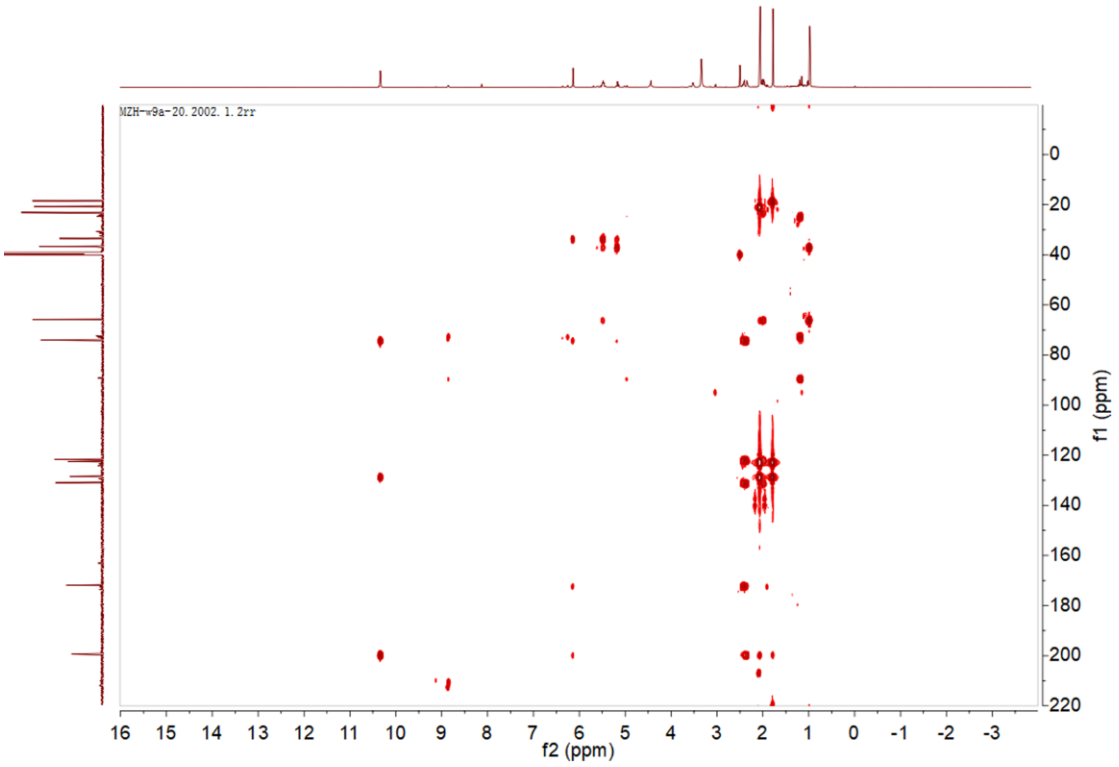


Figure S50. HMBC spectrum of **7**

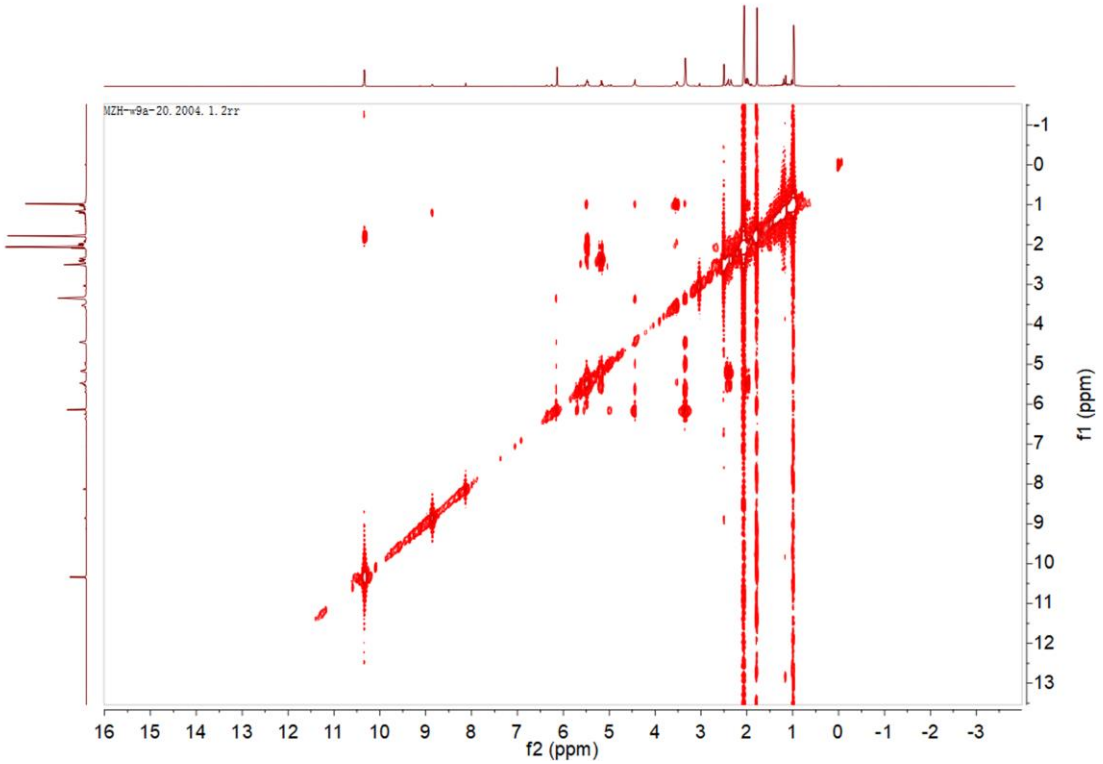


Figure S51. NOESY spectrum of 7

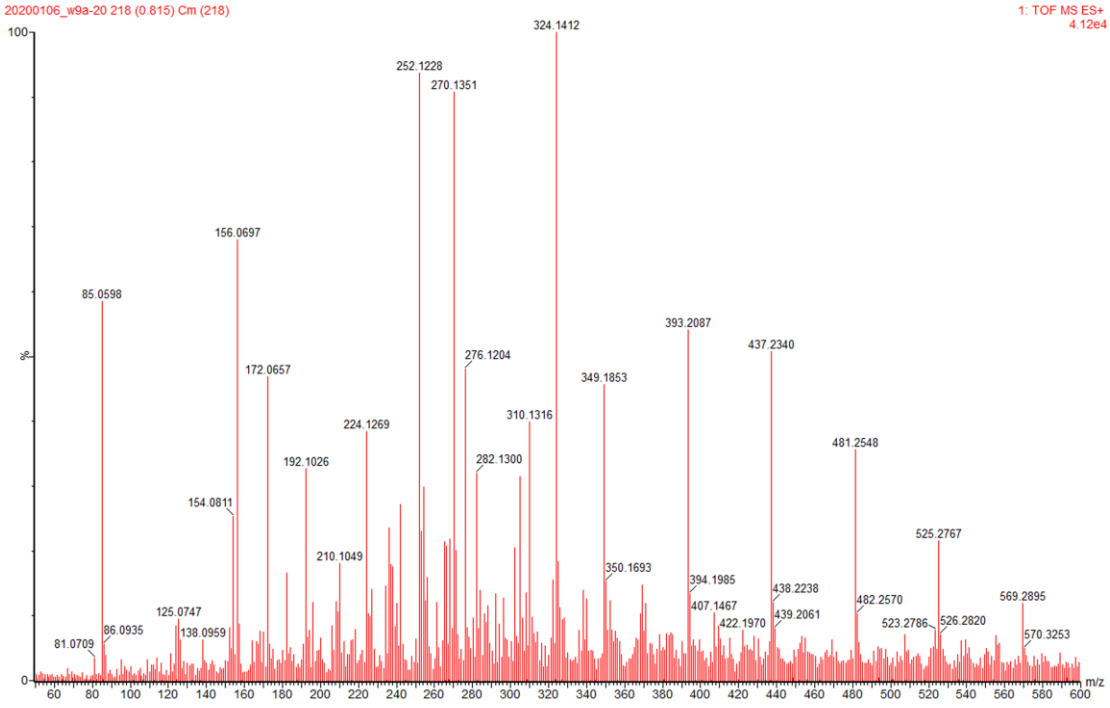


Figure S52. HR-ESI-MS spectrum of 7

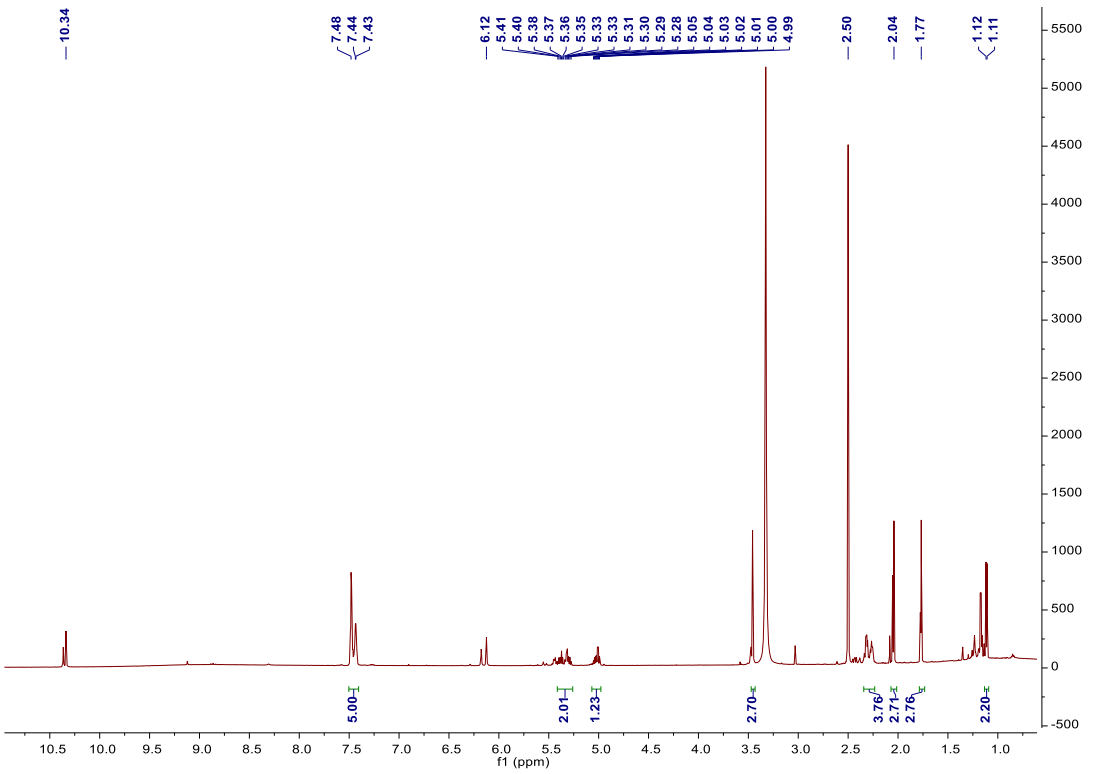


**Figure S53**. $^{1}$H NMR spectrum of (*R*)-MTPA ester of **7**

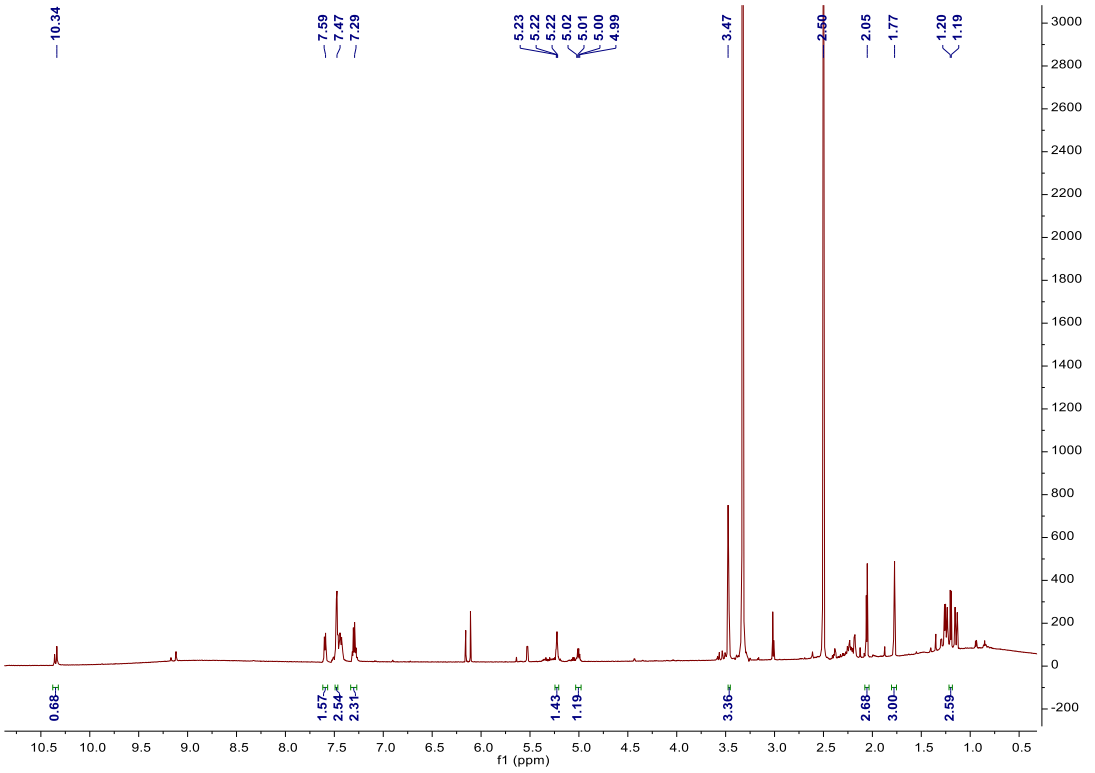


**Figure S54**. $^{1}$H NMR spectrum of (*S*)-MTPA ester of **7**

**Table S2**. Relative free energies[a] and equilibrium populations[b] of conformers for (3*S*, 6*S*, 10*R*)-**2a**[c]

| Conformer | $\Delta G$ | P (%) |
|---|---|---|
| **2a1** | 0.00 | 42.97 |
| **2a2** | 0.52 | 17.90 |
| **2a3** | 0.78 | 11.50 |
| **2a4** | 0.98 | 8.26 |
| **2a5** | 1.11 | 6.62 |
| **2a6** | 1.11 | 6.56 |

[a] B3LYP/6-31G(d), in kcal/mol. [b] From $\Delta G$ values at 298.15 K. [c] in MeOH, no imaginary frequency.

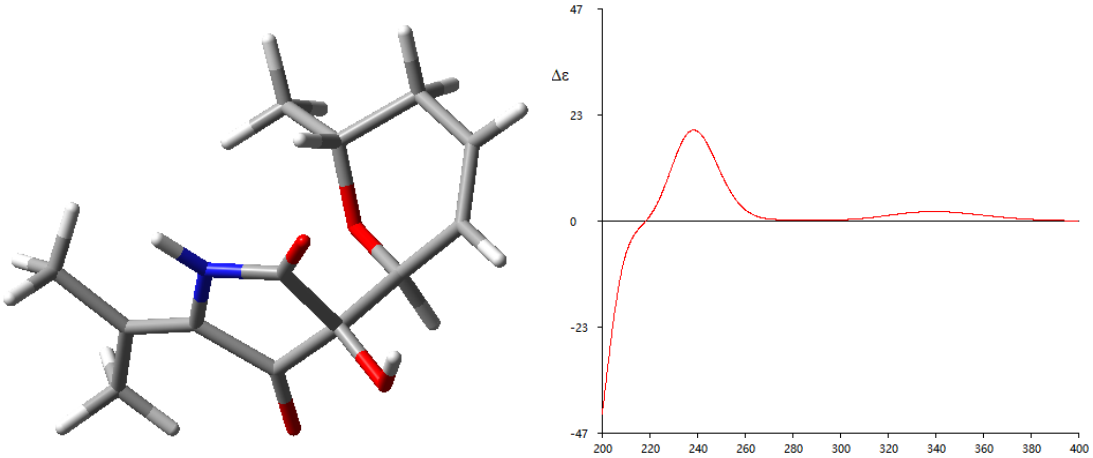


(3*S*, 6*S*, 10*R*)-2**a1**

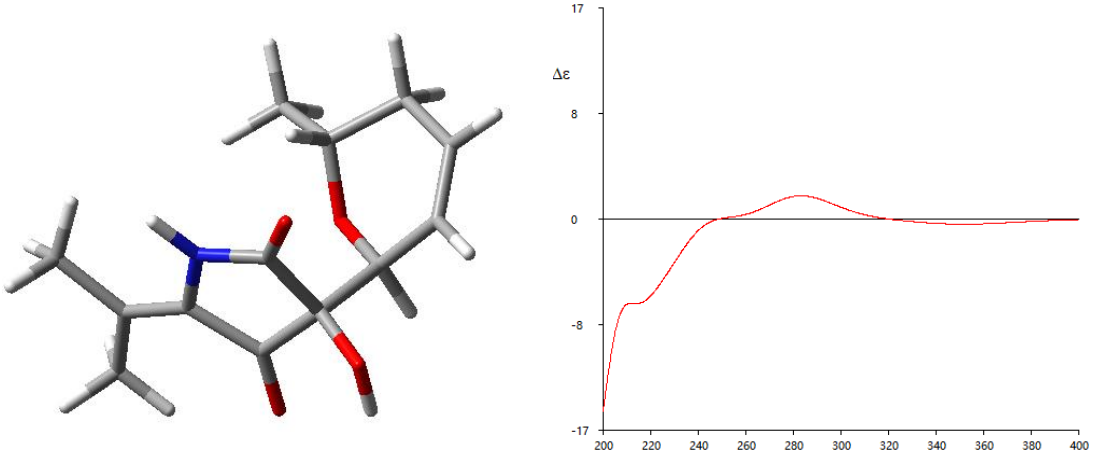


(3*S*, 6*S*, 10*R*)-2**a2**

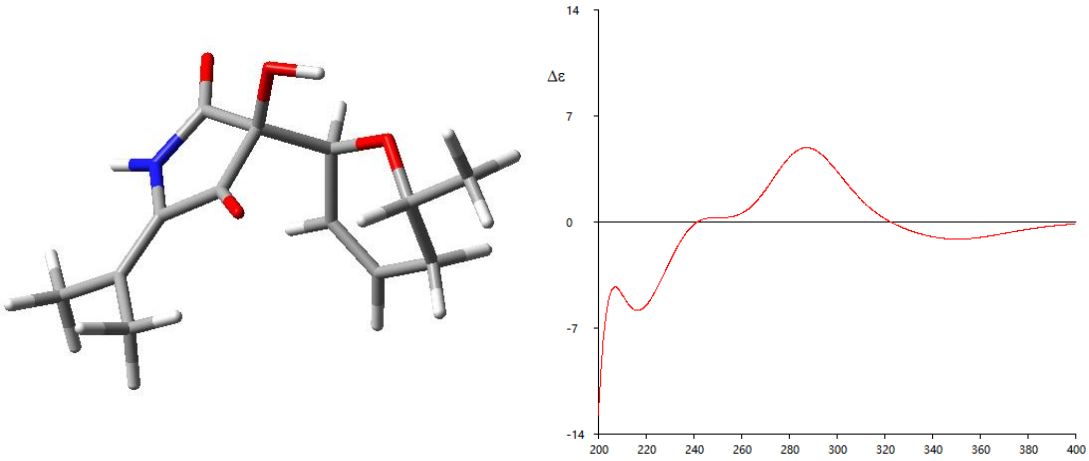


(3*S*, 6*S*, 10*R*)-2**a3**

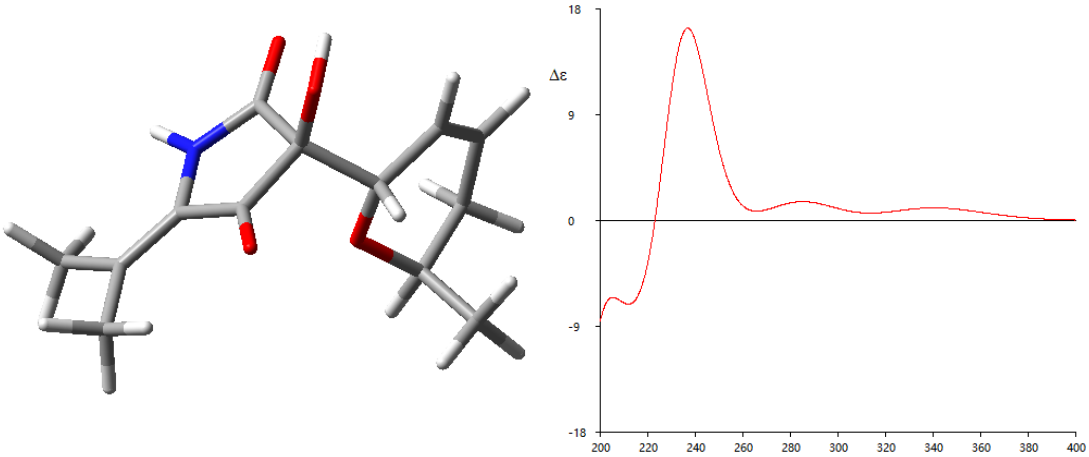


(3*S*, 6*S*, 10*R*)-2**a4**

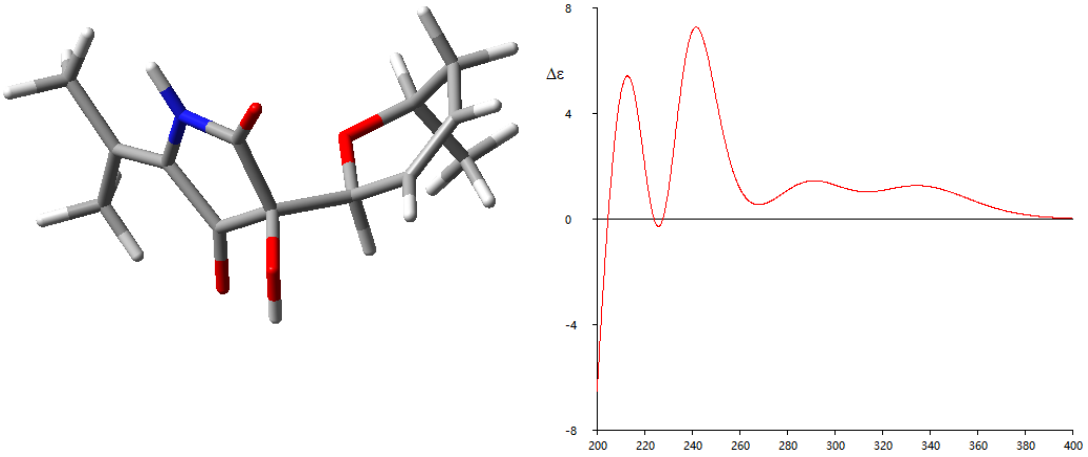


(3*S*, 6*S*, 10*R*)-2**a5**

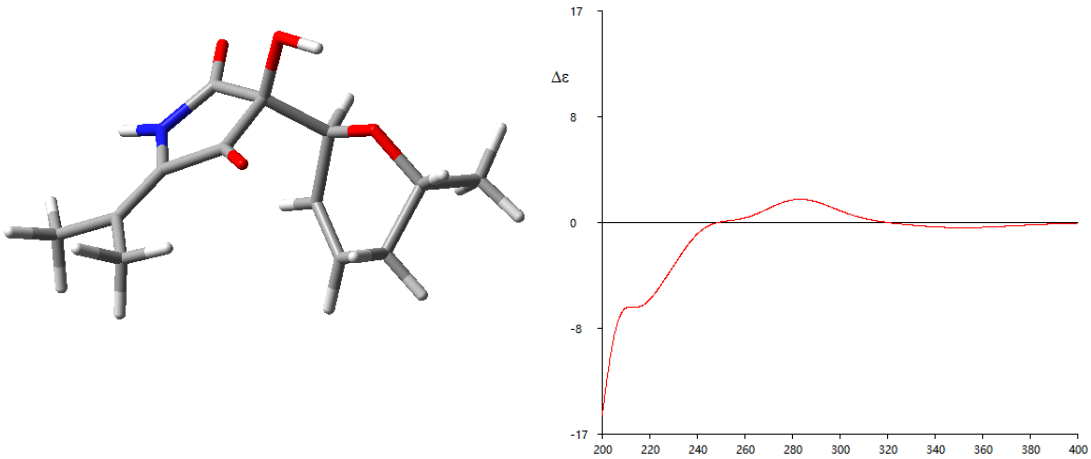


(3*S*, 6*S*, 10*R*)-2**a6**

**Figure S55**. The optimized structures (left) and the calculated CD spectra of conformers (3*S*, 6*S*, 10*R*)-**2a** in MeOH at M06-2X/def2TZVP level (right). σ=0.30 eV.

**Table S3**. Relative free energies[a] and equilibrium populations[b] of conformers for (3*S*, 6*R*, 10*S*)-**2b**[c]

| Conformer | Δ*G* | P (%) |
|---|---|---|
| **2b1** | 0.00 | 51.42 |
| **2b2** | 0.61 | 18.24 |
| **2b3** | 0.65 | 17.19 |
| **2b4** | 0.81 | 13.15 |

[a] B3LYP/6-31G(d), in kcal/mol. [b] From Δ*G* values at 298.15 K. [c] in MeOH, no imaginary frequency.

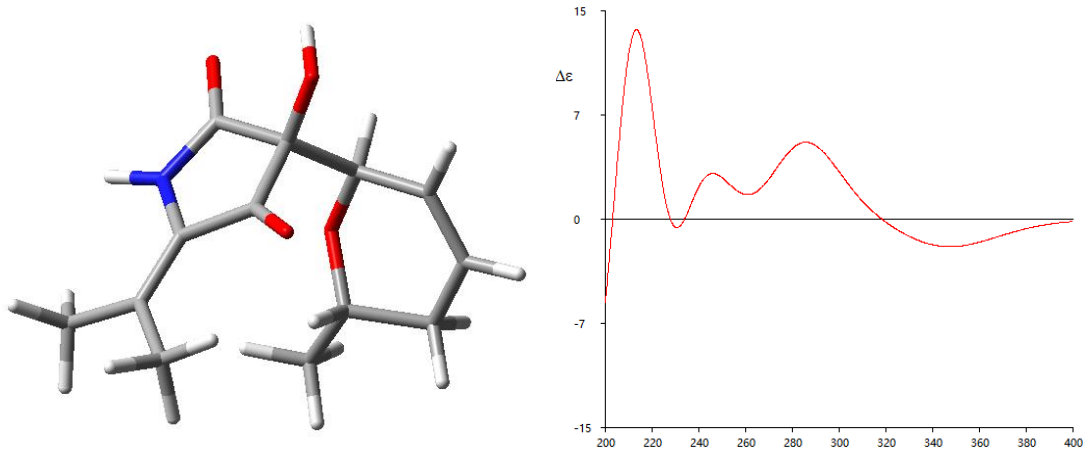


(3*S*, 6*R*, 10*S*)-2**b1**

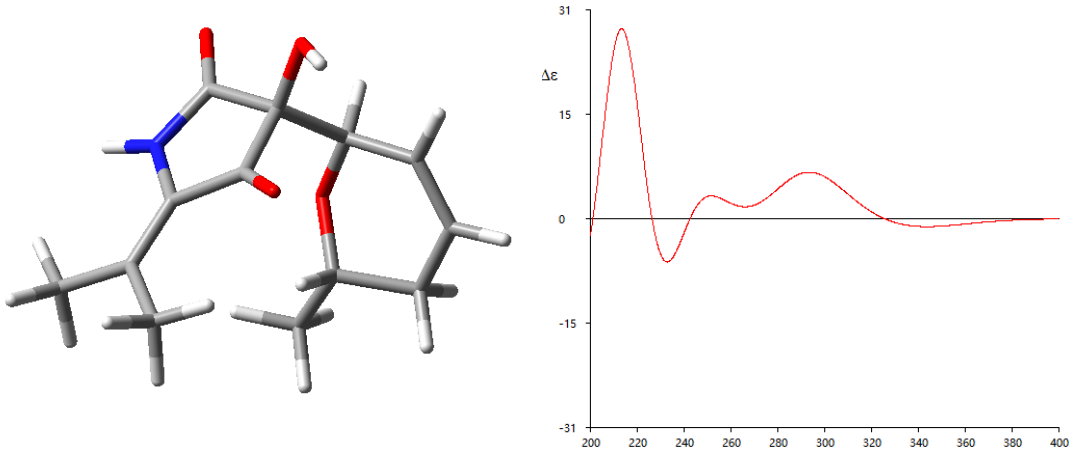


(3*S*, 6*R*, 10*S*)-2**b2**

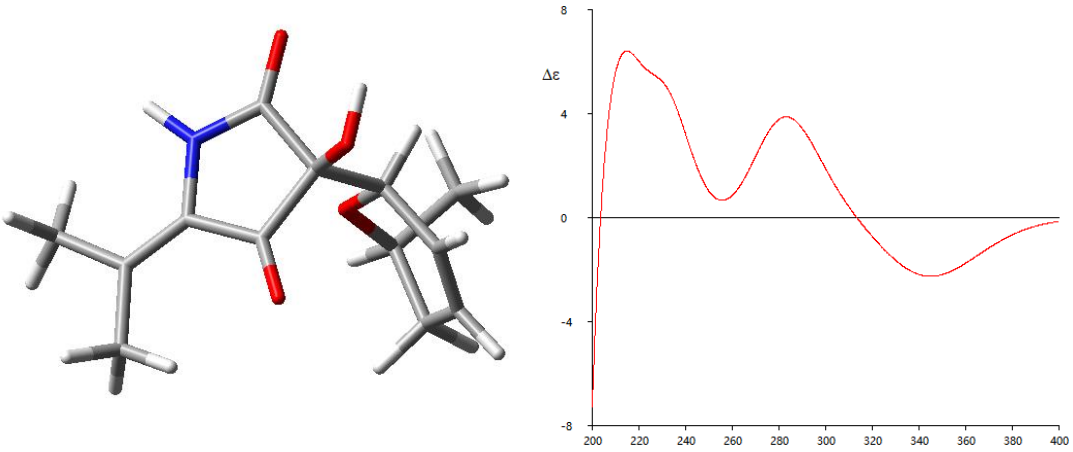


(3*S*, 6*R*, 10*S*)-2**b3**

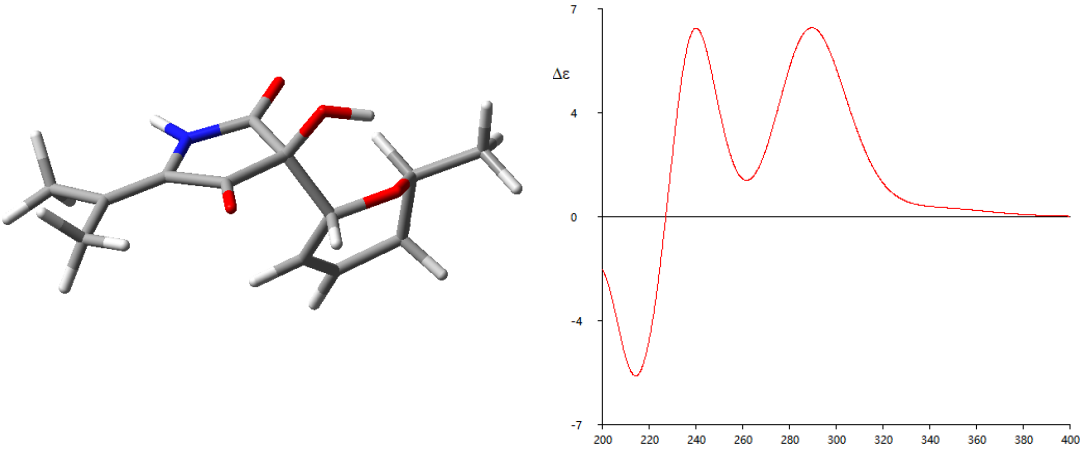


(3*S*, 6*R*, 10*S*)-2**b4**

**Figure S56**. The optimized structures (left) and the calculated CD spectra of conformers (3*S*, 6*R*, 10*S*)-**2b** in MeOH at M06-2X/def2TZVP level (right). σ=0.30 eV.

**Table S4**. Relative free energies[a] and equilibrium populations[b] of conformers for (3*S*, 6*S*, 9*R*)-**3a**[c]

| Conformer | $\Delta G$ | P (%) |
|---|---|---|
| **3a1** | 0.00 | 45.78 |
| **3a2** | 0.47 | 20.56 |
| **3a3** | 0.48 | 20.22 |
| **3a4** | 0.73 | 13.45 |

[a] B3LYP/6-31G(d), in kcal/mol. [b] From $\Delta G$ values at 298.15 K. [c] in MeOH, no imaginary frequency.

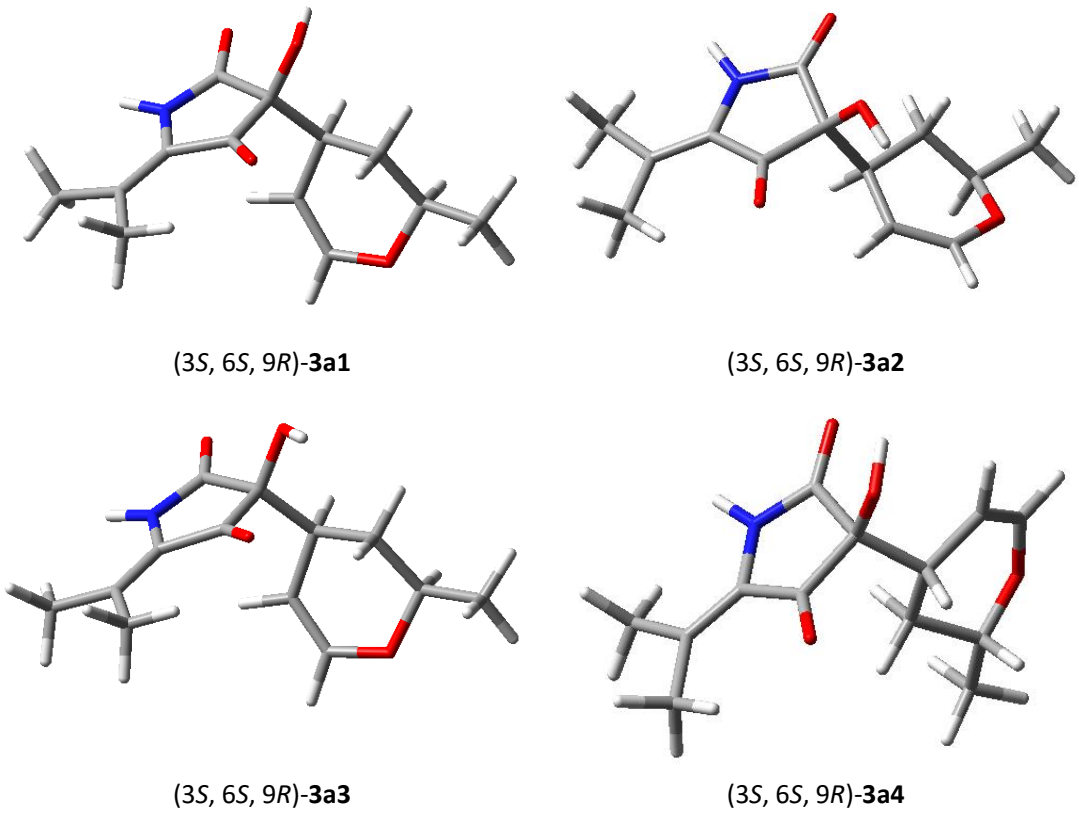

(3*S*, 6*S*, 9*R*)-**3a1** (3*S*, 6*S*, 9*R*)-**3a2**

(3*S*, 6*S*, 9*R*)-**3a3** (3*S*, 6*S*, 9*R*)-**3a4**

**Figure S57**. The optimized structure of conformers for (3*S*, 6*S*, 9*R*)-**3a** in MeOH at B3LYP/6-31G (d) level

**Table S5**. Relative free energies[a] and equilibrium populations[b] of conformers for (3*S*, 6*R*, 9*S*)-3b[c]

| Conformer | $\Delta G$ | P (%) |
|---|---|---|
| **3b1** | 0.00 | 46.24 |
| **3b2** | 0.36 | 25.13 |
| **3b3** | 0.52 | 19.29 |
| **3b4** | 0.95 | 9.34 |

[a] B3LYP/6-31G(d), in kcal/mol. [b] From $\Delta G$ values at 298.15 K. [c] in MeOH, no imaginary frequency.

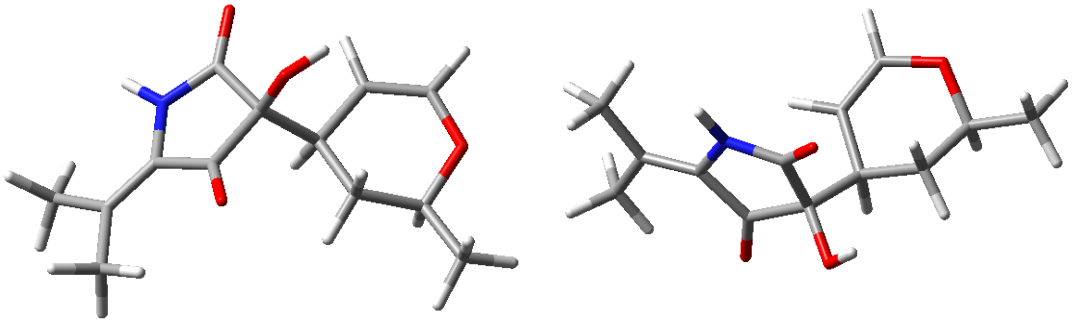

(3*S*, 6*R*, 9*S*)-**3b1**



(3*S*, 6*R*, 9*S*)-**3b2**

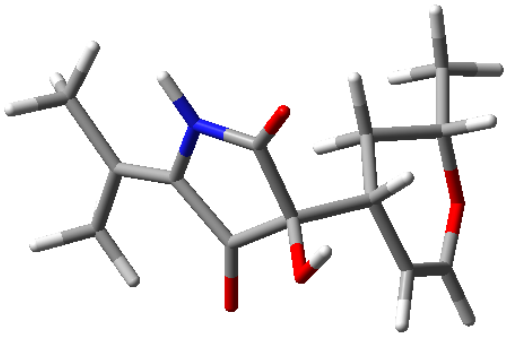

(3*S*, 6*R*, 9*S*)-**3b3**

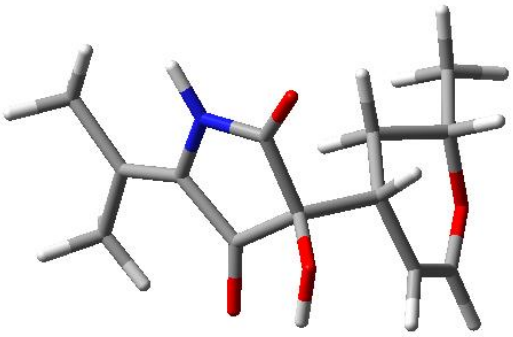

(3*S*, 6*R*, 9*S*)-**3b4**

**Figure S58**. The optimized structure of conformers for (3*S*, 6*R*, 9*S*)-**3b** in MeOH at B3LYP/6-31G (d) level

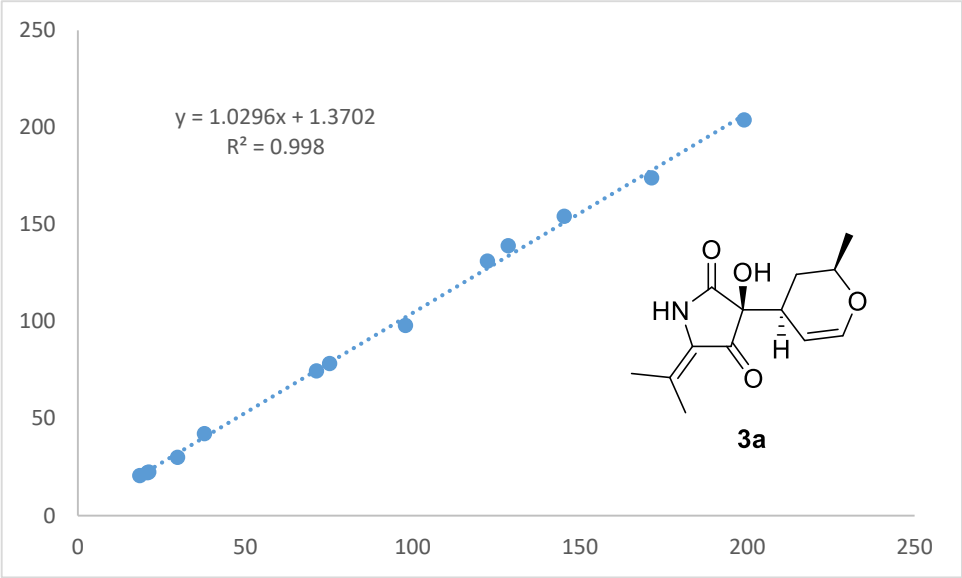

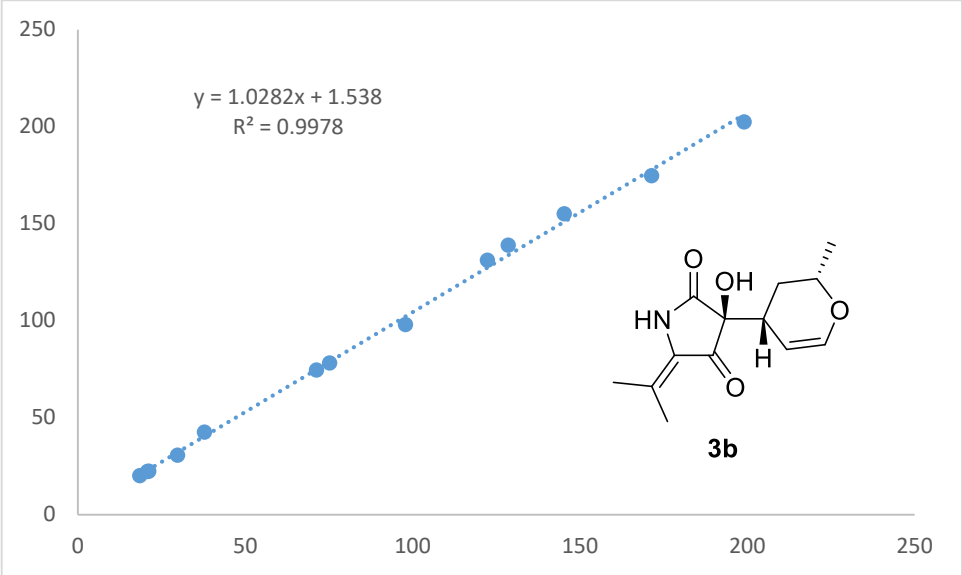


**Figure S59.** Correlation plots of experimental $^{13}C$ NMR chemical shifts versus the corresponding calculated data for (3*S*, 6*S*, 9*R*)-**3a** and (3*S*, 6*R*, 9*S*)-**3b**

| | | DP4+ | 89.66% | 10.34% |
|---|---|---|---|---|
| Nuclei | sp2? | xperimenta | Isomer 1 | Isomer 2 |
| C | x | 122.3 | 131.118 | 131.161 |
| C | x | 199.04 | 203.806 | 202.455 |
| C | | 75.14 | 78.319 | 78.102 |
| C | x | 171.35 | 174.002 | 174.743 |
| C | x | 128.57 | 139.058 | 138.82 |
| C | | 18.49 | 20.49 | 20.138 |
| C | | 20.71 | 22.077 | 22.151 |
| C | | 37.73 | 42.155 | 42.442 |
| C | x | 97.81 | 97.961 | 98.007 |
| C | x | 145.33 | 154.144 | 155.104 |
| C | | 71.2 | 74.538 | 74.579 |
| C | | 29.7 | 30.025 | 30.613 |
| C | | 21.17 | 22.413 | 22.364 |

**Figure S60**. DP4+ probabilities (%) for conformers (3*S*, 6*S*, 9*R*)-**3a** (isomer 1) and (3*S*, 6*R*, 9*S*)-**3b** (isomoer 2)

**Table S6**. Relative free energies[a] and equilibrium populations[b] of conformers for (3*S*,6*S*,9*S*)-**4a**[c]

| Conformer | Δ*G* | P (%) |
|---|---|---|
| **4a1** | 0.00 | 56.61 |
| **4a2** | 0.35 | 31.47 |
| **4a3** | 1.30 | 6.28 |
| **4a4** | 1.37 | 5.64 |

[a] B3LYP/6-31G(d), in kcal/mol. [b] From Δ*G* values at 298.15 K. [c] in MeOH, no imaginary frequency.

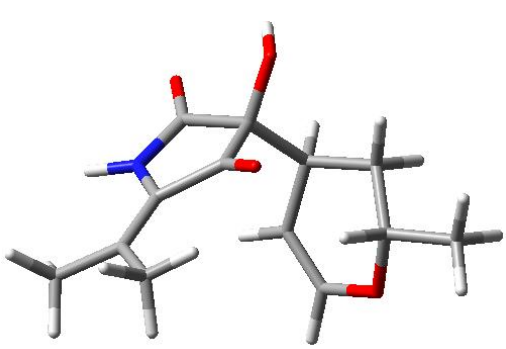

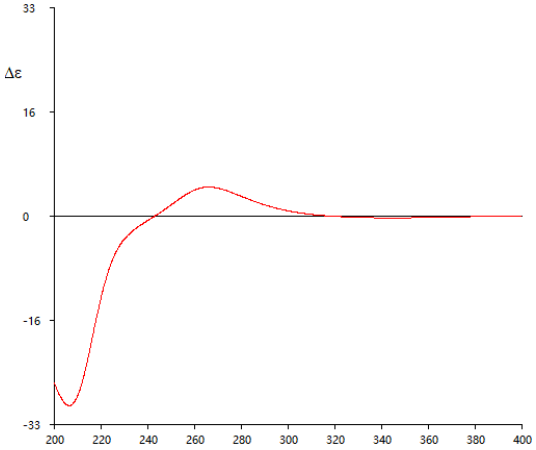


(3*S*,6*S*,9*S*)-4**a1**

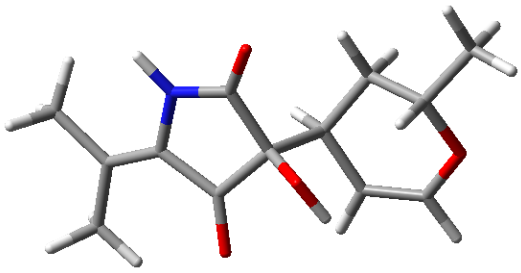

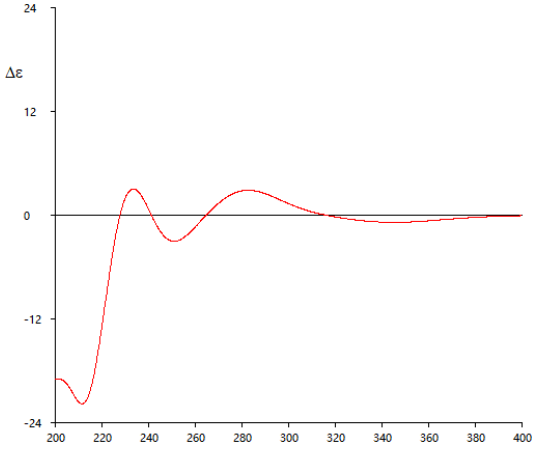


(3*S*,6*S*,9*S*)-4**a2**

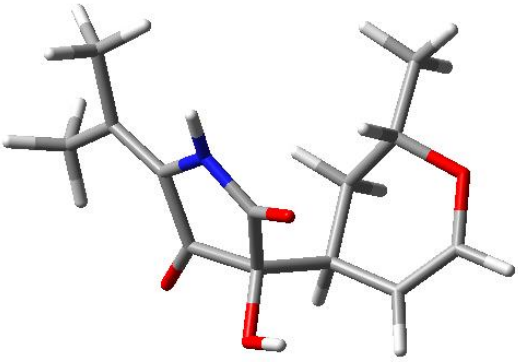

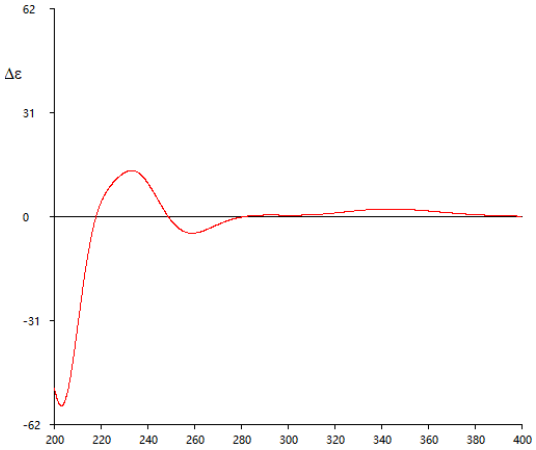


(3*S*,6*S*,9*S*)-4**a3**

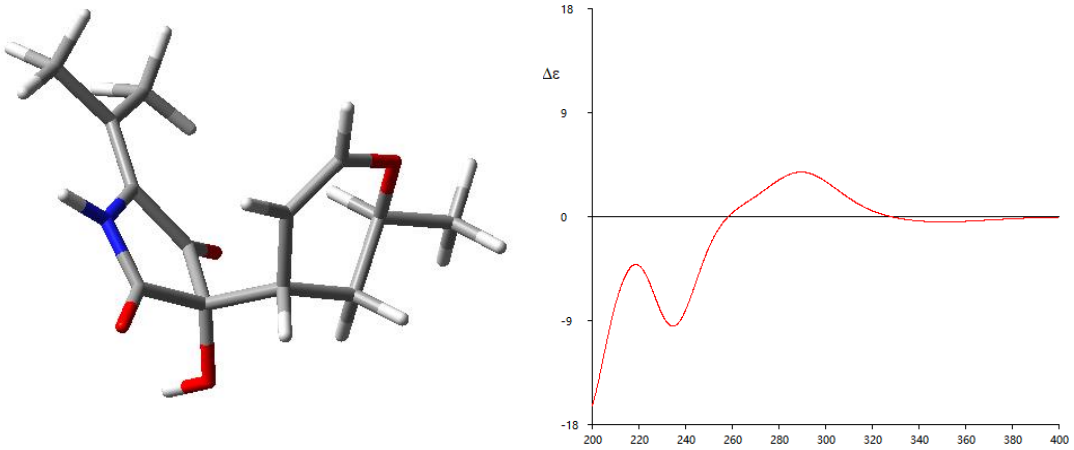


(3*S*,6*S*,9*S*)-4**a4**

**Figure S61**. The optimized structures (left) and the calculated CD spectra for conformers (3*S*,6*S*,9*S*)-**4a** in MeOH at M06-2X/def2TZVP level (right). σ=0.30 eV.

**Table S7**. Relative free energies[a] and equilibrium populations[b] of conformers for (3*S*,6*R*,9*R*)-**4b**[c]

| Conformer | Δ*G* | P (%) |
|---|---|---|
| **4b1** | 0.00 | 58.58 |
| **4b2** | 0.34 | 32.79 |
| **4b3** | 1.13 | 8.63 |

[a] B3LYP/6-31G(d), in kcal/mol. [b] From Δ*G* values at 298.15 K. [c] in MeOH, no imaginary frequency.

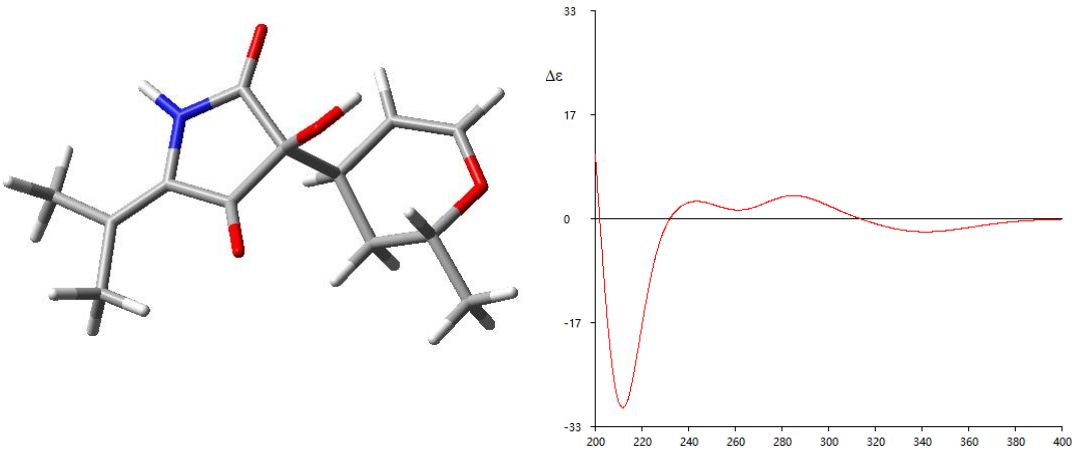


(3*S*,6*R*,9*R*)-**4b1**

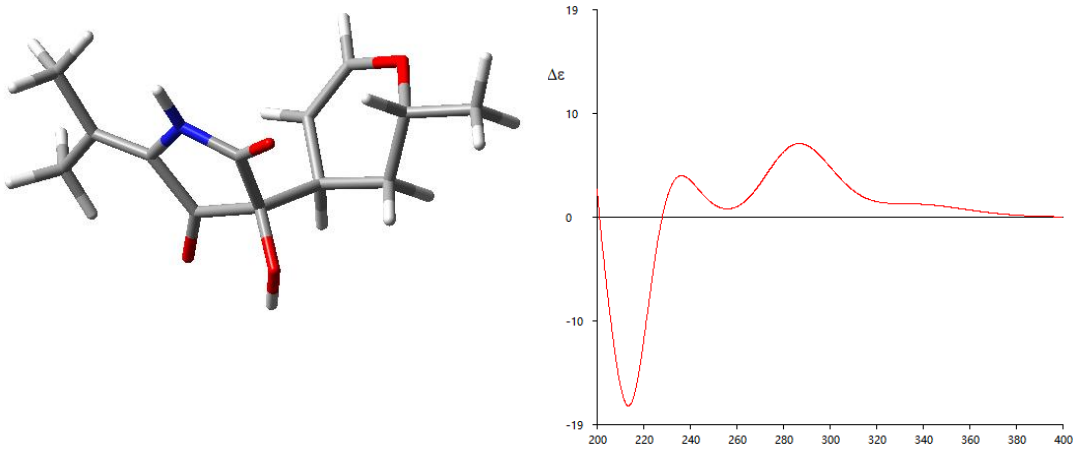


(3*S*,6*R*,9*R*)-**4b2**

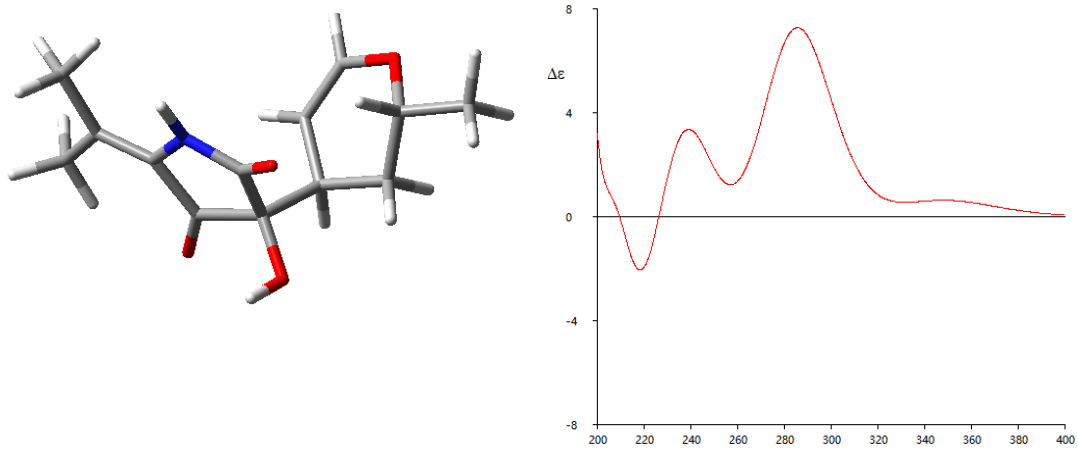


(3*S*,6*R*,9*R*)-**4b3**

Figure S62. The optimized structures (left) and the calculated CD spectra for conformers (3*S*,6*R*,9*R*)-**4b** in MeOH at M06-2X/def2TZVP level (right). σ=0.30 eV.

Table S8. Relative free energies[a] and equilibrium populations[b] of conformers for (3*R*,6*R*,9*R*)-**4c**[c]

| Conformer | Δ*G* | P (%) |
|---|---|---|
| **4c1** | 0.00 | 57.30 |
| **4c2** | 0.36 | 31.09 |
| **4c3** | 1.34 | 5.95 |
| **4c4** | 1.37 | 5.65 |

[a] B3LYP/6-31G(d), in kcal/mol. [b] From Δ*G* values at 298.15 K. [c] in MeOH, no imaginary frequency.

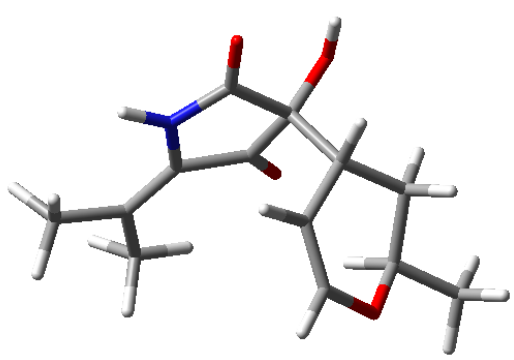

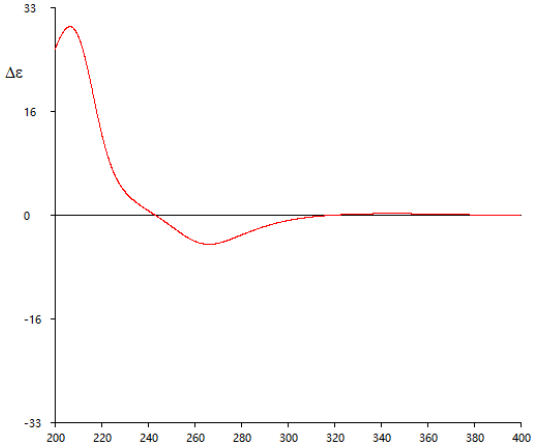


(3*R*,6*R*,9*R*)-**4c1**

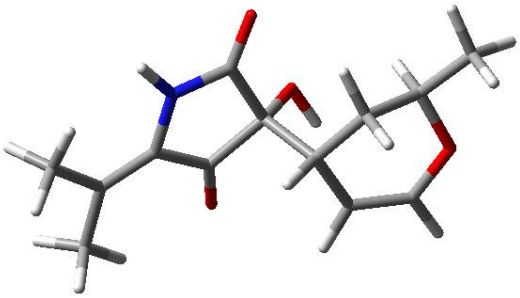

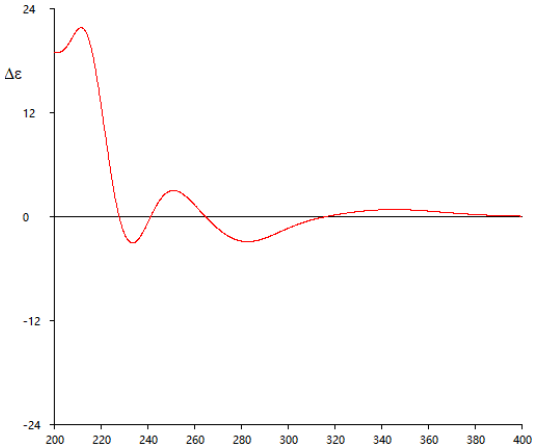


(3*R*,6*R*,9*R*)-**4c2**

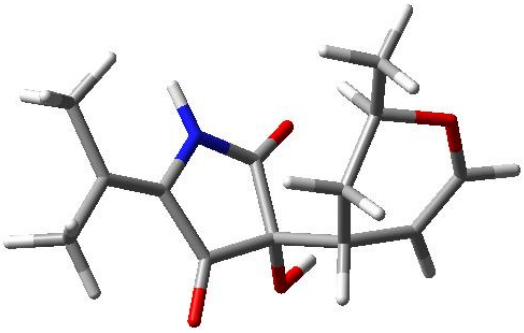

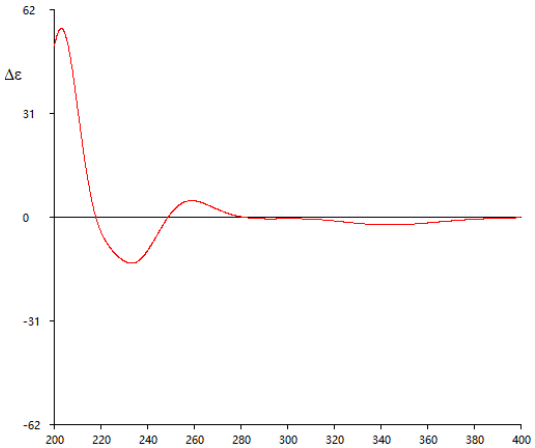


(3*R*,6*R*,9*R*)-**4c3**

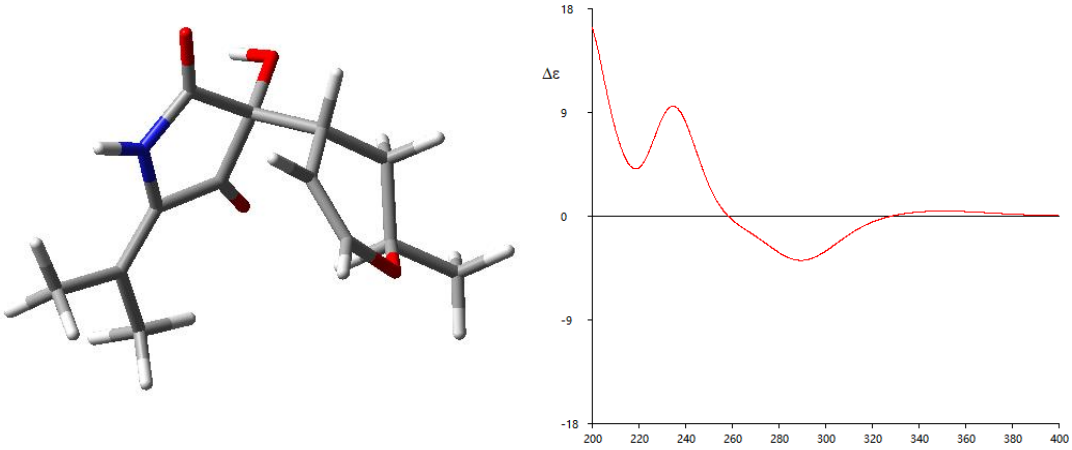


(3*R*,6*R*,9*R*)-**4c4**

**Figure S63.** The optimized structures (left) and the calculated CD spectra for conformers (3*R*,6*R*,9*R*)-**4c** in MeOH at M06-2X/def2TZVP level (right). σ=0.30 eV.

**Table S9**. Relative free energies[a] and equilibrium populations[b] of conformers for (3*R*,6*S*,9*S*)-**4d**[c]

| Conformer | Δ*G* | P (%) |
|---|---|---|
| **4d1** | 0.00 | 54.38 |
| **4d2** | 0.34 | 30.43 |
| **4d4** | 1.13 | 8.00 |
| **4d4** | 1.20 | 7.19 |

[a] B3LYP/6-31G(d), in kcal/mol. [b] From Δ*G* values at 298.15 K. [c] in MeOH, no imaginary frequency.

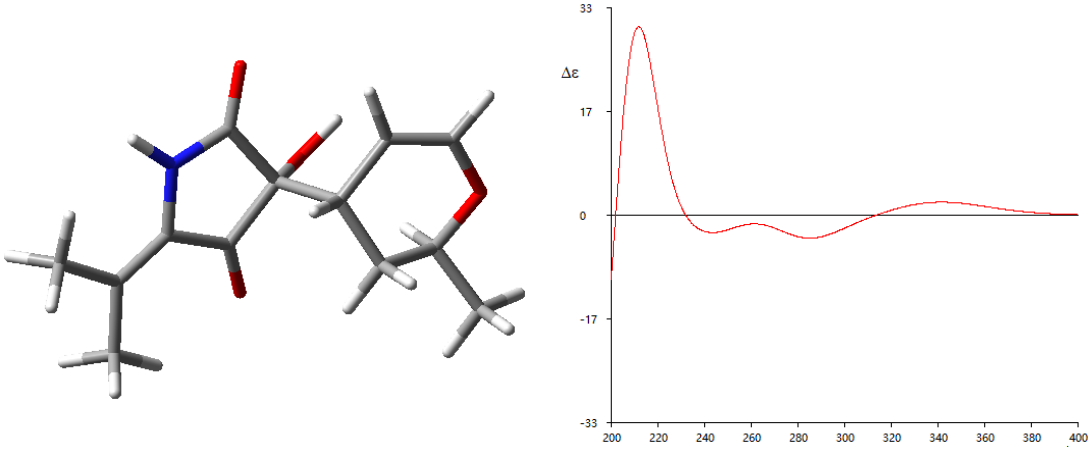


(3*R*,6*S*,9*S*)-**4d1**

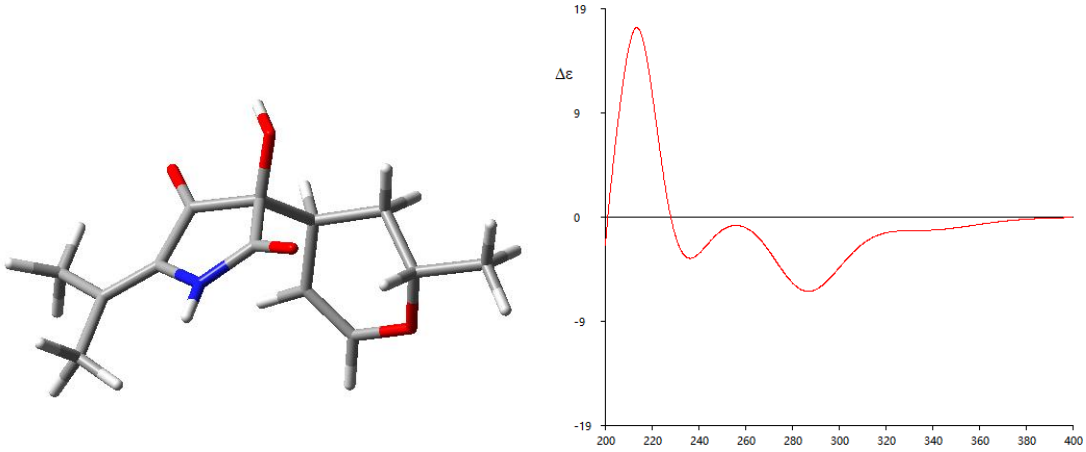


(3*R*,6*S*,9*S*)-**4d2**

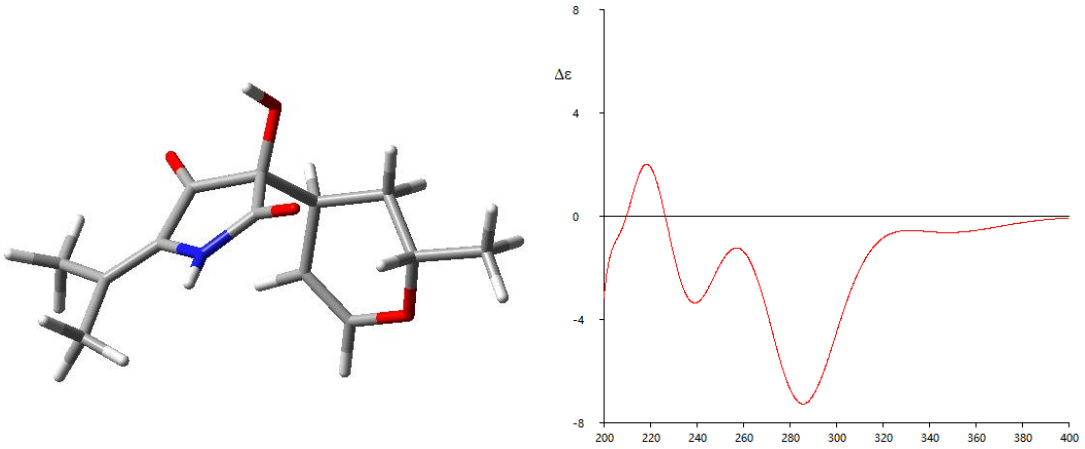


(3*R*,6*S*,9*S*)-**4d3**

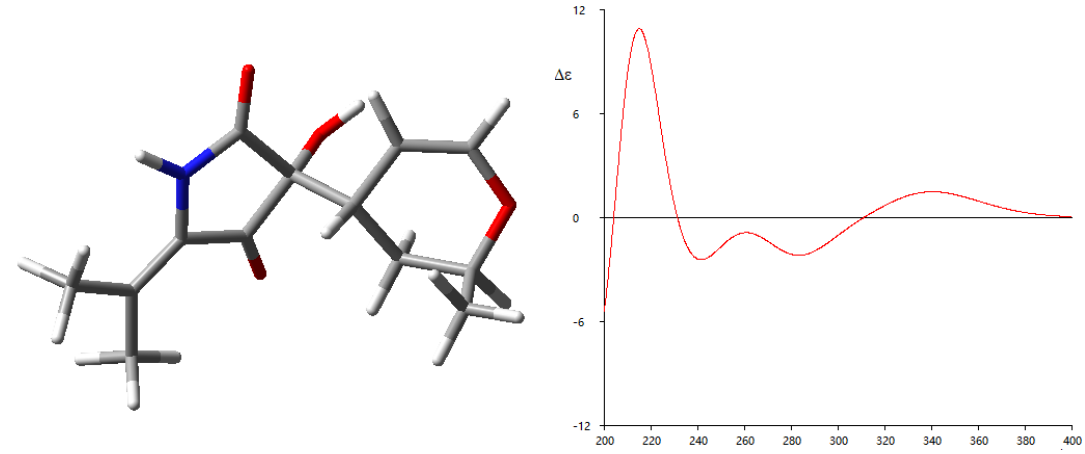


(3*R*,6*S*,9*S*)-**4d4**

**Figure S64.** The optimized structures (left) and the calculated CD spectra for conformers (3*R*,6*S*,9*S*)-**4d** in MeOH at M06-2X/def2TZVP level (right). σ=0.30 eV.

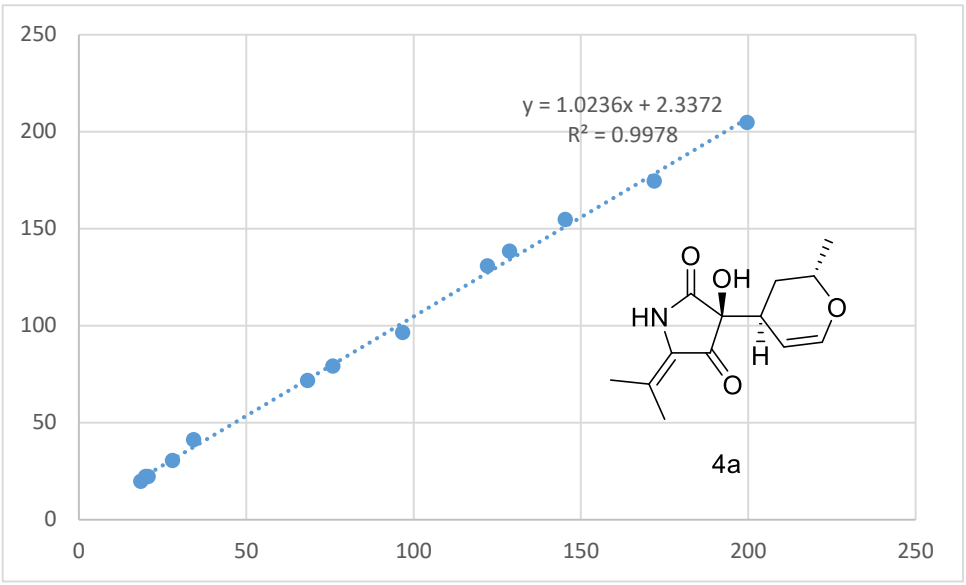


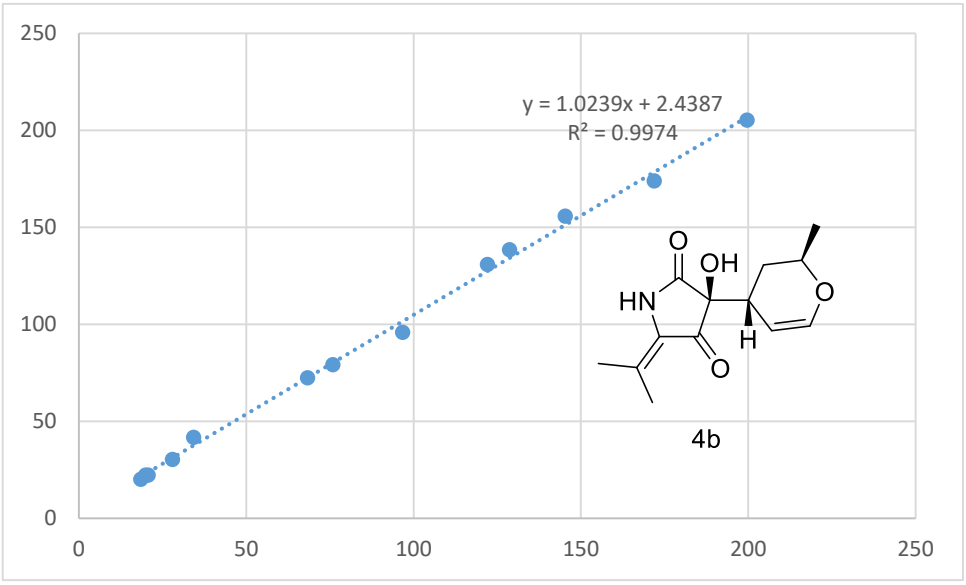


**Figure S65**. Correlation plots of experimental $^{13}$C NMR chemical shifts versus the corresponding calculated data for (3*S*, 6*S*, 9*S*)-**4a** and (3*S*, 6*R*, 9*R*)-**4b**

| | | DP4+ | 91.53% | 8.47% |
|---|---|---|---|---|
| Nuclei | sp2? | xperimenta | Isomer 1 | Isomer 2 |
| C | x | 122.07 | 130.833 | 130.781 |
| C | x | 199.64 | 204.715 | 205.3 |
| C | | 75.86 | 79.184 | 79.225 |
| C | x | 171.89 | 174.492 | 173.923 |
| C | x | 128.6 | 138.448 | 138.369 |
| C | | 18.44 | 19.821 | 20.057 |
| C | | 19.91 | 22.225 | 22.203 |
| C | | 34.26 | 41.124 | 41.651 |
| C | x | 96.65 | 96.549 | 95.898 |
| C | x | 145.25 | 154.707 | 155.726 |
| C | | 68.28 | 71.742 | 72.405 |
| C | | 27.95 | 30.437 | 30.371 |
| C | | 20.63 | 22.192 | 22.205 |

Figure S66. DP4+ probabilities (%) for conformers of (3*S*, 6*S*, 9*S*)-**4a** (isomer 1) and (3*S*, 6*R*, 9*R*)-**4b** (isomoer 2).

Table S10. Relative free energies[a] and equilibrium populations[b] of conformers for (3*S*, 6*R*, 8S, 9*S*)-**5a**[c]

| Conformer | $\Delta G$ | P (%) |
|---|---|---|
| **5a1** | 0.00 | 24.26 |
| **5a2** | 0.10 | 20.40 |
| **5a3** | 0.15 | 18.97 |
| **5a4** | 0.17 | 18.20 |
| **5a5** | 0.17 | 18.17 |

[a] B3LYP/6-31G(d), in kcal/mol. [b] From $\Delta G$ values at 298.15 K. [c] in MeOH, no imaginary frequency.

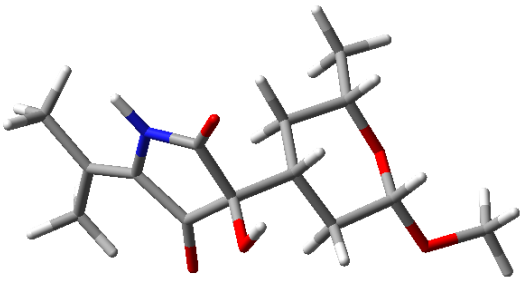

(3*S*,6*R*,8*S*,9*S*)-**5a1**

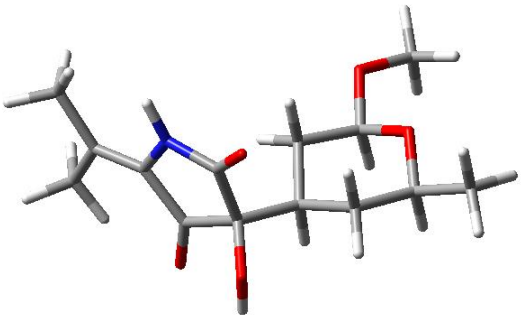

(3*S*,6*R*,8*S*,9*S*)-**5a2**

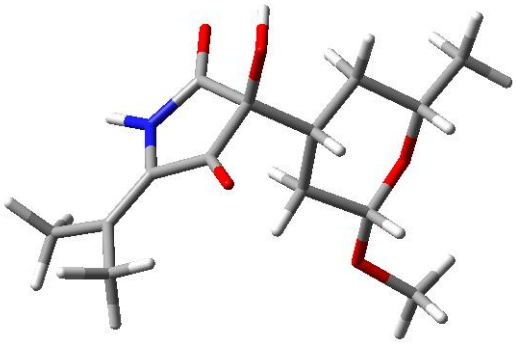

(3*S*,6*R*,8*S*,9*S*)-**5a3**

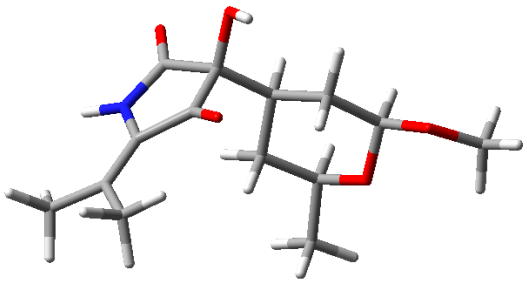

(3*S*,6*R*,8*S*,9*S*)-**5a4**

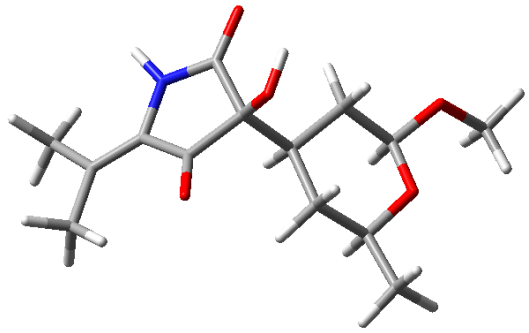

(3*S*,6*R*,8*S*,9*S*)-**5a5**

**Figure S67**. The optimized structure of conformers for (3*S*,6*R*,8*S*,9*S*)-**5a** in MeOH at B3LYP/6-31G (d) level

**Table S11**. Relative free energies[a] and equilibrium populations[b] of conformers for (3*S*,6*S*,8*R*,9*R*)-**5b** [c]

| Conformer | Δ*G* | P (%) |
|---|---|---|
| **5b1** | 0.00 | 48.08 |
| **5b2** | 0.32 | 28.22 |
| **5b3** | 0.65 | 16.14 |
| **5b4** | 1.10 | 7.56 |

[a] B3LYP/6-31G(d), in kcal/mol. [b] From Δ*G* values at 298.15 K. [c] in MeOH, no imaginary frequency.

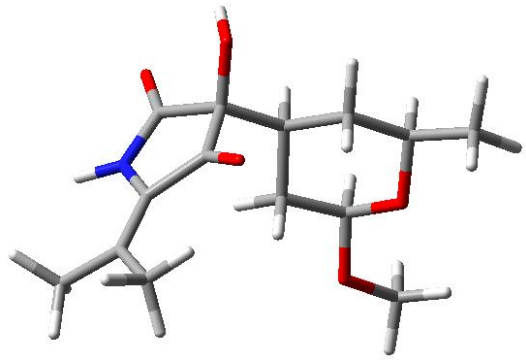

(3*S*,6*S*,8*R*,9*R*)-**5b1**

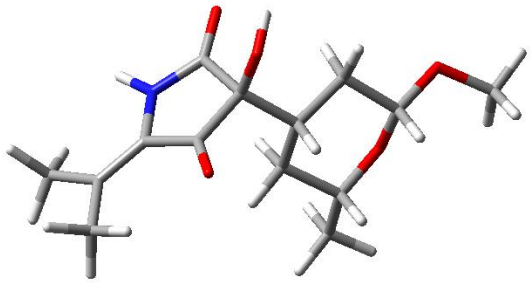

(3*S*,6*S*,8*R*,9*R*)-**5b2**

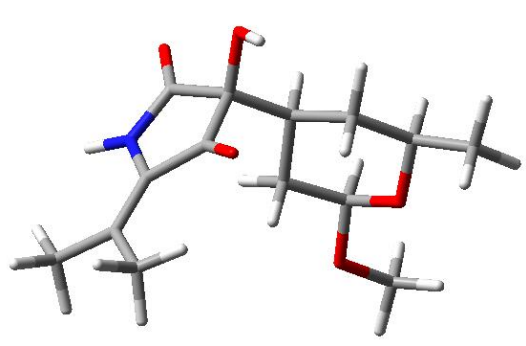

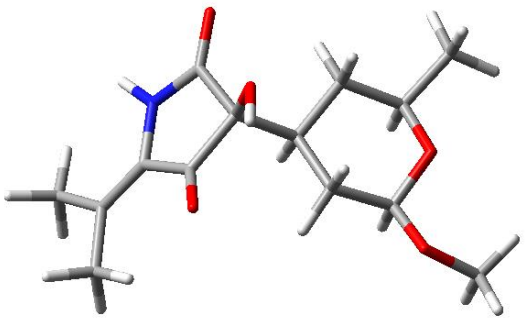

(3*S*,6*S*,8*R*,9*R*)-**5b3** (3*S*,6*S*,8*R*,9*R*)-**5b4**

**Figure S68.** The optimized structure of conformers for (3*S*,6*S*,8*R*,9*R*)-**5b** in MeOH at B3LYP/6-31G (d) level

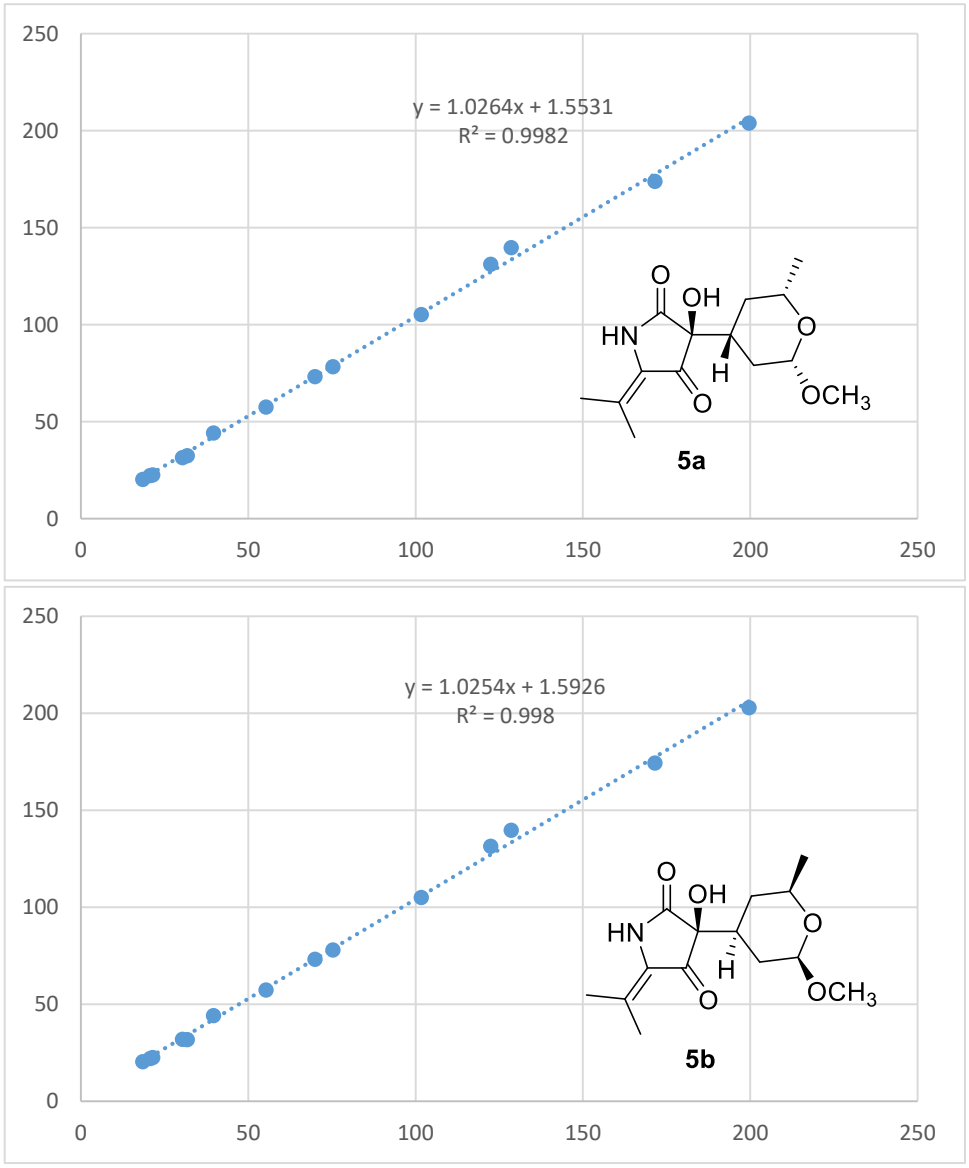


**Figure S69**. Correlation plots of experimental $^{13}C$ NMR chemical shifts versus the corresponding calculated data for (3*S*,6*R*,8*S*,9*S*)-**5a** and (3*S*,6*S*,8*R*,9*R*)-**5b**.

| | | DP4+ | 86.42% | 13.58% |
|---|---|---|---|---|
| Nuclei | sp2? | xperimenta | Isomer 1 | Isomer 2 |
| C | x | 122.44 | 131.238 | 131.53 |
| C | x | 199.59 | 203.942 | 203.056 |
| C | | 75.29 | 78.338 | 78.149 |
| C | x | 171.51 | 173.932 | 174.402 |
| C | x | 128.5 | 139.759 | 139.848 |
| C | | 18.46 | 20.382 | 20.534 |
| C | | 20.69 | 22.232 | 22.16 |
| C | | 39.6 | 44.243 | 44.288 |
| C | | 30.31 | 31.56 | 31.994 |
| C | | 101.66 | 105.23 | 105.176 |
| C | | 69.93 | 73.333 | 73.261 |
| C | | 31.72 | 32.473 | 31.823 |
| C | | 21.45 | 22.653 | 22.652 |
| C | | 55.32 | 57.549 | 57.509 |

**Figure S70**. DP4+ probabilities (%) for conformers of (3*S*,6*R*,8*S*,9*S*)-**5a** (isomer 1) and (3*S*,6*S*,8*R*,9*R*)-**5b** (isomoer 2).

**Table S12**. Relative free energies[a] and equilibrium populations[b] of conformers for (3*S*,6*S*,8*R*,9*S*)-**6a** [c]

| Conformer | Δ*G* | P (%) |
|---|---|---|
| **6a1** | 0.00 | 68.40 |
| **6a2** | 0.72 | 20.24 |
| **6a3** | 1.06 | 11.35 |

[a] B3LYP/6-31G(d), in kcal/mol. [b] From Δ*G* values at 298.15 K. [c] in MeOH, no imaginary frequency.

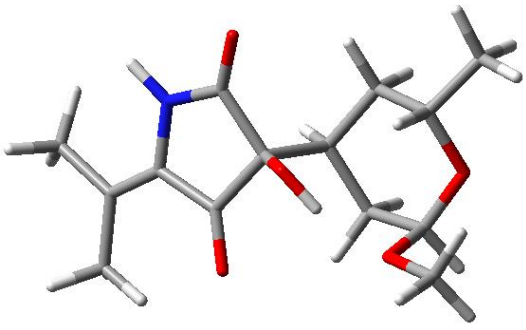

(3*S*,6*S*,8*R*,9*S*)-**6a1**

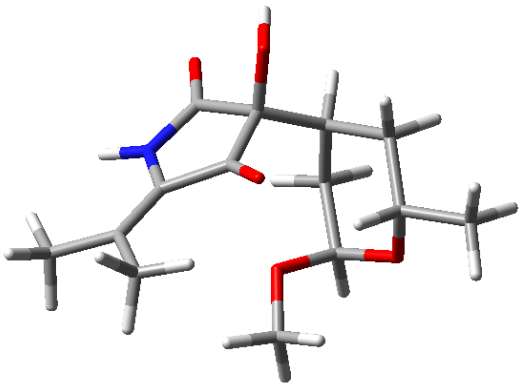

(3*S*,6*S*,8*R*,9*S*)-**6a2**

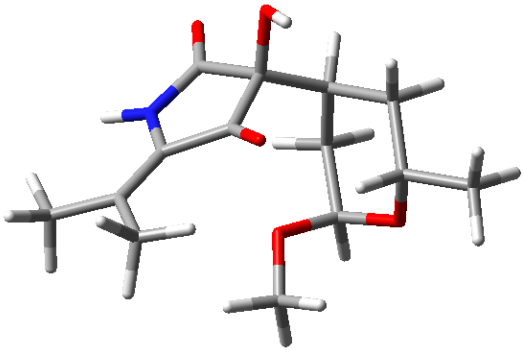

(3*S*,6*S*,8*R*,9*S*)-**6a3**

**Figure S71**. The optimized structure of conformers for (3*S*,6*S*,8*R*,9*S*)-**6a** in MeOH at B3LYP/6-31G (d) level.

**Table S13**. Relative free energies[a] and equilibrium populations[b] of conformers for (3*S*,6*R*,8*S*,9*R*)-**6b** [c]

| Conformer | $\Delta G$ | P (%) |
|---|---|---|
| **6b1** | 0.00 | 77.82 |
| **6b2** | 0.98 | 14.77 |
| **6b3** | 1.39 | 7.41 |

[a] B3LYP/6-31G(d), in kcal/mol. [b] From $\Delta G$ values at 298.15 K. [c] in MeOH, no imaginary frequency.

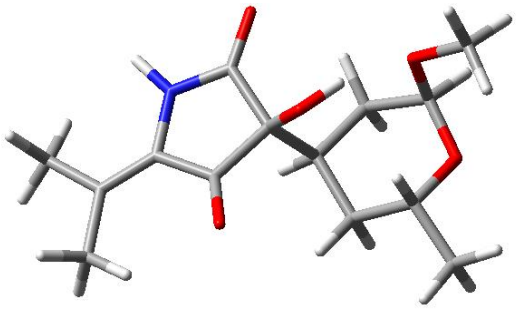

(3*S*,6*R*,8*S*,9*R*)-**6b1**

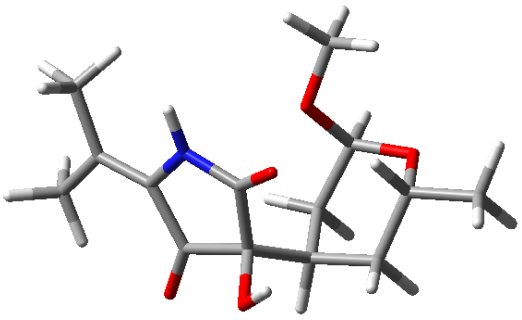

(3*S*,6*R*,8*S*,9*R*)-**6b2**

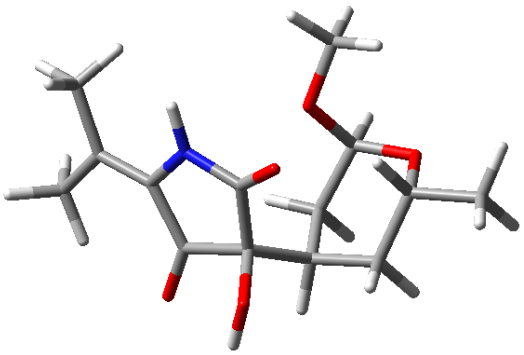

(3*S*,6*R*,8*S*,9*R*)-**6b3**

**Figure S72**. The optimized structure of conformers for (3*S*,6*R*,8*S*,9*R*)-**6b** in MeOH at B3LYP/6-31G (d) level.

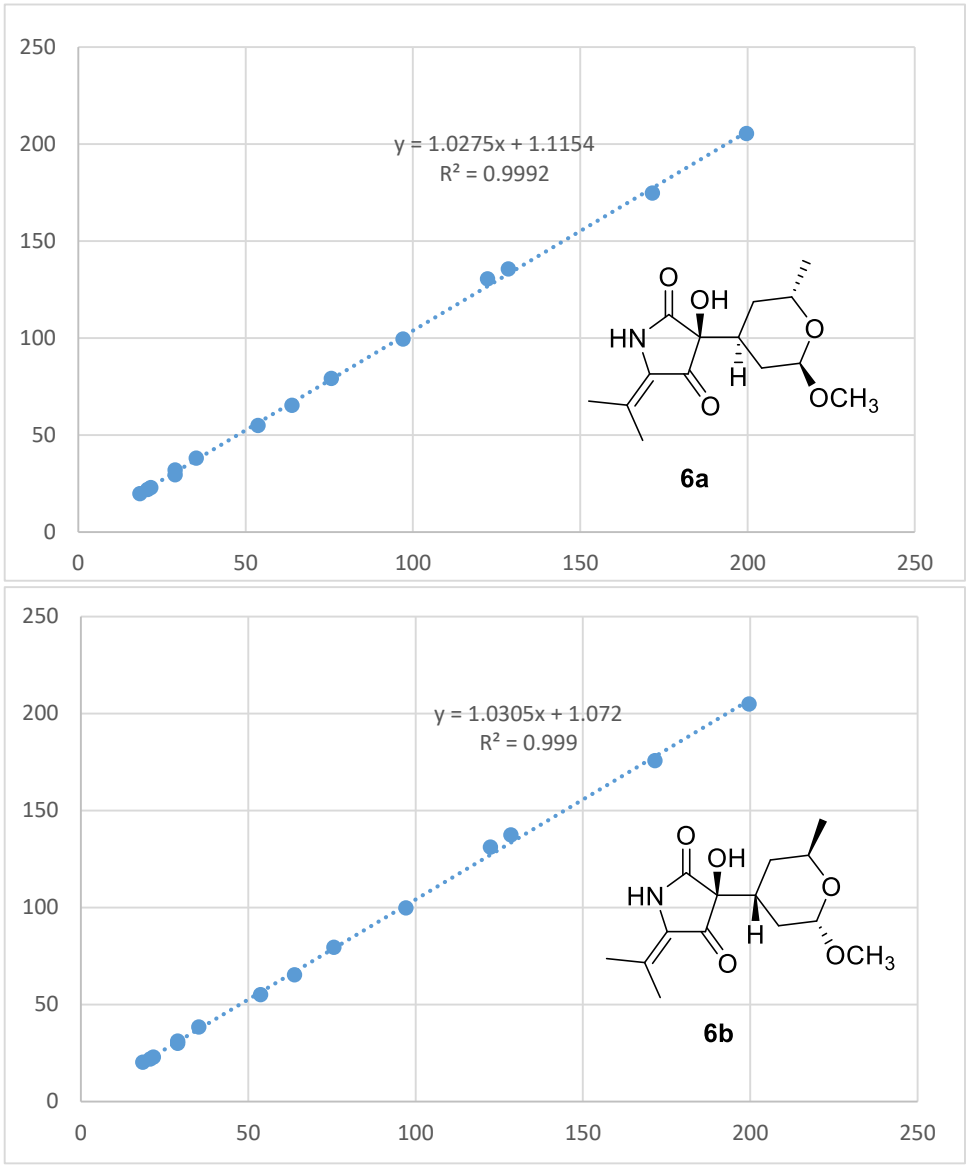


**Figure S73**. Correlation plots of experimental $^{13}C$ NMR chemical shifts versus the corresponding calculated data for (3*S*,6*S*,8*R*,9*S*)-**6a** and (3*S*,6*R*,8*S*,9*R*)-**6b**

| | | DP4+ | 86.61% | 13.39% |
|---|---|---|---|---|
| Nuclei | sp2? | xperimenta | Isomer 1 | Isomer 2 |
| C | x | 122.28 | 130.626 | 131.05 |
| C | x | 199.65 | 205.514 | 204.922 |
| C | | 75.55 | 79.267 | 79.475 |
| C | x | 171.53 | 174.733 | 175.655 |
| C | x | 128.44 | 135.751 | 137.446 |
| C | | 18.43 | 19.937 | 20.266 |
| C | | 20.66 | 22.002 | 21.895 |
| C | | 35.23 | 38.188 | 38.331 |
| C | | 28.86 | 29.628 | 29.974 |
| C | | 97.05 | 99.607 | 99.78 |
| C | | 63.82 | 65.342 | 65.329 |
| C | | 28.86 | 32.037 | 31.086 |
| C | | 21.6 | 22.914 | 22.846 |
| C | | 53.67 | 54.999 | 55.092 |

**Figure S74**. DP4+ probabilities (%) for conformers of (3*S*,6*S*,8*R*,9*S*)-**6a** (isomer 1) and (3*S*,6*R*,8*S*,9*R*)-**6b** (isomoer 2).

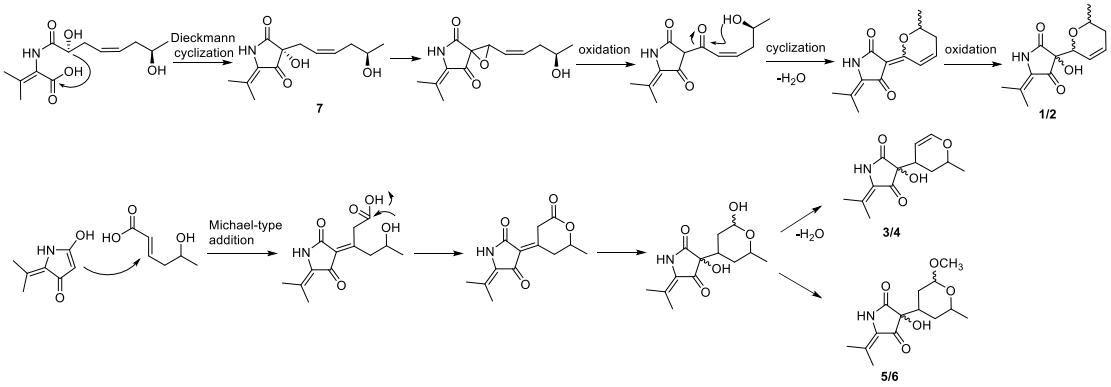


**Figure S74**. Proposed biosynthetic pathway of compounds **1–7** [1,2].

[1] Rischer, M.; Lee, S. R.; Eom, H. J.; Park, H. B.; Vollmer, J.; Kaster, A. K.; Shin, Y. H.; Oh, D. C.; Kim, K. H.; Beemelmanns, C. Spirocyclic cladosporicin A and cladosporiumins I and J from a Hydractinia-associated Cladosporium sphaerospermum SW67. *Org. Chem. Front.* **2019**, *6*, 1084-1093.

[2] Mo, X.; Gulder, T. Biosynthetic strategies for tetramic acid formation. *Nat. Prod. Rep*. **2021**, *38*, 1555-1566.